การพัฒนาสูตรตำรับยาแขวนตะกอนซีลีค็อกซิบ-ไซโคลเดกซ์ทรินสำหรับนำส่งทางตา

ร้อยตำรวจเอกภาคิน กุลศิรโชติ

วิทยานิพนธ์นี้เป็นส่วนหนึ่งของการศึกษาตามหลักสูตรปริญญาเภสัชศาสตรมหาบัณฑิต
สาขาวิชาเภสัชกรรม ภาควิชาวิทยาการเภสัชกรรมและเภสัชอุตสาหกรรม
คณะเภสัชศาสตร์ จุฬาลงกรณ์มหาวิทยาลัย
ปีการศึกษา 2559

FORMULATION DEVELOPMENT OF CELECOXIB-CYCLODEXTRIN SUSPENSIONS FOR OPHTHALMIC DELIVERY

Police Captain Pakin Kulsirachote

A Thesis Submitted in Partial Fulfillment of the Requirements
for the Degree of Master of Science in Pharmacy Program in Pharmaceutics
Department of Pharmaceutics and Industrial Pharmacy
Faculty of Pharmaceutical Sciences
Chulalongkorn University
Academic Year 2016

Thesis Title	FORMULATION DEVELOPMENT OF CELECOXIB-CYCLODEXTRIN SUSPENSIONS FOR OPHTHALMIC DELIVERY
By	Police Captain Pakin Kulsirachote
Field of Study	Pharmaceutics
Thesis Advisor	Phatsawee Jansook, Ph.D.

Accepted by the Faculty of Pharmaceutical Sciences, Chulalongkorn University in Partial Fulfillment of the Requirements for the Master's Degree

.....Dean of the Faculty of Pharmaceutical Sciences
(Assistant Professor Rungpetch Sakulbumrungsil, Ph.D.)

THESIS COMMITTEE

.....Chairman
(Associate Professor Parkpoom Tengamnuay, Ph.D.)

.....Thesis Advisor
(Phatsawee Jansook, Ph.D.)

.....Examiner
(Dusadee Charnvanich, Ph.D.)

.....External Examiner
(Assistant Professor Warisada Sila-on, Ph.D.)

ภาคิน กุลศิรโชติ : การพัฒนาสูตรตำรับยาแขวนตะกอนซีลีค็อกซิบ-ไซโคลเดกซ์ทรินสำหรับนำส่งทางตา (FORMULATION DEVELOPMENT OF CELECOXIB-CYCLODEXTRIN SUSPENSIONS FOR OPHTHALMIC DELIVERY) อ.ที่ปรึกษาวิทยานิพนธ์หลัก: อ. ภก. ดร.ภาสวีร์ จันทร์สุก, หน้า.

ยาซีลีค็อกซิบเป็นยาต้านอาการอักเสบที่ไม่ใช่สเตียรอยด์ สามารถนำไปใช้ในการรักษาโรคจอประสาทตาเสื่อมและภาวะเบาหวานขึ้นจอตาโดยผ่านการยับยั้งเอนไซม์ COX-2 ที่จอประสาทตา ปัจจุบันมีรูปแบบการบริหารยาเพื่อนำส่งยาเข้าสู่บริเวณส่วนหลังของลูกตา เช่นการบริหารโดยการรับประทาน การฉีดเข้าน้ำวุ้นลูกตา การฉีดเข้าใต้เยื่อบุตา และการหยอดตา ในวิถีการบริหารยาทั้งหมด การบริหารยาโดยการหยอดตาเป็นวิธีที่ทำให้ยาออกฤทธิ์เฉพาะที่ และไม่ทำลายเนื้อเยื่อดวงตา อย่างไรก็ตามเนื่องจากยาซีลีค็อกซิบเป็นยาที่ละลายน้ำได้น้อยจึงเป็นข้อจำกัดในการนำส่งยาเข้าสู่ภายในลูกตา ดังนั้นการศึกษานี้จึงมีวัตถุประสงค์เพื่อพัฒนายาแขวนตะกอนซีลีค็อกซิบในรูปแบบยาหยอดตา ที่มีไซโคลเดกซ์ทรินและพอลิเมอร์เป็นองค์ประกอบเพื่อนำส่งยาไปสู่ส่วนหลังของลูกตา ศึกษาเฟสการละลายของสารประกอบเชิงซ้อน และคุณลักษณะของสารประกอบเชิงซ้อนของยาซีลีค็อกซิบกับไซโคลเดกซ์ทริน 5 ชนิดได้แก่ อัลฟา (alpha-CD) บีต้า (beta-CD) แกมมา (gamma-CD) ไฮดรอกซีโพรพิลบีต้า (HP-beta-CD) และแรนดอมลีเมทิลเลตบีต้า (RM-beta-CD) ไซโคลเดกซ์ทริน และพอลิเมอร์ยึดติดเยื่อเมือก 3 ชนิดได้แก่ ไฮดรอกซีโพรพิลเมทิลเซลลูโลส (HPMC) ไคโตซาน และกรดไฮยาลูโรนิก (HA) จากผลการศึกษาพบว่าไซโคลเดกซ์ทรินชนิด RM-beta-CD มีคุณสมบัติในการละลายยาสูงกว่าไซโคลเดกซ์ทรินชนิดอื่นที่นำมาทดสอบ HPMC มีประสิทธิภาพที่ดีในการเกิดสารประกอบเชิงซ้อนตติยภูมิ ซึ่งสูงกว่าสารประกอบเชิงซ้อนทุติยภูมิซีลีค็อกซิบ/RM-beta-CD ถึง 11 เท่า เมื่อทำการประเมินการเกาะกลุ่มของขนาดอนุภาคสารประกอบเชิงซ้อนตติยภูมิ พบขนาดของอนุภาคอยู่ในช่วง 250 - 350 นาโนเมตร ส่งผลทำให้การละลายของซีลีค็อกซิบสูงขึ้น จากข้อมูลที่ได้รับจากเทคนิค DSC PXRD FTIR และ ^{1}H-NMR ชี้ให้เห็นว่ามีการเกิดสารประกอบเชิงซ้อนของยาซีลีค็อกซิบและไซโคลเดกซ์ทริน การเตรียมสูตรตำรับยาหยอดตาซีลีค็อกซิบ ได้มีการเตรียมแบบไม่ใช้ความร้อนและการใช้ความร้อนโดยการผ่านคลื่นความถี่สูงที่อุณหภูมิ 70 องศาเซลเซียส เป็นเวลา 1 ชั่วโมง ประเมินคุณลักษณะทางเคมีและกายภาพ คุณสมบัติการยึดติดเยื่อเมือก และการประเมินการซึมผ่านภายนอกร่างกาย ผลการประเมินคุณสมบัติทางเคมีกายภาพของสูตรตำรับ ได้แก่ลักษณะทางกายภาพ ความเป็นกรด-ด่าง ออสโมลาลิตี และความหนืดอยู่ในช่วงที่ยอมรับได้ ขนาดอนุภาคต่ำกว่า 10 ไมโครเมตร บ่งชี้ว่าอาจจะไม่ก่อให้เกิดการระคายเคืองต่อดวงตา สูตรตำรับที่มีพอลิเมอร์ชนิด HA เป็นองค์ประกอบแสดงคุณสมบัติการยึดติดเยื่อเมือกที่ดี ส่วนสูตรตำรับที่ผ่านความร้อนส่วนใหญ่พบว่ามีปริมาณของยาซีลีค็อกซิบที่อยู่ในรูปสารละลายมากขึ้น ส่งผลทำให้ปริมาณยาที่ซึมผ่านเยื่อเลือกผ่านและการซึมผ่านน้ำวุ้นลูกตาจำลองเพิ่มขึ้น โดยเฉพาะสูตรตำรับที่มี RM-beta-CD และ HA ร้อยละ 0.5 โดยน้ำหนักต่อปริมาตร ดังนั้นสูตรตำรับดังกล่าวจึงอาจเป็นสูตรตำรับที่เหมาะสมในรูปแบบยาหยอดตาแขวนตะกอนที่สามารถนำส่งยาซีลีค็อกซิบไปยังบริเวณส่วนหลังของลูกตาในการรักษาโรคจอประสาทตาเสื่อมและภาวะเบาหวานขึ้นจอตาได้

ภาควิชา วิทยาการเภสัชกรรมและเภสัชอุตสาหกรรม ลายมือชื่อนิสิต .....

สาขาวิชา เภสัชกรรม ลายมือชื่อ อ.ที่ปรึกษาหลัก .....

ปีการศึกษา 2559

5776126033 : MAJOR PHARMACEUTICS

KEYWORDS: CELECOXIB / CYCLODEXTRIN / SUSPENSION / OPHTHALMIC DELIVERY

PAKIN KULSIRACHOTE: FORMULATION DEVELOPMENT OF CELECOXIB-CYCLODEXTRIN SUSPENSIONS FOR OPHTHALMIC DELIVERY. ADVISOR: PHATSAWEE JANSOOK, Ph.D., pp.

Celecoxib (CCB), a nonsteroidal anti-inflammatory drug (NSAID), could be beneficial in the treatment of age-related macular degeneration (AMD) and diabetic retinopathy (DR) through the inhibition of COX-2 enzyme. Currently, the several methods can deliver drugs to the back of the eye. i.e., oral, intravitreal injection, subconjunctival injection and topical. Among routes of administration, topical eye drop is non-invasive method and local effects. However, due to low aqueous solubility of CCB, it hampers ocular bioavailability. Thus, the aim of this study was to develop topical eye drop suspensions containing cyclodextrin (CD) and polymer delivering to the posterior segment of the eye. CDs, the solubilizer, i.e., alpha-CD, beta-CD, gamma-CD, HP-beta-CD and RM-beta-CD and mucoadhesive polymers i.e., hydroxypropylmethylcellulose (HPMC) chitosan and hyaluronic acid (HA) were used. The phase solubility profiles and CCB/CD complex characteristics were investigated. RM-beta-CD exhibited the greatest solubilizer among CDs tested. HPMC was the potential polymer to form ternary complex with CCB/RM-beta-CD which gave 11-folds complexation efficiency higher than that of its binary complex. The aggregate size of ternary complexes in solution were found in the range of 250 - 350 nm which could solubilize themselves resulting in increasing CCB solubility. The data obtained from FT-IR, DSC, PXRD and ^{1}H-NMR indicated that there were interaction of CCB with CD as inclusion complex. The CCB eye drops formulations were prepared by unheated and heating method (sonication at the temperature of 70°C for 1 hour). The physicochemical and chemical characterizations, mucoadhesive properties and *in-vitro* permeation were determined. The physicochemical properties i.e., appearance, pH, osmolality and viscosity were in acceptable range. The particle sizes below 10 μm indicated possibly no irritation to the eye. The formulation containing HA showed the excellent mucoadhesive properties. The increasing of % CCB content in most cases by heat resulting in higher flux permeation through semipermeable membrane and through simulated artificial vitreous humor, especially the formulation containing RM-beta-CD and HA (0.5% w/v). Therefore, it may be a promising candidate as topical formulation which can deliver CCB to the posterior segment of eye to treat AMD and DR.

Department: Pharmaceutics and Industrial Pharmacy Student's Signature .....

Advisor's Signature .....

Field of Study: Pharmaceutics

Academic Year: 2016

ACKNOWLEDGEMENTS

My thesis would not be accomplished without my thesis adviser, Phatsawee Jansook, Ph.D. and I would like to express my sincere thanks for his invaluable advice, guidance, understanding, helpfulness and all kind of supports throughout my study.

I would like to thank my thesis committee for invaluable suggestions and precious comments that exceed the completion of this thesis.

Special thanks are giving to Chulalongkorn University Centenary Academic Development Project for providing research facilities.

I would like to express grateful thanks to the Thailand Research Fund (TRF) for granting financial support to fulfill this study.

I would like to special thanks to Unison Laboratories Co.,Ltd., Thailand for supplying celecoxib to my study.

The other special thanks to Scientific Promotion Co.,Ltd., Thailand for supporting in mixer mill.

Moreover, I am grateful to all staff and lab members in the Department of Pharmaceutics and Industrial Pharmacy, Faculty of Pharmaceutical Sciences, Chulalongkorn University for facilities and instruments support. Their useful suggestion, thoughtfulness and their encouragement are also deeply appreciated.

Finally, my deepest gratitude goes to my family for their love and all kind supports throughout my life. Without their encouragement and understanding, it could not have been possible for inspire me to achieve this thesis.

CONTENTS

Page

Page

Page

LIST OF TABLES

Page

APENDIX B

APPENDIX C

APENDIX D

LIST OF FIGURES

Page

APENDIX A

APENDIX D

LIST OF ABBREVIATION

%	percentage
°C	degree Celsius
μg	microgram (s)
μl	microliter (s)
μm	micrometer (s)
μM	micro-molar
α-CD	alpha-cyclodextrin
β-CD	beta-cyclodextrin
γ-CD	gamma-cyclodextrin
AMD	age-related macular degeneration
ATR	attenuated total reflectance
A°	angstrom
BCS	Biopharmaceutical Classification System
BAC	benzalkonium chloride
CCB	celecoxib
CD	cyclodextrin
CNV	choroid neovascularization
COX-2	cyclooxygenase-2
CE	complexation efficiency
CS	chitosan
DR	diabetic retinopathy
DSC	differential scanning calorimetry
DLS	dynamic light scattering
EDTA	ethylenediaminetetraacetic acid disodium salt
e.g.	for example
Eq.	equation
FT-IR	fourier-transform infra-red spectroscopy
FD	freeze dried

F	sedimentation volume
HP-β-CD	hydroxypropyl-beta-cyclodextrin
HPMC	hydroxypropyl methylcellulose
HPLC	high performance liquid chromatography
HA	hyaluronic acid
^{1}H-NMR	proton nuclear magnetic resonance
IC_{50}	half maximal inhibitory concentration
K	stability constant
kDa	kilodalton
mA	milliamps
MWCO	molecular weight cut-off
NSAID	nonsteroidal anti-inflammatory drug
nm	nanometer
PVP	Polyvinylpyrrolidone
PXRD	powder X-ray diffraction
PEG	polyethylene glycol
PM	physical mixture
P_{app}	permeation coefficient
RM-β-CD	randomly methylated-beta-cyclodextrin
RPE	retina pigment epithelium
rpm	revolutions per minute
RSD	relative standard deviation
R^2	coefficient of determination
SBE-β-CD	sulfobutylether-beta-cyclodextrin
STF	simulated tear fluid
SD	standard deviation
TEM	transmission electron microscopy
UV/VIS	ultraviolet/visible,
VEGF	Vascular Endothelial Growth Factor

CHAPTER I
INTRODUCTION

Presently, age-related macular degeneration (AMD) and diabetic retinopathy (DR) are two key prevailing causes of vision impairment. The two disorders combined account for over 60% of cases of blindness in the US (Congdon et al., 2004). AMD is the major cause of central vision loss, typically individual ≥ 65 years of age. The early phase of AMD is characterized by drusen located under the retina pigment epithelium (RPE), and pigment alteration. Two clinically recognized subtypes of AMD are dry and wet AMD. The former represents the severe atrophy of photoreceptors and the underlying RPE and choriocapillaris. The latter accompanies choroidal neovascularization (CNV) in invading the subretinal and sub-RPE space. Patients with neovascular (wet) AMD have a mean age of 70.5 years, compared with 56.8 years for those with dry AMD. It was also found that incidence of disorder was not significantly different from the gender. (Janoria et al., 2007). Some reports showed that the prevalence of AMD in Asian populations was lower than that in Caucasian populations (Jager, Mieler, and Miller, 2008; Yuzawa et al., 1997). Based on the population of Thailand, there were 3% from 10,788 participants diagnosed as having AMD. The mean age was 62.1 (in range 50–98) years old. There were 2.7% and 0.3% participants with early AMD and late AMD, respectively. Of the late AMD, 74.1% were wet AMD and 25.9% were geographic atrophy (Jenchitr et al., 2011).

DR often leads to neovascularization and proliferative retinopathy as well as macular edema. DR is the third leading cause of blindness in the US and the leading cause of new blindness among the age group 20 to 74 years old. Macular edema involves swelling of the macula due to sub-retinal fluid buildup. Macular edema occurs in approximately 10% of diabetics. Focal macular edema is caused by foci of vascular abnormalities, primarily micro-aneurysms, which tend to leak fluid whereas diffuse macular edema is caused by dilated retinal capillaries. Non-proliferative diabetic retinopathy and proliferative diabetic retinopathy have incidences of 56% and 29%, respectively. The current standard of care for DR involves photocoagulation

and vitrectomy. These are only used in late stage disease and there is a need for earlier pharmacologic intervention. Antiangiogenics, steroids and neuroprotectants may all play a role in the treatment of DR (Hughes et al., 2005).

Vascular endothelial growth Factor (VEGF) seems to be a major contributory factor to vascular leakage and plays an important role in the pathophysiology of neovascular AMD and DR (Kompella et al., 2010). Currently, therapeutic approaches to treat these disorders are limited, although there is a significant interest and research initiative in discovering therapies to combat the progression of these disorders. During the last few years, therapeutic agents have been introduced into the market, to treat DR and AMD i.e. Ozurdex®, an injectable implant containing dexamethasone, an anti-inflammatory corticosteroid (Pacella et al., 2013), Pegatinib (Macugen®), an anti VEGF aptamer, and ranibizumab (Lucentis®) , an anti-VEGF antibody fragment were approved for treating the wet form of AMD in 2004 and 2005, respectively (Ozkiris, 2010). Thus, it is evident that anti-inflammatory agents and VEGF-inhibition are viable therapeutic options for treating DR and AMD (Kompella et al., (2010).

Celecoxib (CCB), a nonsteroidal anti-inflammatory drug (NSAID), is the first selective cyclooxygenase-2 (COX-2) inhibitor used in the treatment of osteoarthritis and rheumatoid arthritis in adult patients. It is also indicated in treatment of acute pain, primary dysmenorrhea, and as an adjuvant in the treatment of familial adenomatous polyposis, a genetic disorder (Davies et al., 2000). In addition, CCB has VEGF inhibitory effects as demonstrated in several anticancer studies using different cell types through the inhibition of COX-2 enzyme and demonstrated to have anti-angiogenic and anti-proliferative effects on several cell types including endothelial cells. Thus, the VEGF inhibitory and anti-proliferative effect activity of CCB could be beneficial in the treatment of the proliferative stages of DR and AMD (Amrite and Kompella, 2008; U. Kompella et al., 2010).

Ayalasomayajula and Kompella (2003) have shown that oral administration of CCB can reduce diabetes-induced retinal VEGF mRNA expression and vascular leakage by inhibiting the activity of COX-2 enzyme in a rat model. Nevertheless, the

required dose for these effective levels is very high (50 mg/kg twice a day) resulting in adverse effects and systemic toxicity including cardiovascular problems. Several studies have been performed to overcome the drawbacks of the systemic administration of CCB. The local administration approaches are alternative pathway delivering the drug reach to the posterior segment of the eye. Intravitreal injections can provide high dose of drug concentration to the retina. However, the bolus intravitreal injections can potentially cause retinal toxicity. Moreover, the repeated intravitreal injections have been associated with complications such as retinal detachment and also endophthalmitis. (Raghava, Hammond, and Kompella, 2004). The other route of administration is subconjunctical injection which has several advantages more than those of the intravitreal route. For instance, the drugs can be administered without directly interfere the vision via subconjunctival routes. In addition, the drug solutions/suspensions volumes can be administered as high as 500–5,000 µl in humans. Ayalasomayajula and Kompella (2004) demonstrated that the 1 mg/ml suspension of CCB injected through subconjunctival administration can be distributed to the retina and other ocular tissues including vitreous, sclera, cornea and lens. Moreover, the retinal availability of CCB following subconjunctival administration in the ipsilateral retina is 54-fold higher compared to intraperitoneal administration. There are several studies regarding to periocular injectable formulation. Amrite *et al*. (2006) demonstrated that CCB-poly(D,L-lactide-co-glycolide) (PLGA) microparticles through subconjunctival administration provided sustained drug level in the retina of rat model for 60 days. Cheruvu et al., (2009) prepared CCB in two injectable forms i.e., CCB suspension in 0.5% carboxymethylcellulose and CCB-loaded poly(L-lactide) (PLA) nanoparticles for trans-scleral drug delivery to the retina which aimed to rapid release and sustained release from both platforms. It can be distributed to vitreous humor and retina. Although these studies showed increased delivery of CCB to the posterior segment of the eye, they all required invasive delivery methods. Both intraocular and periocular routes have inherent risks for ocular infections and tissue damage (Lee et al., 2004). In addition, the invasive methods need ophthalmologist operation leading to high cost

of treatment and patient's inconvenient. Currently, there are no safe and patient-friendly drug delivery systems to the posterior segment. Thus, there is a need for development of non-invasive methods as alternative approaches for effective retinal drug delivery (Koevary, 2003; Kurz and Ciulla, 2002).

Conventional ophthalmic dosage forms for non-invasively topical drug delivery to the eye are aqueous solutions, suspensions and ointments. Aqueous solutions are the most common, however; aqueous drug solutions are rapidly removed from the eye surface and drained into the nasolacrimal duct (Urtti and Salminen, 1993). In case of suspensions, the vehicle containing drug particles is an additional factor influencing drug release rate and corneal penetration. However, the development of eye drops may have several limitations that cannot be delivered to the target site. After an eye-drop instillation, usually less than 5% of an applied dose reaches the intraocular tissues. The small amount of drug can penetrate through the cornea membrane because of drug elimination from the pre-corneal area (pre-cornea clearance) resulting in low ocular drug availability. (Loftssona and Jarvinen, 1999). Current trends in ocular therapeutics and novel drug delivery offer improved biopharmaceutical properties and have the capacity to deliver drugs more precisely to the target sites in the predictable manner.

CCB is a low molecular weight (381.38 Da) hydrophobic molecule with a log P 3.47 at pH 7.4. With a pK_a of 11.1, CCB is neutral at physiologic pH and is practically insoluble. The aqueous solubility of CCB is approximately 2 µg/ml (Ayalasomayajula et al., 2004; Ventura et al., 2005). Due to the poor aqueous solubility of CCB, it hampers the drug permeation resulting in inadequate drug levels to the posterior segment of eye. Thus, the CCB eye drop formulation development should focus on increasing the drug solubility in order to enhance the absorption of the drug into the site of action. There are several techniques used to enhance the drug solubilzation i.e., 1) pH adjustment 2) particle size reduction 3) inclusion complexes/complexation 4) co-solvency 5) miceller solubilization, etc. (Chaudhary, 2012). Using cyclodextrin (CD) as inclusion complex is an alternative approach to enhance the solubility of CCB.

CDs are cyclic oligosaccharides with a hydrophilic outer surface and a lipophilic central cavity comprised (α-1,4-)-linked α-D-glucopyranose units. The naturally shaped of CD molecules like cones with secondary hydroxy groups protruding from the wider edge and the primary groups from the narrow edge result in this conformation of CD molecules has a hydrophilic outer surface, whereas the lipophilicity of their central cavity. The natural CDs consist of six, seven and eight glucopyranose units are α-cyclodextrin (α-CD), β-cyclodextrin (β-CD) and γ-cyclodextrin (γ-CD), respectively. In addition, random substitution of the hydroxy groups such as methoxy functions brings about dramatic improvements in their solubility. CD derivatives of pharmaceutical interest include such as hydroxypropyl-β-cyclodextrin (HP-β-CD), hydroxypropyl-γ-cyclodextrin (HP-γ-CD), randomly methylated-β-cyclodextrin (RM-β-CD), sulfobutylether-β-cyclodextrin (SBE-β-CD). The CD has a molecular weight of about 1,000 - 2,000 Da with the negative Log P. Thus, they are poorly absorbed through biological membranes (Loftsson et al., 2005). The various lipophilic drugs can form complex with CD by inserting their moieties or the whole molecules into the cavity of CD in aqueous solutions resulting in increasing the solubility of lipophilic drugs. Reddy et al., (2004) conducted a study of β-CD complexes of CCB. Regarding to phase- solubility profile, the solubility of CCB can be improved by β-CD. Moreover, the result of this study indicated that the dissolution rate of CCB/β-CD complex in solid-state was significantly increased when compared to free CCB. Additionally, HP-β-CD, the β-CD derivative can enhance the dissolution rate of CCB (Sinha et al., 2011)

Recent studies have shown that the addition of polymer can significantly increase the CD solubilization and complexing abilities by ternary complex formation (Loftsson and Brewster, 1996). In this way, the synergistic effect of water-soluble polymer could decrease in CD amount required to prepare soluble drug/CD complexes (Miranda et al., 2011). Using heating method, autoclaving at 121°C for 20-40 minutes or sonication at a temperature of over 70°C for one hour could accelerate the ternary complexes (Loftsson, Hreinsdottir and Masson, 2005; Maragos et al., 2009). The Influence of hydrophilic polymers on CCB/HP-β-CD complexes as

ternary complex was investigated (Chowdary and Srinivas, 2006). It was concluded that polyvinylpyrrolidone (PVP), HPMC and polyethylene glycol (PEG) stabilized the binary complexes consequently to increase the CCB solubility. Besides CDs as solubilizer, they can act as a permeation enhancer by increasing permeability of drug through the lipophilic membrane. Tirucherai and Mitra (2003) studied the effects of HP-β-CD on the solubility and permeability of the acyl ester prodrugs of ganciclovir through the cornea of rabbit eyes. It was found that the permeability of drug increased 2.5 times compared to formulation without HP-β-CD. Since, CDs act as true carriers by keeping and dissolving the hydrophobic drug molecules in solution and delivering them through the mucin layer (aqueous layer) to the surface of the biological membrane similar to increasing drug concentration at the membrane surface lead to increasing permeability. (Loftssona et al., 1999). There was an example of *in-vivo* study using CD as topical eye drop delivering dexamethasone to the anterior and posterior segments of the rabbit eyes. The drug can be absorbed into the eye and distributed to eye tissues such as cornea sclera in large quantities after topical eye drop was applied. It was also found that it could reach to the back of the eye i.e., retina and vitreous, rather than to the intravenous injection (Sigurdsson et al., 2007).

Several researchers have studied the effect of mucoadhesive polymers on lowering drainage rate of instilled eye drop from pre-cornea area. For example, Saettone et al., (1989) studied mucoadhesive properties of polymer with mucin-coated surfaces model for ophthalmic drug delivery. The good to excellent mucoadhesive properties were found in formulation of tropicamide containing hyaluronic acid which is better than formulation containing polyacrylic acid. Similarly, Felt et al. (1999) have studied regarding precorneal retention in eye rabbits of tobramycin eye drop preparation. At least a 3-fold increasing of the corneal contact time was achieved in the presence of chitosan when compared to a commercially available pharmaceutical product (Tobrex®). It was concluded that the ophthalmic formulation containing mucoadhesive polymer helps to deliver the drugs reach to the site of action by inhibiting drug removal from the pre-corneal area.

Although, these studies showed the increasing retention time of eye drop formulation, the eye drop solution with mucoadhesive polymer are not enough residence time to maintain the drug adhered to the eye surface. Combination of the solid particles and mucoadhesive polymer in eye drop preparations is a promising alternative approach. Jansook et al, (2010) studied the permeation of dorzolamide microsuspension eye drops into the rabbit eyes and intraocular drug levels were determined. After eye drops were instilled, the drug level in the aqueous humor can be maintained more than 24 hours while the formulation of it in solution dosage form (Trusopt®) can be maintained in the aqueous humor for just 8 hours. From this study, the particles in suspension were trapped on the eye surface which increased the contact time leading to prolonged drug absorption. However, the size of the particle in formulation should not exceed 10 microns to prevent irritation of the eyes.

This present study was focused on developing new CCB eye drop formulation containing CD platform. They are expected to provide sustained release and mucoadhesive properties to improve ocular bioavailability which aimed to deliver to the posterior segment of the eye. The effect of CDs and mucoadhesive polymer on CCB solubilization was investigated, CCB eye drop formulations were developed, physicochemical properties were characterized and also the mucoadhesive properties and *in-vitro* permeation were evaluated.

Objectives of this study

1. To study the effect of CD and polymer on the CCB solubilization and to investigate the solid and solution CCB/CD complexes.
2. To develop and characterize the CCB eye drop solutions and suspensions containing CD.
3. To determine *in vitro* permeation through semi-permeable membrane and simulated vitreous humor, and mucoadhesive properties of CCB eye drop formulations containing CD.
4. To study the effect of heating process (sonication 70°C, 1 hr) on the dissolved CCB content and *in-vitro* permeation of CCB eye drop suspensions.

CHAPTER II
LITERATURE REVIEWS

1. Celecoxib

1.1 Mechanism of action

Celecoxib (CCB) is a potent cyclooxygenase-2 (COX-2) inhibitor which currently being used as an anti-inflammatory agent for the treatment of rheumatoid arthritis and osteoarthritis. It has been investigated for the treatment of various malignant and premalignant tumors, including colorectal, breast, lung, and prostate cancer (Amrite et al., 2006). In addition, it has been shown to have anti-proliferative effects in several cancer cell types and also in human umbilical vein endothelial cells (HUVEC) cells. This anti-proliferative potential of CCB can be used in the treatment of age-related macular degeneration (AMD), where there is proliferation of retinal endothelial cells and retinal pigment epithelial cells (Amrite et al., 2008)

There are several reported that CCB has been shown to have anti-vascular endothelial growth factor (VEGF) effects on the retinal cells (Amrite et al., 2006; Amrite et al., 2008; Ayalasomayajula et al., 2003) The treatment with CCB leading to a dose-dependent reduce the VEGF expression in the retinal pigment epithelium (RPE). The VEGF inhibition of CCB in the RPE cells was at 0.003-0.006 μM which is the same concentrations as the median IC_{50} of CCB for inhibition of the COX-2 enzyme. It is indicated that the anti-VEGF effect of CCB has potential value in treating diabetic retinopathy (DR) and AMD and other VEGF induced neovascular conditions of the eye (Kompella et al., 2010).

1.2 The physicochemical properties of celecoxib

The chemical name of CCB is (4-[5-(4-Methylphenyl) 3 (trifluoromethyl)-1H-pyrazol-1 -yl] benzenesulfonamide. It does not contain any chiral centers and thus it does not exhibit any optical isomers. Figure 1 showed the chemical structure of CCB.

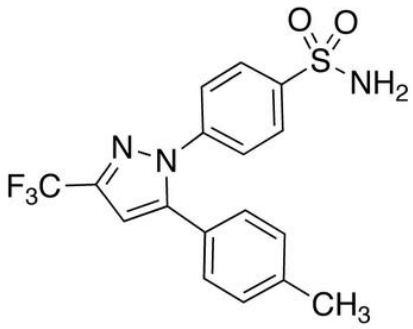

Figure 1 Chemical structure of celecoxib

CCB is an odorless, white to off-white crystalline powder. It is a low molecular weight (381.38 Da) and its melting point is 159 - 161°C. The amide hydrogen is weakly acidic (pKa is 11.1) leaving the molecule uncharged at physiological pH. It has a very poor aqueous solubility (2–7 mg/ml at 40°C, pH 7.0), and was shown to have dissolution rate-limited bioavailability. In addition, CCB is a highly permeable compound (log P is 3.47). Thus, it is categorized into Class II according to the Biopharmaceutical Classification System (BCS) (Ayalasomayajula et al., 2004; Choubey et al., 2013; Sinha et al., 2005).

1.3 The stability of CCB

The stability of CCB was investigated under stress test condition of dry heat, hydrolysis, oxidation and UV degradation. It was found that CCB had acidic and basic stability under condition of heating with aqueous 0.1N hydrochloric acid and 0.1N sodium hydroxide at 80°C for 24 hrs, respectively, and no degradation peak was observed. And also, CCB had photostability and thermal stability after exposed to UV light (254 nm) and heating at 105°C for 24 hrs, respectively. However, the degradation product of CCB was significantly found under condition of heated with 5 % w/v aqueous potassium permanganate solution at 80°C for 3 hrs. It was indicated that CCB had instability under oxidative condition (Srinivasulu et al., 2012).

2. The eye

2.1 The anatomy of eye

The anatomy of eye is shown in Figure 2. The eye can be divided into two sections, an anterior and a posterior segment. The anterior segment of the eye composes of cornea, conjunctiva, iris, lens, Pupil, ciliary muscle, anterior chambers and posterior chambers.

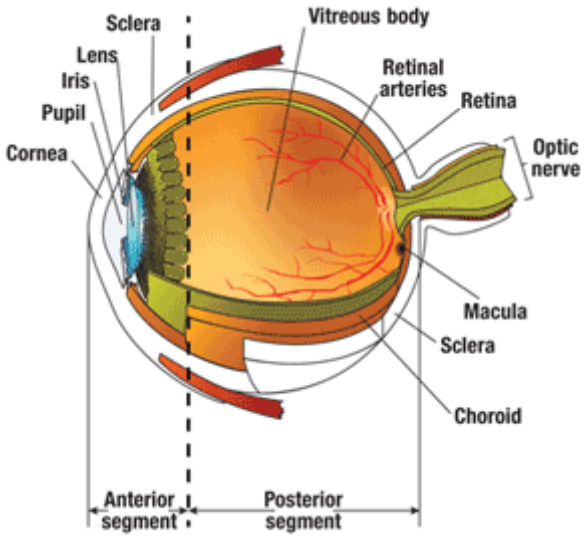

Figure 2 Anatomy of the eye
(https://www.uspharmacist.com/article/understanding-diabetic-retinopathy)

The posterior segment of eye, which is located behind the lens, comprises the optic nerve and the three layers of sclera, choroid and retina which cover the vitreous body. The center of the retina is called the macula. The macula contains a high concentration of photoreceptor cells which convert light into nerve signals (Dhanapal and Ratna, 2012).

2.2 Drug deliver to posterior segment of the eye

Figure 3 shows the several routes of administration for drug delivery to the posterior segment of the eye. Oral administration is a systemic approach and self-medication; however, it was limited accessibility to the targeted eye tissues. It is possible that the drugs are diffused to all tissues in the body including the retina and

optic nerve. Only a small quantity of drugs can penetrate the barriers of the eye requiring frequent administration of high doses such as penicillins, cephalosporins and aminoglycosides (Barza, 1978). The nonspecific absorption of systemically administered agents leads to unwanted side effects and potentially serious toxicities (Janoria et al., 2007).

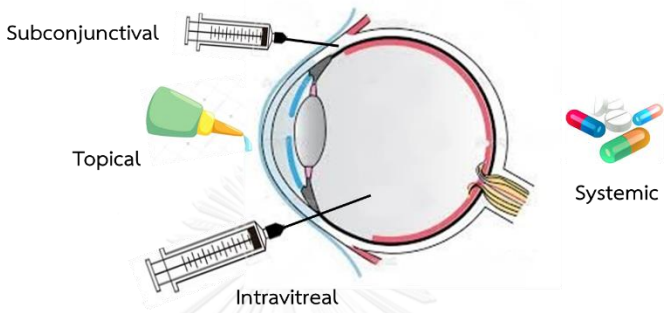

Figure 3 The several routes of administration for drug delivery to the posterior segment of the eye.

Currently, intravitreal injections are common administration. Although drug delivery through this route can achieve increased drug concentrations in the neural retina, the bolus intravitreal injections can potentially cause retinal toxicity. The repeated intravitreal injections have been associated with complications such as retinal detachment and also endophthalmitis (Raghava et al., 2004). The periocular route i.e., subconjunctival, subtenon, retrobulbar, and peribulbar administration is considered to be a localized and minimally invasive drug delivery technique to the posterior segment of eye. The drug applied by periocular injections can reach the posterior segment by three different pathways: trans-scleral pathway; systemic circulation through the choroid; and the anterior pathway through the tear film, cornea, aqueous humor, and the vitreous humor (Gaudana et al., 2010). Following a subconjunctival injection, drug delivery through periocular is located in close proximity to sclera and may directly diffuse through the sclera to reach choroid (Kim et al., 2002). As a result, vitreal drug level can be observed 20-30 min after administration (Janoria et al., 2007). Despite of delivering adequate drug levels to the

retina, they all required invasive delivery methods. Both intraocular and periocular routes have inherent risks for ocular infections and tissue damage (Lee et al., 2004). Topical administration, non-invasive method, is an alternative approach for delivering the drugs. Typically, this route is applied by topical eye drops, but they have only a short residence time on the eye surface. The duration of drug action, can be prolonged by formulation design (Dhanapal et al., 2012).

2.3 Topical eye drop drug delivery to the posterior segment of eye

The treatment of posterior segment diseases is more complicated and challenging. Besides the longer penetration distance, the path of a topically applied drug is obstructed by various eye tissues such as the corneal epithelium and endothelium, conjunctiva, sclera and vitreous humor. Primarily, the penetration of drugs into the cornea and conjunctiva is driven by the concentration gradient, lipophilicity and molecular weight of the drug. The epithelial layers of the cornea and conjunctiva act as rate-limiting barriers for drug absorption. Depending on the lipophilicity, the hydrophilic drugs enter the epithelial layers via the paracellular route, while lipophilic drugs through the transcellular pathway (Lach, Huang, and Schoenwald, 1983). After instillation of topical eye drop, aqueous eye drop solution and suspension will mix with the tear fluid and be dispersed over the eye surface. The ocular absorption was limited by several pre-corneal factors such as drug metabolism, normal tear turnover, induced lacrimation and nasolacrimal drainage resulting in the shorten residence time of applied drugs. Typically, less than 5% of applied dose reaches the intra ocular tissue (Loftssona et al., 1999). The absorption from topical delivery to the posterior segment of the eye has been described as occurring by two routes i.e., corneal and non-corneal (conjunctiva) pathways (Figure 4) (Hughes et al., 2005). Following corneal absorption, the drug enters the anterior chamber and distributes to surrounding ocular tissues such as the lens, iris-ciliary body, vitreous and posterior retina and also penetrate through the cornea diffuse laterally into the sclera and distribute among other intraocular tissues. According to non-corneal absorption, it can occur in three ways: 1) diffusion of the drug through

the conjunctiva, sclera, choroid and reaching the retina. 2) clearance of the drug by the conjunctival blood vessels into the systemic circulation and re-entering the eye from systemic circulation. 3) lateral diffusion of the drug from the conjunctiva into the cornea or iris/ciliary body, and hence into the anterior chamber and other intraocular tissues (Boddu, Gupta, and Patel, 2014).

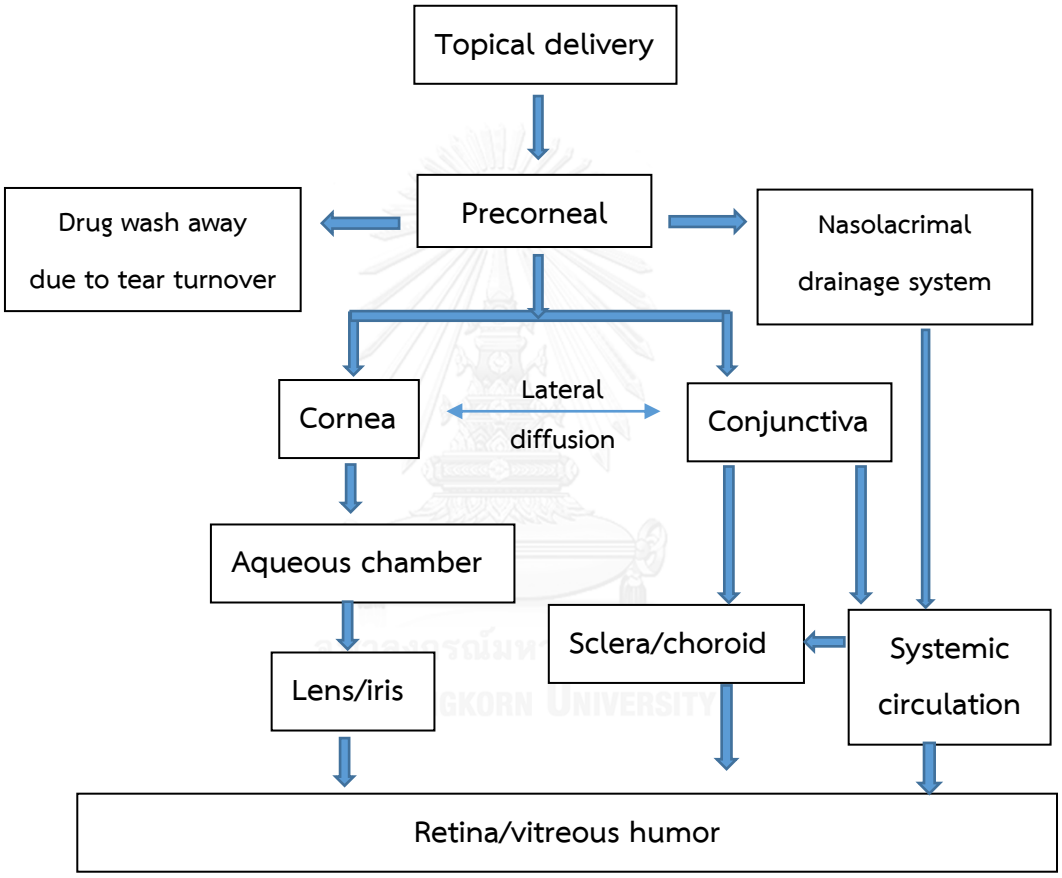

Figure 4 General ocular penetration pathways for topically applied drugs (modified from Boddu et al., (2014) and Hughes et al., (2005))

Although topical administration is an alternative and patient-friendly route, both the physiological barrier and biological membrane barrier are the limitation of the conventional topical eye drop delivering to the posterior segment of the eye. Several techniques can improve ocular bioavailability such as liposome (Al-Muhammed et al., 1996), niosome (Vyas et al., 1998), nanomicellar (Mitra, Velagaleti,

and Grau, 2010; Velagaleti et al., 2010) and nanoparticles (Kompella, Singh and Sundaram, 2009; Zimmer and Kreuter, 1995). Using Cyclodextrins (CDs) are also an alternative approach in topical ophthalmic formulations for increasing solubility and permeability of drugs (Loftsson, Hreinsdottir, and Stefansson, 2007; Sigurdsson et al., 2007).

3. Cyclodextrin

Cyclodextrins (CDs) are cyclic oligosaccharides with a hydrophilic outer surface and a lipophilic central cavity. They consist of (α-1,4-)-linked α-D-glucopyranose units (Figure 5). Due to the chair formation of the glucopyranose units, CD molecules are shaped like cones with secondary hydroxy groups extending from the wide edge and the primary groups from the narrow edge. This gives CD molecules a hydrophilic outer surface, whereas the lipophilicity of their central cavity is comparable to an aqueous ethanolic solution .The most common natural CDs consist of six (α-CD), seven (β-CD) and eight (γ-CD) glucopyranose units (Loftsson and Brewster, 2012).

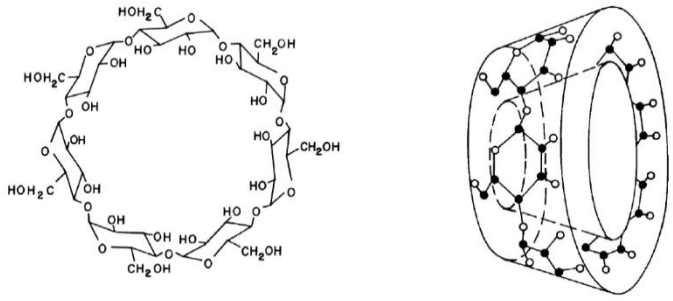

Figure 5 The chemical structure and the conical shape of the β-cyclodextrin molecule (Loftsson et al., 2005)

Although the natural CDs and their complexes are hydrophilic, their aqueous solubility is rather limited, especially that of β-CD. This is thought to be due to relatively strong binding of the CD molecules in the crystal state (i.e., relatively high crystal lattice energy). Random substitution of the hydroxy groups, even by hydrophobic moieties such as methoxy functions, will result in dramatic improvements in their solubility. The physicochemical properties of natural CDs and selected CD derivatives and their pharmaceutical applications are shown in Table 1.

Table 1 Some physicochemical properties and the pharmaceutical applications of natural CDs and selected CD derivatives (modified form Loftsson et al., 2005)

Cyclodextrin	Substitution[a]	MW (Da)	Solubility[b] (mg/ml)	Applications
α-Cyclodextrin	-	972	145	Oral, parenteral, topical
β-Cyclodextrin	-	1135	18.5	Oral, topical
2-Hydroxypropyl-β-cyclodextrin	0.65	1400	>600	Oral, parenteral, topical
Randomly methylated-β-cyclodextrin	1.8	1312	>500	Oral, topical
Sulfobutyl ether β-cyclodextrin sodium salt	0.9	2163	>500	Oral, parenteral, topical
γ-Cyclodextrin	-	1297	232	Oral, parenteral[c], topical
2-Hydroxypropyl-γ-cyclodextrin	0.6	1576	>500	Oral, parenteral, topical

[a] Average number of substituents per glucopyranose unit, [b] solubility in pure water at 25°C,
[c] in vary limited amounts.

The main reason for the solubility enhancement is that the random substitution transforms the crystalline CDs into amorphous mixtures of isomeric derivatives. CD derivatives of pharmaceutical interest include the hydroxypropyl derivatives of β- and γ-CD, the randomly methylated β-CD, sulfobutylether β-CD. CD molecules are relatively large (molecular weight ranging from almost 1000 to > 2000 Da) with a large number of hydrogen donors and acceptors, and are consequently poorly absorbed through biological membranes (Loftsson et al., 2005).

3.1 Drug/CD complex formation

In aqueous solutions, CDs are able to form inclusion complexes with various drugs by taking up a drug molecule or lipophilic moiety of the molecule into the central cavity (Loftsson et al., 2005). No covalent bonds are formed or broken during the complex formation, and drug molecules in the complex are in rapid equilibrium with free molecules in the solution. The driving forces for the complex formation include release of enthalpy-rich water molecules from the cavity, electrostatic interactions, Van der Waals' interactions, hydrophobic interactions, hydrogen bonding, the release of conformational strain and charge-transfer interactions (Loftsson and Brewster, 1996). The physicochemical properties of free drug

molecules are different from those bound to the CD molecules. The inclusion complex formation can be investigated by a number of physicochemical method. Phase solubility studies were used to determine the solubility of drug/CD complex in solution state.

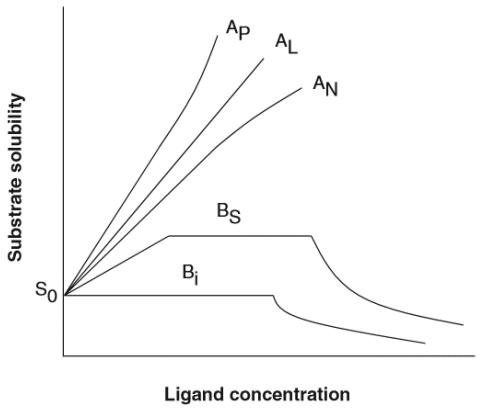

Figure 6 Phase-solubility profiles and classification of complexes (Loftsson et al., 2005)

The effect of CD as complexation on drug solubility was indicated by phase-solubility profiles that classified by Higuchi and Connors (1965) in Figure 6. A-type phase solubility profiles are acquired from the increasing substrate (drug) solubility with increasing ligand (CD) concentration. A_L-type phase solubility profiles are obtained when the complex is first order with respect to ligand and first or higher order with respect to substrate (Cappello et al., 2007; Nagarsenker and Joshi, 2005). In case of A_P-type phase solubility profiles, the complex is first order with respect to the substrate, but second or higher order with respect to the ligand (Patel and Patel, 2012; Rajesh and Bhanudas, 2010). A_N-type phase solubility profiles can be difficult to interpret. B-type phase solubility profiles indicate formation of complexes with limited solubility in the aqueous complexation medium (Shen et al., 2012). In general, the water-soluble CD derivatives form A-type phase solubility profiles, whereas the less soluble natural CDs frequently form B-type profiles (Loftsson et al., 2005).

The phase solubility profiles do not verify formation of inclusion complexes but they only describe how the increasing CD concentration influences drug

solubility. The most common type of CD complex is the 1:1 drug/CD complex (D/CD) in which one drug molecule (D) forms a complex with one CD molecule (CD):

$$D + CD \overset{K_{1:1}}{\leftrightarrow} D/CD$$

Under such conditions an A_L-type phase solubility diagram, with slope less than unity, would be observed, and the stability constant ($K_{1:1}$) of the complex can be calculated from the slope and the intrinsic solubility (S_0) of the drug in the aqueous complexation media i.e., drug solubility when no CD is present.

$$K_{1:1} = \frac{\text{Slope}}{S_o(1 - \text{Slope})}$$

For 1:1 drug/CD complexes, the complexation efficiency (CE) can be calculated from the slope of the phase solubility profiles:

$$CE = S_o . K_{1:1} = \frac{\text{Slope}}{1 - \text{Slope}}$$

When selecting CD or complexation conditions during formulation development, it can frequently be more convenient to compare the CE than $K_{1:1}$ values. The most common stoichiometry of higher order drug/CD complexes is the 1:2 drug/CD complex resulting in A_P-type phase solubility diagram. Consecutive complexation is assumed where the 1:2 complex is formed when one additional CD molecule forms a complex with an existing 1:1 complex:

$$D/CD + CD \overset{K_{1:2}}{\leftrightarrow} D/CD_2$$

The stoichiometry of the system can be proved by curve fitting of the diagram with a quadratic model:

$$[S_t] - [S_o] = K_{1:1}[S_o][CD] + K_{1:1}K_{1:2}[S_o][CD]^2$$

Here [CD] represents the concentration of free CD, but it is customary to plot the total amount of dissolved drug (S_t) against the total amount of CD in solution ($[CD]_t$), assuming that the extent of complexation is low (i.e., [CD] ~ $[CD]_t$). The value of $K_{1:2}$ is frequently between 10 and 500 M^{-1}, or significantly lower than that of $K_{1:1}$ (Loftsson et al., 2005).

The other techniques that used to characterize drug/CD complex in solution i.e., UV/VIS absorbance (Keipert et al., 1996), fluorescence spectroscopy (Schuette and Warner, 1994), pH-potentiometric titration (Yousef, Zughul, and Badwan, 2007), the chemical shifts of nuclear magnetic resonance (NMR) (Mura, 2014; Sinha et al., 2005) and effects on drug permeability through semipermeable membranes (Loftsson Másson, and Sigurdsson, 2002).

For the complex in solid state, several methods have been used to characterize drug/CD inclusion complex. The most often used methods are differential scanning calorimetry, powder X-ray diffraction and fourier-transform infra-red spectroscopy (Mura, 2015).

3.2 Preparation of drug/CD complexation

Various methods can be applied to prepare drug/CD complexes, including the solution method, the co-precipitation method, neutralization method, the slurry method, the kneading method and the grinding method (Hedges, 1998). In most cases, the presence of at least some water is essential for successful complex formation. In solution, CD complexes are usually prepared by the addition of excess amount of drug to an aqueous CD solution. The suspension formed is equilibrated at the desired temperature and then filtered or centrifuged to obtain clear drug/CD complex solution. For preparation of solid complexes, the water is removed from the

aqueous drug/CD solution by evaporation (e.g., spray drying) or sublimation (e.g., lyophilization) (Sinha et al., 2005; Ventura et al., 2005).

Several techniques have been used in an effort to enhance CD complexation of drugs. These include addition of auxiliary substances such as polymer to the complexation media (Medarevic et al., 2015; Mura, Faucci, and Bettinetti, 2001), drug ionization and salt formation, addition of hydroxyl carboxylic acids, volatile acids or bases to the complexation media, the present of organic salts, and co-solvents in drug/CD complex solutions, etc. (Loftsson et al., 2005).

3.3 Formation of ternary complexes

The ternary complexes formation obtained from three components in the system. For instance, a water-soluble polymer, a CD and a drug are mixed together in a solution. it is possible to increase drug solubilization, when compared to the polymer and CD separately, which is a result of the synergistic effect between these components (Loftsson et al., 1994). Formulations containing drug/CD complexes with the addition of a water-soluble polymer have proven to be capable of increasing the bioavailability of formulations while reducing the amount of CD by up to 80% (Mura et al., 2001). The interaction of water-soluble polymers with drug molecules may occur by means of ion-ion, ion-dipole, dipole-dipole electrostatic bonds and Van der Waals force (Ribeiro, Ferreira, and Veiga, 2003). Likewise, the interaction between polymers and CDs and drug/CD complexes begins to occur on the external surface of the CD molecule. CDs, polymers and drug/CD complexes form aggregates capable of solubilizing drugs and other hydrophobic molecules (Loftsson et al., 2007). In aqueous solutions, polymers stabilize micelles and other types of aggregates, reduce CD mobility and increase the solubility of complexes by changing the hydration properties of CD molecules (Loftsson et al., 2005).

This process can be accelerated by heating the ternary system. Thus, it is possible to activate the bonds between system components during the preparation of complexes by heating method i.e., heating by autoclave (120 to 140°C) for 20 - 40 minutes and heating by ultrasound bath (over 30°C) for 1-2 hour (Loftsson et al.,

2005). Studies have proven that HPMC, PVP and PEG6000 can increase the complexation efficiency of felodipine when present β-CD as ternary complex. This study performed to accelerate by sonicating for 1 hr in ultrasonic bath and heated for 2 hrs in oven at 90°C (Shankar Kuchekar and Narkhede, 2007). The other investigators studied the effects of PVP and HPMC on vinpocetine complexation with β-CD and its sulfobutyl ether derivative in solution and solid state. The ternary complexes were prepared by sonicated for 15 min and then heated in an autoclave at 120°C for 20 min. it showed the benefit on the addition of water-soluble polymers to promote higher complexation efficiency (Ribeiro et al., 2003). The most commonly used polymers for this purpose may be classified as natural, semi-synthetic and synthetic (Miranda et al., 2011) as detailed in Table 2.

Table 2 The most commonly used polymers as ternary complex (modified from Miranda et al. (2011))

Nature of polymers	Polymer
Natural	Pectin
	Mucin
	Agar
	Alginic acid
	Carrageenin
	Casein
	Gelatin
Semi-synthetic	Methyl cellulose (MC)
	Hydroxyethyl cellulose (HEC)
	Hydroxypropyl cellulose (HPC)
	Hydroxyethyl methyl cellulose (HEMC)
	Carboxymethyl cellulose (CMC)
Synthetic	Povidone (PVP)
	Polyethylene glycol (PEG)
	Polyvinyl alcohol (PVA)

4. Cyclodextrins in ocular drug delivery

In general, the ocular bioavailability of topically applied drugs is very low, frequently less than 5%. The main ocular barrier to drug permeability into the eye consists of lipophilic membranes (i.e., cornea, conjunctiva and sclera) but the membrane exterior consists of aqueous tear fluid and a hydrophilic mucin layer (aqueous layer barrier) at the membrane surface (Figure 7).

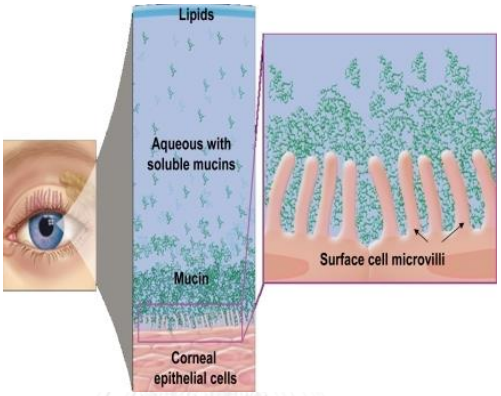

Figure 7 The membrane exterior consist of aqueous tear fluid and a hydrophilic mucin layer (aqueous layer barrier) at the membrane surface of the eye (https://openi.nlm.nih.gov/detailedresult.php?img=PMC2720680_opth-3-405f2&req=4)

The drug molecule must be somewhat hydrophilic (i.e. water-soluble) to be able to permeate through this aqueous exterior of the eye surface while the molecule must be somewhat hydrophobic (i.e. lipid-soluble) to be able to penetrate the ocular barrier membrane into the eye (Loftssona et al., 1999). The CD molecules are relatively large (molecular weight ranging from almost 1000 to > 2000 Da) with a large number of hydrogen donors and acceptors, and are consequently poorly absorbed through biological membranes (Loftsson et al., 2005). However, CDs act as true carriers by keeping the hydrophobic drug molecules in solution and delivering them through the aqueous mucin layer to the surface of absorption e.g. the cornea and the conjunctiva membrane (Figure 8).

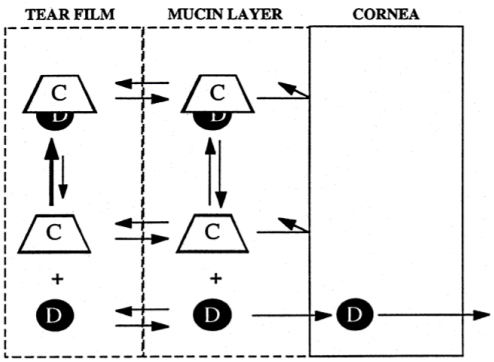

Figure 8 The proposed mechanism of drug penetration from aqueous CD containing eye drop solution in to the eye; C: CD; D: drug. (Loftssona et al., 1999)

According to this model the delivery of drug through the aqueous mucin layer is diffusion controlled but drug delivery through the corneal membrane is membrane controlled (Loftssona et al., 1999). In case of topical eye drop preparations, the eye drop solution composed of drug/CD complexes is limited research for retinal delivery. Sigurdsson et al. (2007) studied the topical and systemic absorption of dexamethasone eye drop solution containing RM-β-CD in rabbit eyes. The authors concluded that the absorption after topical administration dominates in the anterior segment. The topical absorption was an important role in delivering dexamethasone to posterior segment of the rabbit eye. Approximately 60% of the dexamethasone concentration reaches to the vitreous and retina resulted from topical administration.

The previous study showed the benefits of eye drop suspensions are better than eye drop solutions. Since, the particles in suspension increased significantly the contact time of the drug on the aqueous eye surface cause to increase ocular bioavailability. Another studied the dexamethasone/γ-CD eye drop suspension delivering to the retina in rabbits. After topical administration of the aqueous eye drop suspension, the dexamethasone/γ-CD particles were existed on the eye surface where they were rather slowly dissolved. The relatively high dexamethasone concentrations were acquired from the posterior segment of the eye but low concentrations in the blood after the eye drop suspension administration. This indicated that dexamethasone/γ-CD eye drop suspension is more site specific with

regard to posterior segment of eye than conventional eye drop solutions (Loftsson, Hreinsdottir, and Stefansson, 2007).

5. Mucoadhesive polymer for ophthalmic drug delivery

According to the physicochemical properties and structure of the tear film, various factors will influence the mucoadhesion of ocular delivery systems. Various theories (electronic, mechanical, adsorption, wetting, diffusion and cohesive) were proposed to explain bioadhesion or mucoadhesion (Saraswathi, Balaji, and Umashankar, 2013). The attachment of mucin to the epithelial surface may be considered as an interaction of a number of charged and neutral polymer groups with the mucin through non-covalent bonds (Thomas et al., 2003). In order to be a good mucoadhesive adjuvant, the polymer of the drug delivery system must make closely contact with the mucus layer. The polymer chains must be mobile and flexible enough to inter-diffuse into the mucus and penetrate to a sufficient depth in order to create a strong entangled network. They should interact with mucins by hydrogen bonding, electrostatic and hydrophobic interactions. These interactions depend on the ionic strength and pH of the vehicle, because changes in ionization of functional groups or shielding of charges influence electrostatic repulsion and expansion of the mucus network (Ludwig, 2005).

Hui and Robinson (1984) displayed the advantage of mucoadhesive polymers in enhancing the ocular bioavailability of progesterone. Saettone et al. (1989) demonstrated a series of bioadhesive vehicles for ocular delivery of pilocarpine and tropicamide. They found that hyaluronic acid was the most promising mucoadhesive polymer. The *in-vivo* pre-corneal residence time of the complex formation consisting of a ternary system of cationic drug (tetrazoline HCl), anionic polymer (hyaluronan) and gelatin to eye rabbit was investigated. These system showed ocular bioavailability improvement as well as were able to maintain levels of tetrazoline HCl detectable until 20 min while the drug solution was not detectable since 3 min after instillation (Sandri et al., 2006).

The most commonly used for mucoadhesive polymers are macromolecular hydrocolloids with numerous hydrophilic functional groups capable of forming hydrogen bonds (such as carboxyl, hydroxyl, amide, and sulfate groups). Table 3 showed a better mucoadhesive capacity of charged polymers both anionic and cationic in comparison to non-ionic cellulose-ethers or polyvinyl alcohol (PVA).

Table 3 Mucoadhesive polymer screened for ocular mucoadhesion (modified form Ludwig, 2005)

Polymer	Charge	Mucoadhesive capacity
Poly(acrylic acid) (neutralized)	A	+++
Carbomer (neutralized)	A	+++
Hyaluronan	A	+++
Chitosan	C	++
Na carboxymethylcellulose	A	++(+)
Poly(galacturonic acid)	A	++
Na alginate	A	++
Pectin	A	++(+)
Xanthan gum	A	++(+)
Xyloglucan gum	A	+
Scleroglucan	A	+
Poloxamer	NI	+(+)
Hydroxypropylmethylcellulose	NI	+
Methylcellulose	NI	+
Poly(vinyl alcohol)	NI	+
Poly(vinyl pyrrolidone)	NI	+

Charge: A: anionic; C: cationic; NI: non-ionic. Mucoadhesive capacity: +++: excellent; ++: good; +: poor/absent.

6. *In-vitro* permeation of drug CD complexation

Most biological membrane barriers are lipophilic membrane with an aqueous exterior, which forms a structured water layer at the membrane surface frequently referred to as unstirred diffusion layer. If drug permeation through the aqueous diffusion layer is the rate-limiting step, CDs can frequently enhance the permeation. However, CDs are in most cases unable to enhance drug permeation through a lipophilic membrane barrier. The excess cyclodextrin (more than is needed to dissolve the drug) was possible to obstruct drug permeation through the membrane (Loftsson et al., 2005; Masson et al., 1999). The chemical structure of CDs (i.e., the large number of hydrogen donors and acceptors), their MW (i.e., > 970 Da) and their very low octanol/water partition coefficient (approximately log Po/w between -3 and 0.00) are all characteristics of compounds that do not readily permeate biological membranes (Lipinski et al., 2001). Only the free form of the drug, which is in equilibrium with the drug/CD complex, is capable of permeation lipophilic membranes (Uekama, Hirayama, and Irie, 1998).

The investigation of fluxes value through semipermeable membranes have been used to evaluate release of drugs from CD containing vehicles (Másson et al., 1999). The permeation of drug molecules from aqueous CD formulation through semi-permeable membranes follows the same pattern as permeation across lipophilic biological membranes. However, this flux pattern is obtained for semipermeable membranes with MW cut-off (MWCO) well above the MW of CD. Therefore, both of CD molecules and their complexes are able to permeate the semipermeable membranes similar to permeate through an aqueous diffusion barrier at the surface of a biological membrane (Loftsson et al., 2002).

Regarding to the drug transportation into the posterior segment of the eye, the general pathway is the passive diffusion of the drug through cornea and conjunctiva absorption. The drug enters the biological membrane in to the anterior and diffuses to ocular tissue such as iris-ciliary body, vitreous humor and posterior retina. Xu et al. (2000) studied the permeability and diffusion of acid orange 8 as a model agent by developing simulated bovine vitreous humor model. Because the vitreous humor is

the clear, avascular, relatively stagnant and large component, it is an attractive site for controlled-release delivery of therapeutic drugs to treat vitreo-retinal diseases. This experiment concluded that it can predict the transport mechanism of drug within the vitreous humor.

CHARPTER III

MATERIALS AND METHODS

Materials

The following materials were used as received;

- Celecoxib (CCB) was generously donated by Unison Laboratories Co., Ltd.,Thailand)
- α-cyclodextrin (Wacker Chemie, AG, Germany)
- β-cyclodextrin (Wacker Chemie, AG, Germany)
- γ-cyclodextrin (Wacker Chemie, AG, Germany)
- Hydroxypropyl β-cyclodextrin (Wacker Chemie, AG, Germany)
- Randomly methylated β-cyclodextrin (RM-β-CD) (Wacker Chemie, AG, Germany)
- Chitosan (Fluka Fine Chemical, Japan)
- Hyaluronic acid (Soliance, France)
- Hydroxypropyl methylcellulose 4000 (Dow Chemical Company, USA)
- Acetonitrile HPLC grade (Burdick & Jackson, Korea)
- Benzalkonium chloride (Sigma-Aldrich, USA)
- Ethylenediaminetetraacetic acid disodium salt (Ajax Finechem Pty LTD, Ajax Finechem Pty LTD)
- Mucin from porcine stomach type II (Sigma-Aldrich, USA)
- Agar (Perl mermaid, Thailand)
- Sodium chloride (Ajax Finechem Pty LTD, Australia)
- Sodium hydroxide (Merck, Germany)
- Sodium carbonate (Merck, Germany)
- Calcium chloride (Merck, Germany)
- Disodium hydrogen phosphate (Sigma-Aldrich, USA)
- Sodium dihydrogen phosphate (Merck, Germany)
- Dialysis Membrane (Spectra/Por, Dialysis Membrane Standard RC Tubing, Canada)

Equipments

- Analytical balance (MettlerToledo AG285, Germany)
- High speed refrigerator micro centrifuge (TOMY, MX-305, Japan)
- High performance liquid chromatography (HPLC) instrument equipped with the following
    - Liquid chromatograph pump (LC-20AB binary pump, Shimadzu, Japan)
    - UV-VIS detector a SPD-20A, Shimadzu, Japan)
    - Auto sampler (SIL-20ATH, Shimadzu, Japan)
    - C18 column (Shiseido, 5μm, 150x4.6 mm ID reverse-phase column)
- Optical Microscope (Nikon eclipse E200, Japan)
- pH meter (MettlerToledo, sevenCompact, Germany)
- Scanning Electron Microscope (SEM JEOL, JSM-6610LV, USA).
- Shaker Incubator (DLabTech, LSI-4018A, India)
- Transmission Electron Microscope (TEM JEOL, JEM-2100F, USA)
- Ultrasonic bath (GT sonic, China)
- Viscometer (Brookfield, LVDV-II+, USA).
- Powder X-ray Diffractometer (Rigaku, model MiniFlex II, Japan)
- Fourier transform infrared spectroscopy (Thermo Scientific, model Nicolet iS10, USA)
- Proton nuclear magnetic resonance spectroscopy (^{1}H-NMR, BRUKER, model AVANCE III HD, USA)
- Differential scanning calorimetry (MettlerToledo, model DSC822^{e}STAR System, Germany)
- Freeze dryer (Dura-Dry MP, Canada)
- Orbital shaker (Stuart Scientific, Mini Orbital Shaker SO5, UK)
- Mixer media mill (RETSCH, MM400, Germany)
- Osmometer (Gonotec, OSMOMAT 3000 basic, Germany)
- Nanosizer (Zetasizer, Nano-ZS with software version 7.11, Malvern, UK)
- Autoclave (Hirayama, HICLAVE HVE-50, Japan)

Methods

1. Thermal stability of CCB on cycles of autoclaving

The stability of the CCB in the aqueous solution containing 0.5% w/v β-CD was determined by heating method (Loftsson et al., 2005). Excess amount of CCB was dissolved in purified water and equilibrated at 30°C ± 1°C for 24 hrs under constant agitation. The supernatant was filtered through 0.45 µm nylon filter and mixed with 1% w/v β-CD solution at 1:1 ratio. The solution was then divided into three sealed vials that were heated in an autoclave for one, two, and three heating cycles, each cycle consisted of heating to 121°C for 20 min. The drug concentrations in the vials were then determined by a high-performance liquid chromatographic method (HPLC).

2. Quantitative analysis of CCB

Calibration curve of CCB

A stock solution was prepared by accurately weighing CCB reference standard (10.0 mg) into 100-ml volumetric flask. Then, it was dissolved and diluted to volume with mixture of acetonitrile:water (55:45 v/v) to a final concentration of 100 µg/ml. This solution was further diluted to give a range of CCB 0.05-16 µg/ml. Each solution was subjected to HPLC analysis in triplicate. Peak area was recorded for all the solutions and the equation was calculated from the relationship between peak area of CCB and their concentrations.

The sample preparation

The filtrate of sample was further diluted with mixture of acetonitrile:water (55:45) with appropriate dilution. A portion of the sample was filtered through 0.45 µm nylon filter membrane and subjected to HPLC analysis. The CCB content in the sample was then calculated against the CCB calibration curve.

HPLC conditions

The quantitative determination of CCB was performed on a reversed-phase HPLC component system from Shimadzu™ consisting of a LC-20AB binary pump, a SPD-20A multiple wavelength detectors, a SIL-20ATH auto sampler and LCsolution software. The modified HPLC condition (Ventura et al., 2005) was described as follows:

Mobile phase	: Acetonitrile:water (55:45% v/v)
Chromatographic column	: Shiseido™ C18 column, 5 µm, 4.6x150 mm ID with C18 guard cartridge column MGII 5µm, 4x10 mm.
Flow rate	: 1.0 ml/min
Oven temperature	: Ambient temperature
UV detector wavelength	: 252 nm
Injection volume	: 20 µl
Run time	: 15 minutes

3. Validation for the quantitative analysis of CCB

Specificity

The specificity of the analyze method investigated by injecting of CCB and all components i.e., α-CD, β-CD, γ-CD, HP-β-CD, RM-β-CD, chitosan (CS), hyaluronic acid (HA), hydroxypropylmethylcellulose (HPMC), phosphate buffer saline (PBS) pH 7.4, EDTA, Benzalkonium chloride (BAC), and mobile phase to demonstrate the absence of interference with the elution of analyze. The all components were properly diluted before determining by HPLC.

Linearity

Linearity was determined with various amounts of properly diluted stock standard solutions in the range of 0.05-16.0 µg/ml of CCB. For each concentration three measurements were performed and the calibration curves were obtained by plotting the peak area versus nominal concentration expressed in µg/ml of CCB. The

slope, intercept and coefficient of determination (R^2) of each calibration curve were evaluated.

Precision

Within run precision

The within run precision was determined by analyzing five sets of three standard solutions of CCB in the same day. The coefficients of variation of the peak area responses (%CV) for each concentration were determined.

Between run precision

The between run precision was determined by comparing each concentration of CCB standard solution which prepared and injected on different days. The percentage coefficient of variation (%CV) CCB of peak area responses from three standard solution on different days was calculated.

Accuracy

The recovery of CCB from blank formulation were assessed by spiking blank formulation (all components except the drug) with CCB in triplicate at three level spanning 80-120% of amount of CCB in the formulation. The average recovery and the coefficient of variation (%CV) were calculated.

4. Phase solubility studies

4.1 The effect of CD on CCB solubility

Excess amount of CCB was added to a solution containing 0 to 15% (w/v) CD (α-CD, β-CD, γ-CD, HP-β-CD and RM-β-CD) in pure water. The drug suspensions were saturated through heating in an autoclave 121°C for 20 min and allowed to cool to room temperature (Loftsson et al., 2005). Then a small amount of solid drug was added to the suspensions to promote drug precipitation. The suspensions were equilibrated at 30°C ± 1°C for 7 days under constant agitation. After equilibrium was attained, the suspensions were filtered through 0.45 μm syringe filter, the filtrates were diluted with the mobile phase and analyzed by HPLC as described in section 2.

Each sample was done in triplicate. The apparent stability constants for CCB/CD complexes ($K_{1:1}$ and/or $K_{1:2}$) and the complexation efficiency (CE) were determined according to the phase-solubility method of Higuchi and Connors (Higuchi & Connors, 1965)

$$CE = S_o . K_{1:1} = \frac{Slope}{1 - Slope} \quad \textbf{Eq. 1}$$

$$[S_t] - [S_o] = K_{1:1}[S_o][CD] + K_{1:1}K_{1:2}[S_o] \quad \textbf{Eq. 2}$$

Where S_0 is intrinsic solubility of CCB, S_t is the concentration of CCB at CD concentration [CD].

4.2 The effect of polymer on solubility of CCB/CD complexes

The phase solubility of CCB was determined in pure aqueous γ-CD and RM-β-CD solutions containing various water-soluble polymers. HPMC (0.1%), HA (0.01%) or CS (0.1%) (all %w/v) were selected as non-ionic, negatively and positively charged polymer, respectively. The polymer was dissolved in the aqueous solutions containing 0-10% w/v CD. Then the excess of CCB was added to form drug suspensions and then heated in an autoclave 121℃ for 20 min. The phase-solubility was determined as described above. $K_{1:1}$, $K_{1:2}$ and CE were calculated.

5. Morphology and aggregates particle size analysis

The morphology and the particle size and size distribution of the aggregated in CCB saturated 10%w/v γ-CD and 7.5% RM-β-CD with polymer (0.01 %w/v HA and 0.1%w/v HPMC) mixture thereof were analyzed using transmission electron microscope and dynamic light scattering.

5.1 Dynamic light scattering (DLS) measurement

The particle size of CCB/CD based aggregates in solution was measured by DLS technique (Zetasizer™ Nano-ZS with software version 7.11, Malvern, UK). The

samples were properly diluted with purified water. A sample was put in a quartz glass cuvette and placed in the instrument. Measurements were carried out at 25°C, 180 degrees scattering angle. Particle size and size distribution was automatically calculated and analyzed by the curve plotted between size distribution and percentage intensity. Each obtained value was carried out in triplicate.

5.2 Transmission electron microscope (TEM) analysis

The morphology of CCB/CD based aggregates was evaluated by TEM (JEOL, JEM-2100F, USA). Initially, the sample was placed on a formvar-coated grids to permit the adsorption. After blotting the grid with a filter paper, the grid was transferred onto the drop of negative straining. Aqueous phosphotungstic acid solution (2%) was used as a negative strain. The sample was air dried under room temperature. Finally, the samples were examined with TEM.

6. Preparation and characterization of binary CCB/CD complexes and ternary CCB/CD/polymer complexes

6.1 Solid-state characterization

6.1.1 Sample preparations

1:1 molar ratio (m:n; D_mCD_n where m and n represents the total moles of drug and CD, respectively) of CCB and CDs (γ-CD and RM-β-CD) with polymer (0.01%w/v HA and 0.1 %w/v HPMC) mixture thereof were prepared by freeze drying method. The obtained Freeze dried mixture were performed through heating in an autoclave 121°C for 20 min and equilibrated at 30°C ± 1°C for 7 days under constant agitation. The filtrated solutions were frozen and then freeze-dried at -52°C for 48 hrs using a Freeze-dryer (Dura-Dry MP, Canada), yielding a solid complex powder (FD). Identical physical mixtures (PM) were prepared by careful blending CCB and CDs in a mortar with pestle. The samples were characterized in solid state as follows: pure CCB, γ-CD, RM-β-CD, PM and FD of CCB/CD (CCB/γ-CD and CCB/RM-β-CD), and FD ternary complexes i.e., CCB/γ-CD/HA, CCB/γ-CD/HPMC, CCB RM-β-CD/HA, CCB/RM-β-CD/HPMC.

6.1.2 Differential scanning calorimetry (DSC)

DSC thermograms were determined in a scanning calorimeter (Mettler Toledo™, DSC822 STAR System, Germany). The samples (3-5 mg) were heated (10°C/min) in sealed aluminium pans under nitrogen. The temperature range was from 30-250°C. An empty aluminium pan was used as reference.

6.1.3 Powder X-ray diffraction (PXRD) studies

The PXRD patterns were recorded using Powder X-ray diffractometer (Rigaku™ model MiniFlex II, Japan) and operated at a voltage of 30 kV and a current of 15 mA. The samples were analyzed as the 2θ angle range of 3° to 40° and process parameters were set as follows: step size of 0.020° (2θ), and scan speed of 2° per minute.

6.1.4 Fourier transform infra-red (FT-IR) spectroscopy

The FTIR spectra of samples were measured on FT-IR spectrometer (Thermo Scientific™ model Nicolet iS10, USA) using Attenuated Total Reflectance (ATR) technique. The data was obtained in the range of 400-4500 cm^{-1} for each sample. Analyses were performed at room temperature.

6.2 Solution state characterization

6.2.1 Sample preparations

The pure compound of CCB, γ-CD, RM-β-CD and their complexes of CCB and CD i.e., CCB/γ-CD and CCB/RM-β-CD, which were prepared by freeze drying method as described in section 6.1.1, were characterized in solution state. The samples were prepared by dissolving in CD_3OD:D_2O (50:50 v/v) in a capillary tube and then carried out by proton nuclear resonance spectroscopy measurements.

6.2.2 Proton nuclear magnetic resonance (^{1}H-NMR) spectroscopy

^{1}H-NMR spectroscopy measurements was using a 500 MHz ^{1}H-NMR spectrometer (BRUKER™ model AVANCE III HD, USA). The spectrum and chemical shift values were recorded. The resonance at 4.6500 ppm due to residual solvent (OD) was used as reference (Ventura et al., 2005).

7. Formulation of celecoxib ophthalmic preparation

7.1 Celecoxib ophthalmic solution

Celecoxib ophthalmic solution was prepared by dissolved 0.1% w/v of CCB in aqueous 7.5% w/v RM-β-CD solution. EDTA, BAC and polymer were then added and mixed. The composition of CCB eye drop solutions was given in Table 4. The obtained CCB solution was adjusted pH to 7.4 with sodium hydroxide and adjusted isotonicity with sodium chloride before adjusting to the desired volume with purified water. After that, all formulations were passed through heating process in an autoclave 121°C for 20 min and allowed to cool to room temperature.

Table 4 Composition of CCB eye drop solutions

Ingredient [a]	Formulation (gm) [b]					
	F1	F2	F3	F4	F5	F6
Celecoxib	0.1	0.1	0.1	0.1	0.1	0.1
RM-β-CD	7.5	7.5	7.5	7.5	7.5	7.5
HPMC	-	-	-	0.1	0.25	0.5
HA	0.1	0.25	0.5	-	-	-
EDTA	0.1	0.1	0.1	0.1	0.1	0.1
BAC	0.02	0.02	0.02	0.02	0.02	0.02
Purified water qs. to 100 ml						

[a] RM-β-CD; randomly methylated -β-cyclodextrin, HPMC; Hydroxypropyl methylcellulose, HA; Hyaluronic acid, EDTA; Ethylenediaminetetraacetic acid disodium salt, BAC; Benzalkonium chloride

[b] All formulation was adjusted pH to 7.4 with 1N sodium hydroxide solution and was adjusted with sodium chloride to obtain isotonicity.

7.2 Celecoxib ophthalmic suspension (binary complex)

Celecoxib ophthalmic suspension was prepared by suspending 0.5% w/v of CCB in the aqueous CD solutions. EDTA and BAC were added into the obtained suspension and mixed. The compositions of each formulation are shown in Table 5. The particle size reduction of each sample was performed by mixer mill (RETSCH® MM400, Germany) with 1-mm zirconium bead as media mill, the vibration was set at 25 Hz and was operated for 30 minutes. The mucoadhesive polymers was then added and mixed until the polymer was dissolved. The CCB suspension was adjusted pH to 7.4 with sodium hydroxide and adjusted isotonicity with sodium chloride. Finally, the volume was filled-up with purified water.

Table 5 Composition of CCB eye drop suspensions

Ingredient [a]	Formulation (gm) [b]											
	F7	F8	F9	F10	F11	F12	F13	F14	F15	F16	F17	F18
Celecoxib	0.5	0.5	0.5	0.5	0.5	0.5	0.5	0.5	0.5	0.5	0.5	0.5
RM-β-CD	7.5	7.5	7.5	7.5	7.5	7.5	-	-	-	-	-	-
γ-CD	-	-	-	-	-	-	10	10	10	10	10	10
HPMC	-	-	-	0.1	0.25	0.5	-	-	-	0.1	0.25	0.5
HA	0.1	0.25	0.5	-	-	-	0.1	0.25	0.5	-	-	-
EDTA	0.1	0.1	0.1	0.1	0.1	0.1	0.1	0.1	0.1	0.1	0.1	0.1
BAC	0.02	0.02	0.02	0.02	0.02	0.02	0.02	0.02	0.02	0.02	0.02	0.02
Purified water qs. to 100 ml												

[a] RM-β-CD; randomly methylated-β-cyclodextrin, γ-CD; γ-cyclodextrin, HPMC; Hydroxypropyl methylcellulose HA; Hyaluronic acid, Ethylenediaminetetraacetic acid disodium salt, BAC; Benzalkonium chloride

[b] All formulation was adjusted pH to 7.4 with 1N sodium hydroxide solution and was adjusted with sodium chloride to obtain isotonicity.

7.3 Effect of heating method on CCB eye drop suspensions (ternary complex)

To investigate the effect of heating process to promote the ternary complex of CCB/CD/polymer, CCB eye drop suspensions from the section 7.2 were selected to further study. The CCB ophthalmic suspension was prepared following the procedure described in the section 7.2. Before the adjusting volume, the formulations were sonicated in an ultrasonic bath (GT sonic, China) at 70°C for 1 hour.

8. Physicochemical and chemical characterizations of CCB eye drop formulations

8.1 pH determination

The pH value of formulations was measured at room temperature with pH meter (METTLER TOLEDO™, SevenCompact, Germany). The equipment was calibrated at pH 4, 7 and 11 using Beckman standard buffer solutions before measurement.

8.2 Viscosity determination

The viscosity measurement of each formulation was determined by using the viscometer (Brookfield LVDV-II+, USA). All measurement samples in triplicate were performed at a 25 ± 0.1°C.

8.3 Osmolality measurement

The osmolality of formulations was measured by Osmometer (Gonotec, OSMOMAT 3000 basic, Germany) at room temperature using freezing point depression principle. The instrument was calibrated with 0.9% sodium chloride solution before the measurement of sample. The clear formulation volume of 50 µl was measured as value for osmolality concentration in mOsmol/kg. Each sample was measured in triplicate.

8.4 Sedimentation volume determination

For CCB (0.5% w/v) eye drop suspensions, the sedimentation volume (F) was measured during storage without agitation in 10-ml cylinder for a period of 10 days and was recorded at interval time in terms of the ratio of the ultimate settled height (Hu) to the original height (Ho), in the following equation:

$$F = \frac{Hu}{Ho} \qquad \textbf{Eq.3}$$

8.5 Re-dispersion time determination

Celecoxib (0.5% w/v) ophthalmic suspensions were filled in 15-ml colorless glass vials and closured with rubber and aluminium caps. The time required for re-dispersion of the suspensions was measured after standing the vial in an upright position for 5 days. The container was rolled in a horizontal position using a mechanical shaker (Stuart Scientific, Mini Orbital Shaker SO5, UK) at 75 rpm. Re-dispersion time was defined as the required time to become a uniform suspension from the precipitated condition at the bottom of the container. The measurement was done in triplicate and the results are the mean values $\pm$ standard deviation (S.D.).

8.6 The morphology, particle size and size distribution analysis

The samples were centrifuged by High speed micro centrifuge (TOMY™, MX-305, Japan) at 3,500 rpm for 40 minutes to separate the supernatant and the solid particles portions. The supernatant of each formulation was performed by DLS as described in the section 5.1 to detect the particle size and size distribution of CCB-CD based aggregates. For solid particles portion, the particle size was investigated by optical microscopy (Nikon™ eclipse E200, Japan). Before the measurement, the ocular micrometer was calibrated with the stage micrometer. The magnification x 400 was used in all experiments. The sample was dropped on the glass slide covered with cover slip and measured the particle size about 300 particles. The mean of particle size values $\pm$ S.D. was recorded. The morphology of particles was observed

by scanning electron microscope (SEM, JEOL™ JSM-6610LV, USA). The sample of solid particle portion was layered on the slide and dried overnight in desiccator at room temperature. And then, it was mounted on the stubs. The specimen stubs were coated with a thin layer of gold under argon atmosphere at room temperature. Finally, the samples were observed for their surface morphology by SEM.

8.7 Total drug content and dissolved drug content

Total CCB content was determined by diluting 100-µl of sample with mixture of mobile phase, acetonitrile:water (55:45 v/v), and further diluted to appropriate CCB concentration. For amount of dissolved CCB content in suspension, the sample was centrifuged at 3,500 rpm for 40 minutes. The supernatant was further diluted with mobile phase and analyzed by HPLC which described in section 2. The measurement was done in triplicate. The percentage dissolved content calculated by the following Eq. 4.

$$\% \text{ dissolved content} = \frac{[\text{Ds}]\text{x } 100}{[\text{Dt}]} \qquad \textbf{Eq.4}$$

Where [Ds] = drug content of supernatant

[Dt] = total drug content

9. *In-vitro* mucoadhesive studies

The mucoadhesive properties of the formulations were evaluated using equipment described by Bin Choy et al. (2008). This method was modified as follows. Before the measurement, semipermeable membrane (MWCO 12-14,000 Da) was immersed in an aqueous mucin solution (0.1% w/v mucin from porcine stomach, Type II) for 2 hr. Then, 50-µl of each formulation was dropped in the middle of the membrane. The membrane was rinsed with simulated tear fluid (STF) continuously at the flow rate of 1 ml/min for 1 min. Then the remained drug was washed from the membrane by immersing the membrane in volumetric flask containing the mobile phase. After shaking for 20 min, the solutions were filtered through 0.45 µm nylon

filter membrane and the amount of CCB was finally determined by HPLC which described in the section 2. The CCB eye drop formulations without mucoadhesive polymer used as a control were also tested.

10. *In-vitro* permeation studies

10.1 In-vitro permeation through semipermeable membrane

The *in-vitro* permeation of CCB formulation through semipermeable membrane (MWCO 12–14,000 Da) was performed by Franz diffusion cell apparatus consisting of a donor and a receptor compartment. The donor and receptor compartments were separated by the semipermeable membrane. The receptor phase consists of the phosphate buffer saline, pH 7.4 and 2.0% (w/v) γ-CD or RM-β-CD. CDs were added in the receptor phase to allow sink condition. Before the experiment, the receptor medium was sonicated to remove dissolved air and the membrane was soaked overnight in the receptor medium. For the experimental condition, the receptor phase was stirred continuously during the experiment at 150 rpm and controlled temperature at 34±0.5°C. The sample (1.5 ml) of each formulation was placed on the donor phase. A 400-µl aliquot of the receptor medium was withdrawn follow suitable time interval for analysis and replaced immediately by an equal volume of fresh receptor medium. The CCB content was determined by HPLC (described in section 2) and the amount of drug permeation was calculated. Each formulation was done in triplicate. The flux *(J)* was calculated from the linear part of each permeation profile. The steady state flux was calculated as the slope of linear plots of the amount of drug in the receptor chamber (*q*) versus time and the apparent permeation coefficient (P_{app}) determined from equation Eq.5:

$$J = \frac{dq}{A.dt} = P_{app}.Cd \qquad \textbf{Eq.5}$$

Where *A* is the surface area of the mounted membrane (2.27 cm^2) and *Cd* is the dissolved concentration of the drug in the donor chamber.

10.2 In-vitro permeation through simulated artificial vitreous humor

The study of permeation through artificial vitreous humor model was represented the permeation through vitreous humor which aimed to deliver the drug to the posterior segment of eye i.e., retina and optic nerve. The artificial vitreous humor consisted of 0.25 %w/v HA and 0.2 %w/v agar (Kummer et al., 2007). The donor phase and receptor phase were separated by two-layered of semi-permeable membrane (MWCO 3,500 Da and MWCO 12–14,000 Da) and the artificial vitreous humor was filled inside the compartment as depicted in Figure 9. The procedure of this study was done followed by the section 10.1.

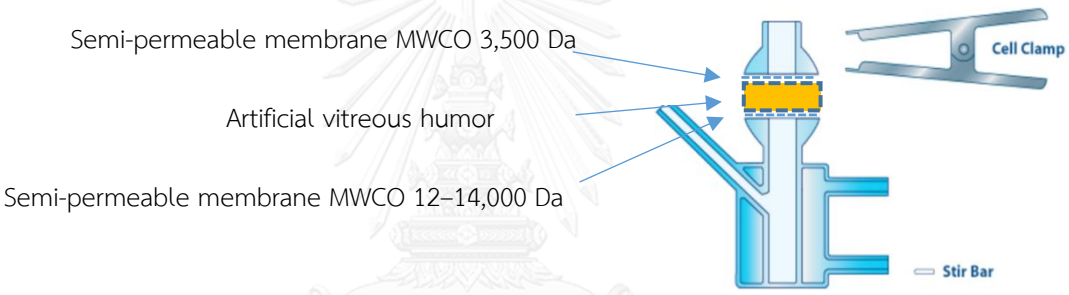

Figure 9 Simulated artificial vitreous humor model

CHAPTER IV
RESULTS AND DISCUSSION

1. Thermal stability of CCB on cycles of autoclaving

Since the phase solubility studies of CCB determined by heating method (Loftsson et al., 2005), the thermal stability of the CCB/CD complexes in the aqueous solution was determined. Table 6 shows the CCB content in aqueous solution containing 0.5% w/v β-CD after zero to three cycles of autoclaving. Each cycle consisted of heating to 121°C for 20 minutes. The amount of CCB in aqueous β-CD solutions in each cycle of autoclaving was not significantly different ($p<0.05$). This result exhibited CCB was relatively stable which no degradation was observed after three cycles of autoclaving. It was concluded that the CCB/CD complexes could be prepared by heating process. The thermal stability of CCB was confirmed by the study of Srinivasulu et al. (2012). The result was shown that there was no thermal degradation of pure CCB when kept it at the temperature of 105°C for 24 hrs.

Table 6 CCB content in aqueous solution containing 0.5% w/v β-CD after zero to three cycles of autoclaving[a]

No. of autoclaving	Content of CCB (µg/ml) (Mean ± S.D.)
0 cycle	1.483 ± 0.038
1 cycle	1.512 ± 0.068
2 cycle	1.525 ± 0.047
3 cycle	1.523 ± 0.051

[a] each cycle consisted of 121°C for 20 minutes

2. Phase solubility studies

2.1 The effect of CD on CCB solubilization

Figure 10 displays the phase solubility diagrams of CCB in aqueous CD solutions i.e., α-CD, β-CD, γ-CD, HP-β-CD and RM-β-CD. In case of β-CD, γ-CD and HP-β-CD, they demonstrated that CCB solubility increased linearly with increasing CD concentration and represented an A_L-type diagram (Figure 10B, 10C and 10D). Whereas, α-CD and RM-β-CD showed a positive deviation from linearity represented A_p-type profile (Figure 10A and 10E) (Higuchi et al., 1965).

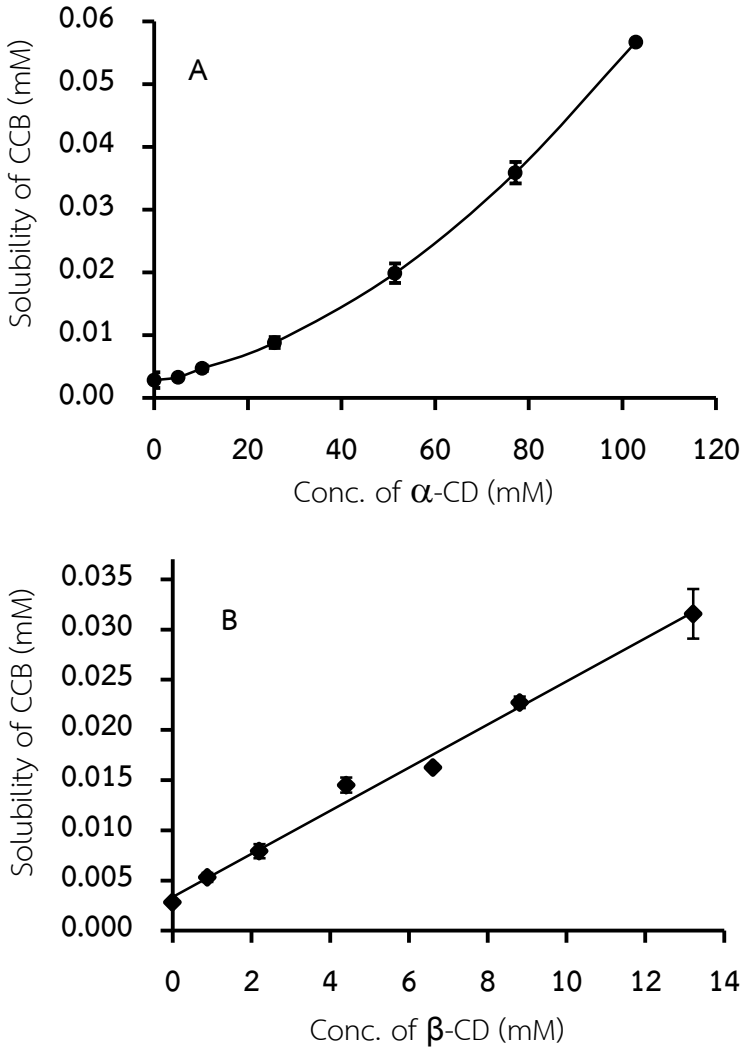

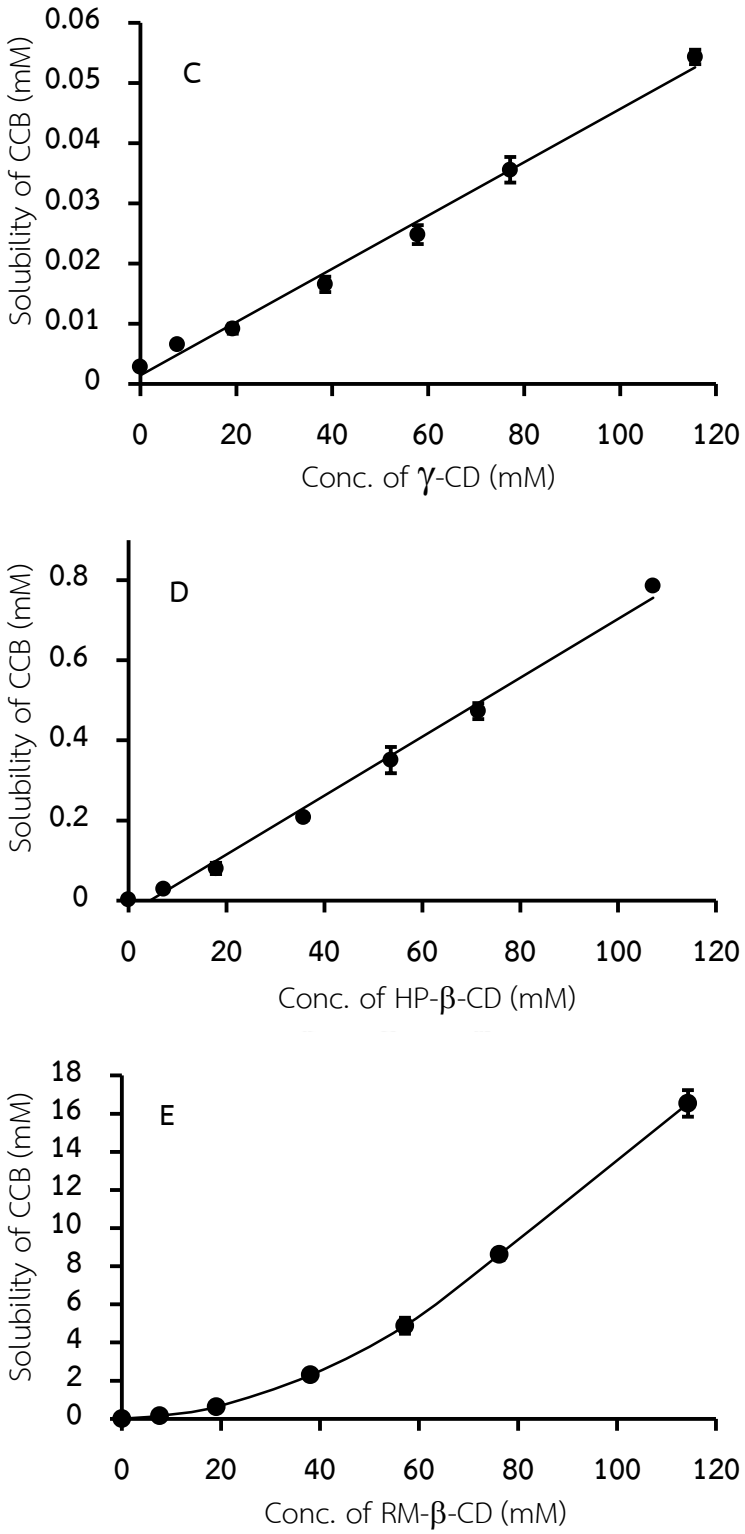

Figure 10 Phase solubility profiles of celecoxib in aqueous cyclodextrin. α-CD solutions (A), β-CD solutions (B), γ-CD solutions (C), HP-β-CD solutions (D) and RM-β-CD solutions (E).

According to A_L-type phase solubility profile, this linear of drug and CD correlation with slope less than 1 suggested the formation of first-order soluble complex assumed that the increasing solubility of CCB as a result of the formation of a 1:1 molar ratio of CCB/CD inclusion complex (Rawat and Jain, 2004). Table 7 shows apparent stability constant values ($K_{1:1}$ and $K_{1:2}$) and the complexation efficiency (CE) of CCB/CD complexes in pure aqueous CD solutions. For α-CD and RM-β-CD, they indicated that the formation of higher order soluble complexes at high CD concentration. Stability constants (K) for the two complexes i.e., CCB/CD and CCB/CD_2 were determined after constructing a plot by using the following Eq.2. They assumed that the 1:1 complex was formed more easily than 1:2 complex.

Table 7 Apparent stability constant values ($K_{1:1}$ and $K_{1:2}$) and the complexation efficiency (CE) of celecoxib/cyclodextrin complexes in pure aqueous cyclodextrin solutions at 30 °C ± 1 °C

Cyclodextrin	Type	$K_{1:1}$ (M^{-1})	$K_{1:2}$ (M^{-1})	CE
α-CD	A_p	49.9	26.2	0.00014
β-CD	A_L	760.2	-	0.00215
γ-CD	A_L	155.3	-	0.00044
HP-β-CD	A_L	2,630.2	-	0.00746
RM-β-CD	A_p	3,139.9	141.0	0.00890

Ventura et al. (2005) investigated that the CCB/dimethyl-β-CD complex was also formed the same stoichiometry complex i.e., 1:1 and 1:2 complex. β-CD displayed the greatest CE among natural CDs. The literature review demonstrated that the cavity diameter of β-CD has been found to be most appropriate size for aromatic and heterocyclic molecules (Del Valle, 2004). However, its aqueous solubility is rather limited due to relatively strong binding of the CD molecules in the crystal state. Random substitution of the hydroxyl groups, even by hydrophobic moieties such as methoxy functions, will result in dramatic improvements in their solubility (Loftsson et al., 2005). This could support that HP-β-CD and RM-β-CD, β-CD

derivatives, could enhance the CE when compared with their unmodified ones (Table 7). Among CDs tested, RM-β-CD showed the highest CE value which referred to the great CCB solubilization. However, the safety profiles of CD should be considered. It was reported that the ranking of CD toxicity in human corneal epithelial cell line (HCE) as following: α-CD > DM-β-CD > SBE-β-CD ≈HP-β-CD > γ-CD (Saarinen-Savolainen et al., 1998). γ-CD is well tolerated and possess favorable toxicological profiles but for RM-β-CD could be used at low concentration in topically aqueous eye drop formulation (Loftssona et al., 1999; Saokham and Loftsson, 2017). Therefore, regarding to the data of phase solubility profiles and safety profile aspects, RM-β-CD and γ-CD were selected to further study.

2.2 The effect of polymer on CCB/CD complex solubilization

Water-soluble polymers can enhance the CD complexation of drugs and also they can increase the drug permeation through biological membranes (Sigurdardottir and Loftsson, 1995). This synergistic effect is possible due to the formation of ternary complexes or co-complexes and their mucoadhesive enhancement (Jarho et al., 1998; Loftsson et al., 1999; Jansook et al., 2010). In this study, the effect of polymers i.e., HPMC, hyaluronic acid (HA) and chitosan (CS) (non-ionic, anionic and cationic polymer, respectively) on RM-β-CD and γ-CD solubilization of CCB was investigated. Figure 11 displays the effect of polymers on phase solubility profiles of CCB in aqueous CD solutions and Table 8 shows the apparent stability constant and CE of CCB/CD complexes in the present of polymer. The results exhibited that the addition of polymers in complexing medium did not alter the type of the phase solubility diagram. Thus, the presence of polymers did not change the stoichiometry of the complex formed.

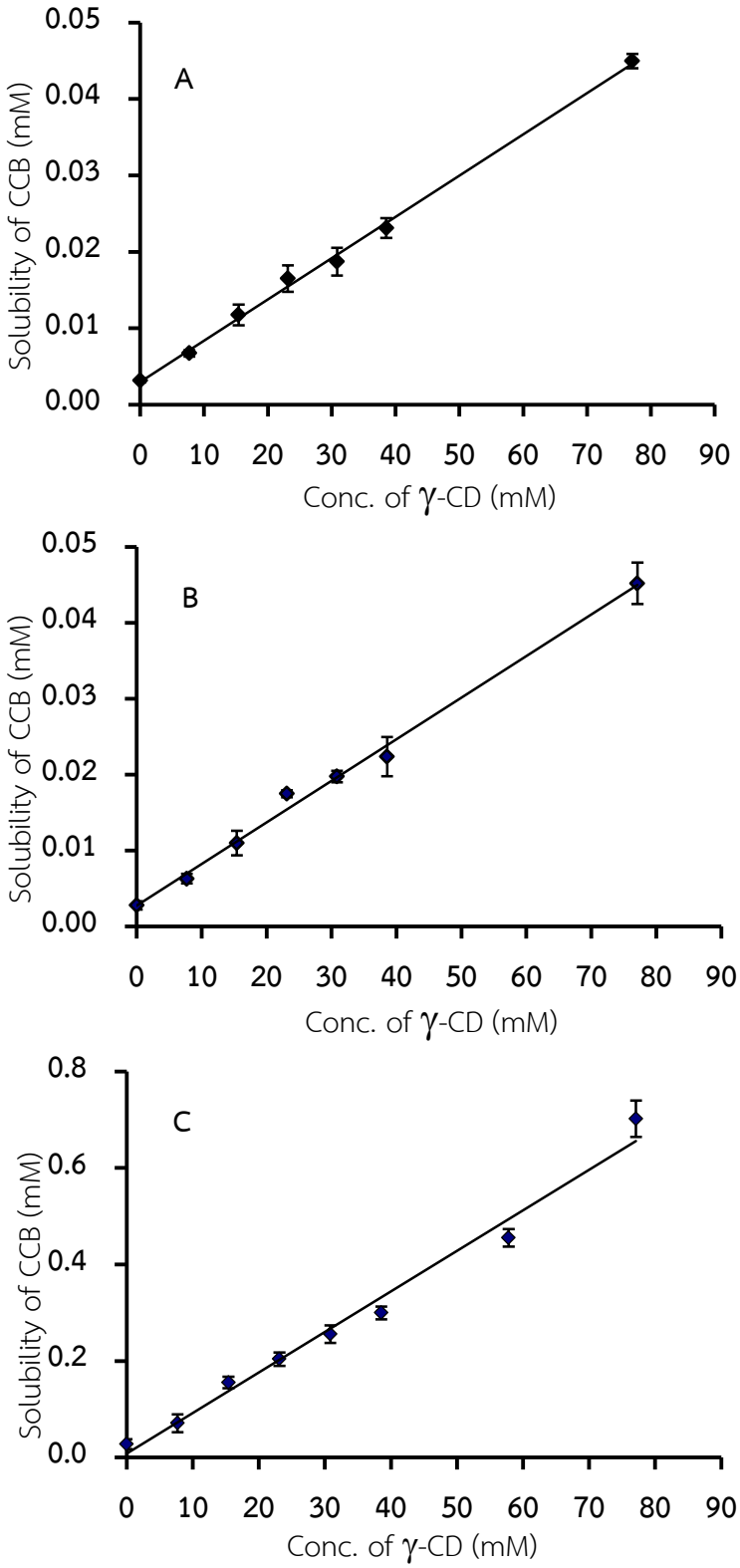
A
Solubility of CCB (mM)
0.05
0.04
0.03
0.02
0.01
0.00
0 10 20 30 40 50 60 70 80 90
Conc. of γ-CD (mM)
B
Solubility of CCB (mM)
0.05
0.04
0.03
0.02
0.01
0.00
0 10 20 30 40 50 60 70 80 90
Conc. of γ-CD (mM)
C
Solubility of CCB (mM)
0.8
0.6
0.4
0.2
0.0
0 10 20 30 40 50 60 70 80 90
Conc. of γ-CD (mM)

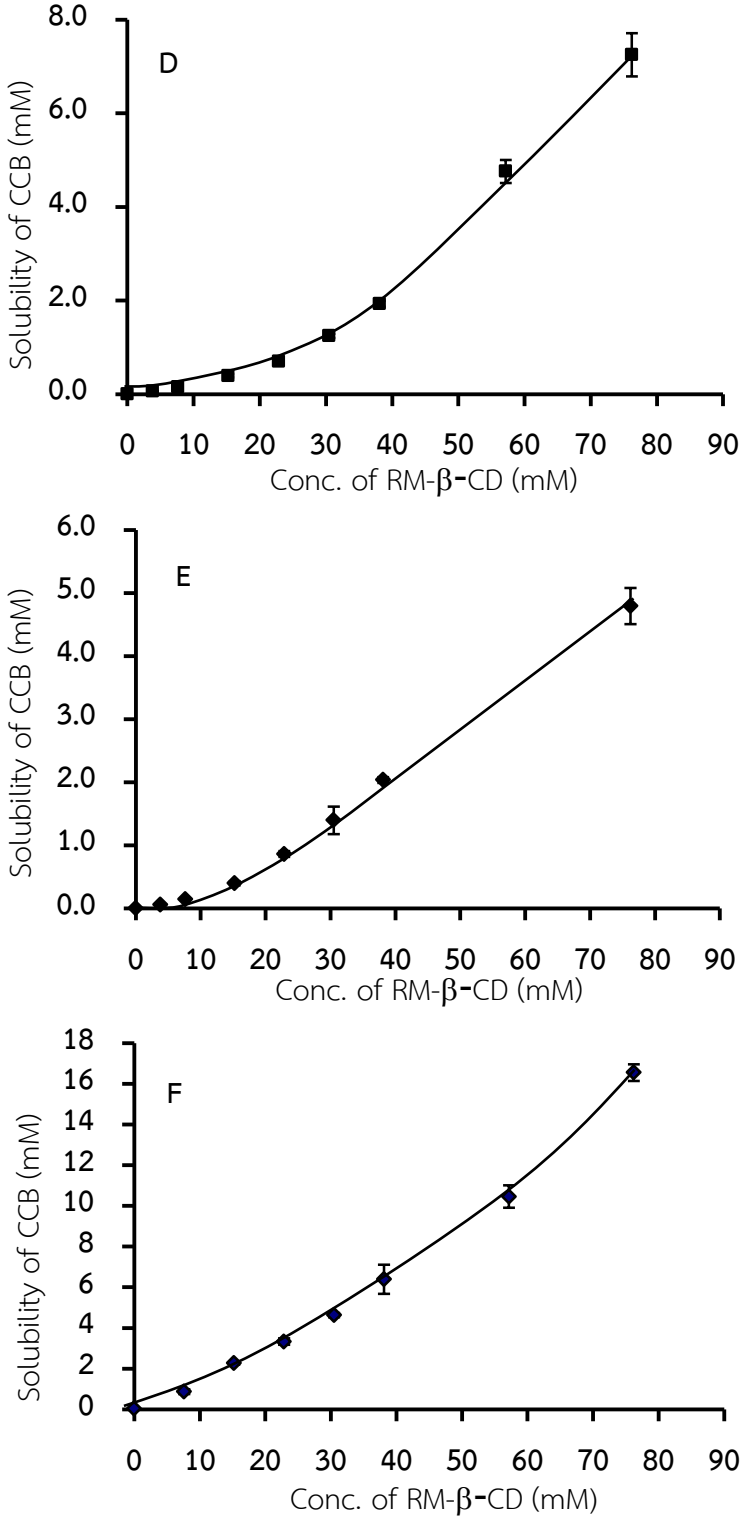

Figure 11 Phase solubility profile of celecoxib in aqueous cyclodextrin containing polymer. γ-CD solutions containing 0.1% w/v chitosan (A), 0.01% w/v hyaluronic acid (B) and 0.1% w/v HPMC (C), and in aqueous RM-β-CD solutions containing 0.1% w/v chitosan (D), 0.01% w/v hyaluronic acid (E) and 0.1% w/v HPMC (F).

Table 8 Apparent stability constant values ($K_{1:1}$ and $K_{1:2}$) and the complexation efficiency (CE) of celecoxib/cyclodextrin complexes in pure aqueous cyclodextrin solutions in the presence of polymer at 30°C ±1°C

Cyclodextrin	Polymer	Type	$K_{1:1}$ (M^{-1})	$K_{1:2}$ (M^{-1})	CE	CE ratio
γ-CD	-	A_L	155.3	-	0.00044	1.00
	0.1 % Chitosan	A_L	170.9	-	0.00048	1.10
	0.01 % HA	A_L	196.4	-	0.00056	1.26
	0.1 % HPMC	A_L	307.5	-	0.00108	2.46
RM-β-CD	-	A_p	3,139.9	141.0	0.00890	1.00
	0.1 % Chitosan	A_p	2,846.1	136.4	0.00900	1.01
	0.01 % HA	A_p	3,532.6	119.8	0.00990	1.11
	0.1 % HPMC	A_p	3,564.4	18.3	0.09820	11.03

Form this results, the apparent stability constant (K) and CE of both binary CCB/RM-β-CD complex and CCB/γ-CD complex were increased when addition of the small amount of polymer due to the synergistic effect between these components (Loftsson et al., 1994). The effect of polymer on the CE of both CCB/γ-CD complex and CCB/RM-β-CD complex showed the same trend as follows: HPMC > HA > CS (Table 8). Addition of chitosan to the complexation media has insignificantly effect on the CE of CCB, thus; it was excluded for further study. Interestingly, HPMC showed the highest increments in solubilizing efficiency (CE ratio) of CCB about 11-folds and 2.5-folds increasing in the CE of CCB/RM-β-CD and CCB/γ-CD, respectively. The dramatically increasing CE of CCB/RM-β-CD with HPMC as ternary complex may be possibly caused by the interaction of multi-components. The synergistic effect with polymer might occur of water-soluble polymers interaction with drug molecules through aggregate formation capable of solubilizing drugs. In addition, the polymers plays the important role in stabilizing micelles and other types of aggregates. These reduce the mobility of CD and change the hydration properties of CD molecules, result in enhancing the solubility of drug and their complexes (Loftsson et al., 2005). This observation was similar to the study of Loftsson et al. (2005). They

demonstrated that HPMC and PVP can increase the CE as ternary complex of acetazolamide, carbamazepine methazolamide and pregnenolone when the present of HP-β-CD.

3. Morphology and aggregates particle size analysis

According to polymer and drug/CD complexes formed aggregates which was able to solubilize the water-insoluble drugs, the aggregated size of ternary complexes i.e., CCB/RM-β-CD/HA, CCB/RM-β-CD/HPMC, CCB/γ-CD/HA, and CCB/γ-CD/HPMC were investigated. Two different techniques were applied to determine aggregation of CCB/CD/polymer complexes, the dynamic light scattering (DLS) technique used to measure the self-assembled aggregates nanoparticles size which was assumed that they have spherical shape, whereas the microscopic methods, transmission electron microscopy (TEM), used to observe the morphology of their aggregates. From the results, the aggregates diameters of the ternary complexes were in the range of 250 - 350 nm (Table 9). As expected, the aggregate diameter of the ternary complexes consisted of CCB/CD containing HPMC were larger than those of CCB/CD with HA. TEM photographs of the ternary complexes are shown in Figure 12. The morphology of all samples was seemed to be spherical in shape and the complex aggregates size was in the same range obtained from the DLS techniques. This was supported that the addition of small amount of water-soluble polymer i.e., HA and HPMC to aqueous CCB/CD complex solutions can enhance the CE of CD through complex aggregate formation.

Table 9 The aggregate size and size distribution of CCB/CD/polymer ternary complex

Cyclodextrin (%w/v)	Polymer (% w/v)	Mean particle size (nm)
10% γ-CD	0.01% HA	273 ± 36
		1.86 ± 0.02
	0.1% HPMC	308 ± 8
		2.10 ± 0.14
7.5% RM-β-CD	0.01% HA	283 ± 36
		2.05 ± 0.25
	0.1 %HPMC	312 ± 29
		2.08 ± 0.48

In general, in aqueous solutions the relative amount of aggregated CD increases with increasing CD concentration. From the literatures, the diameter of CD aggregates is most frequently between 90 and 300 nm (González-Gaitano et al., 2002). However, CD molecule has its own dynamic behavior resulted from rotational freedom of the glucopyranose unit of CD molecule and the overall molecular mobility. The stabilization of nano-particulate aggregates is regulated by Van der Waals forces and hydrogen bonds interactions, which are at all times in competition resulting in the aggregates are very unstable although the ability of CD to self-assemble to form reversible aggregates is well documented (Ryzhakov et al., 2016).

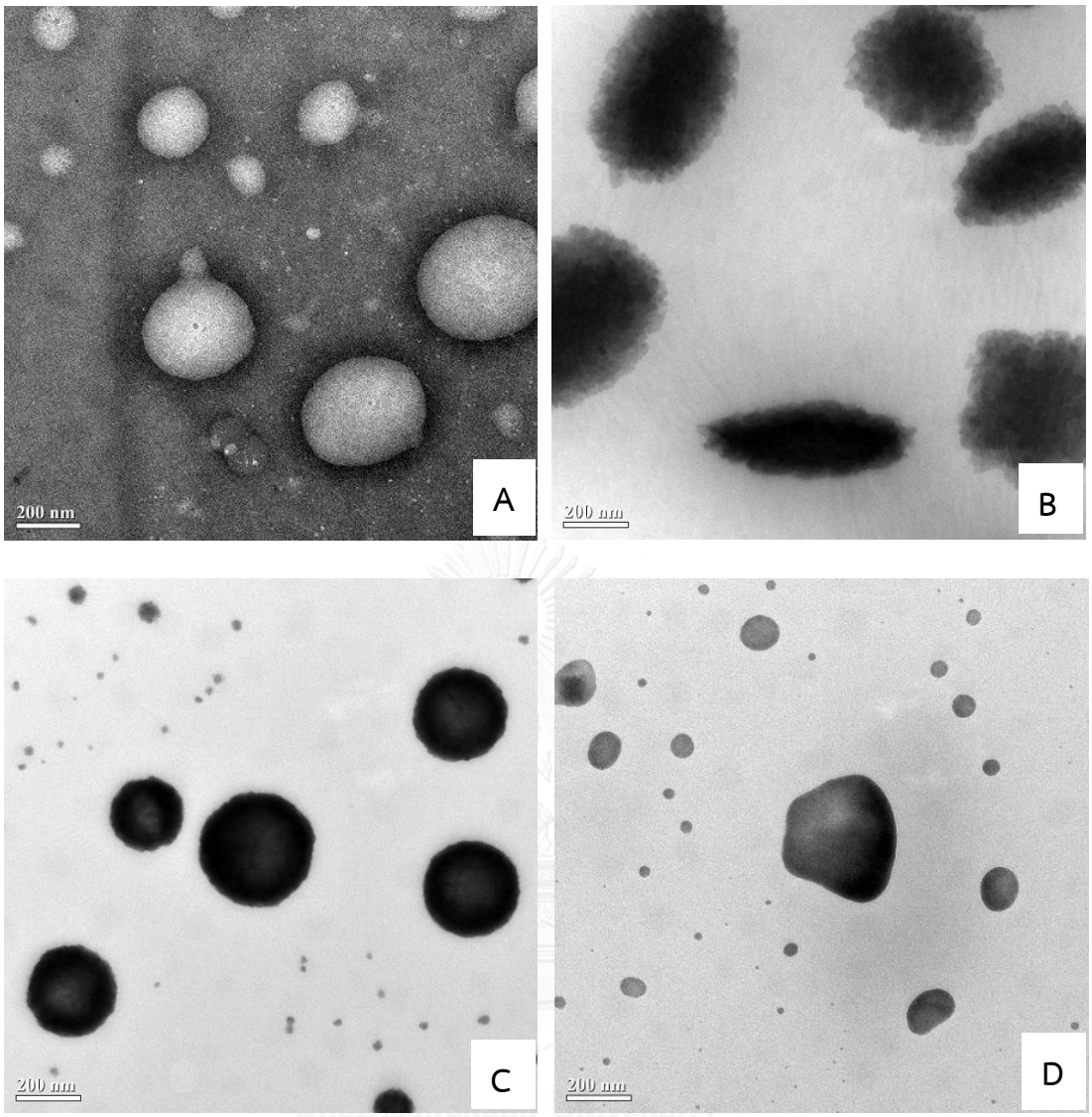

Figure 12 TEM photographs of saturated solution of CCB in CD solution with polymer. (A) CCB/γ-CD/HA, (B) CCB/γ-CD/HPMC, (C) CCB/RM-β-CD/HA, and (D) CCB/RM-β-CD/HPMC.

4. Preparation and characterization of binary CCB/CD complexes and ternary CCB/CD/polymer complexes

4.1 solid-state characterization

4.1.1 Differential scanning calorimetry (DSC)

DSC thermograms of CCB, CDs, their physical mixture (PM) and their freeze dried (FD) samples are shown in Figure 13 and 14. The thermogram of pure CCB

exhibited a sharp endothermic peak at 165.17°C which represented the melting point of the drug (Figure 13A and 14A). Thermogram of γ-CD showed a very broad endothermic peak in the range of 112°C (Figure 13B) due to elimination of water of crystallization (Sinha et al., 2011) while the DSC thermograms of RM-β-CD showed no thermal change (Figure 14B).

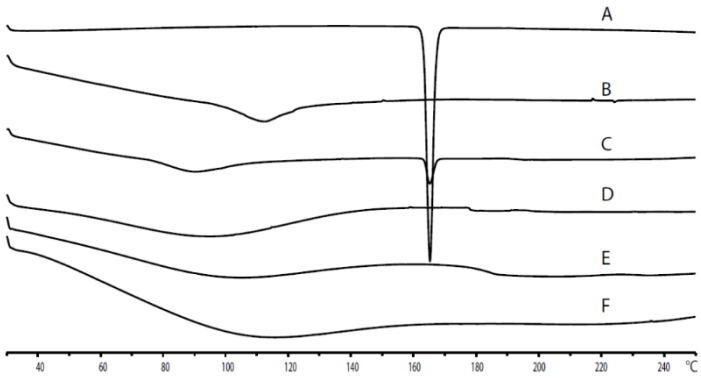

Figure 13 DSC thermograms. (A) pure CCB, (B) pure γ-CD, (C) CCB/ physical mixture γ-CD, (D) freeze-dried CCB/γ-C, (E) freeze-dried CCB/γ-CD/HA, and (F) freeze-dried CCB/γ-CD/HPMC.

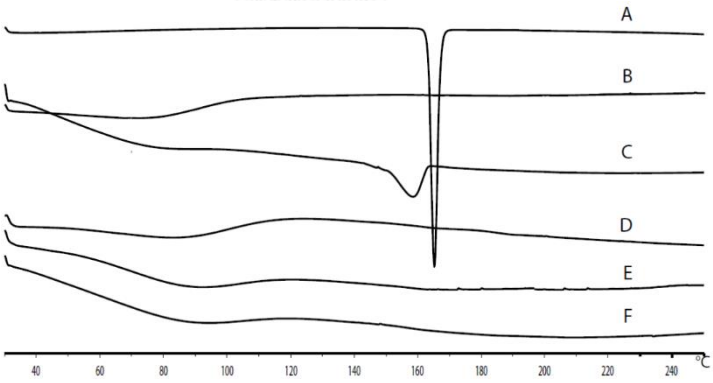

Figure 14 DSC thermograms. (A) pure CCB, (B) pure RM-β-CD, (C) physical mixture CCB/RM-β-CD, (D) freeze-dried CCB/RM-β-CD, (E) freeze-dried CCB/RM-β-CD/HA, and (F) freeze-dried CCB/RM-β-CD/HPMC.

In case of PM, the endothermic peak of the CCB in PM CCB/γ-CD was retained at 165.17°C while the peak of the CCB in PM CCB/RM-β-CD was a broad peak and slightly shifted to lower temperature appeared at 158.67°C. These observations may be attributed to the presence of weak or no interaction between the pure

components in the PM and/or its possibility was an interaction between CCB and RM-β-CD promoted by the heating process in the DSC operation (Nagarsenker et al., 2005). For FD samples, the endothermic peak of binary complex (FD CCB/γ-CD and FD CCB/RM-β-CD) and ternary complex (FD CCB/γ-CD/HA, FD CCB/γ-CD/HPMC, FD CCB/RM-β-CD/HA and FD CCB/RM-β-CD/HPMC) were absent (Figure 13 and 14). The disappearance of an endothermic peak may be attributed to an amorphous state and/or the inclusion complex between CCB and CD in the solid state (Cappello et al., 2007).

4.1.2 Powder X-ray diffractometry (PXRD)

PXRD is used to measure the crystallinity of the formed complexes and the peak position (angle of diffraction) is an indication of a crystal structure. The PXRD spectra of pure CCB, γ-CD, RM-β-CD, their PM, and FD of binary complex and ternary complex are presented in Figure 15 and 16.

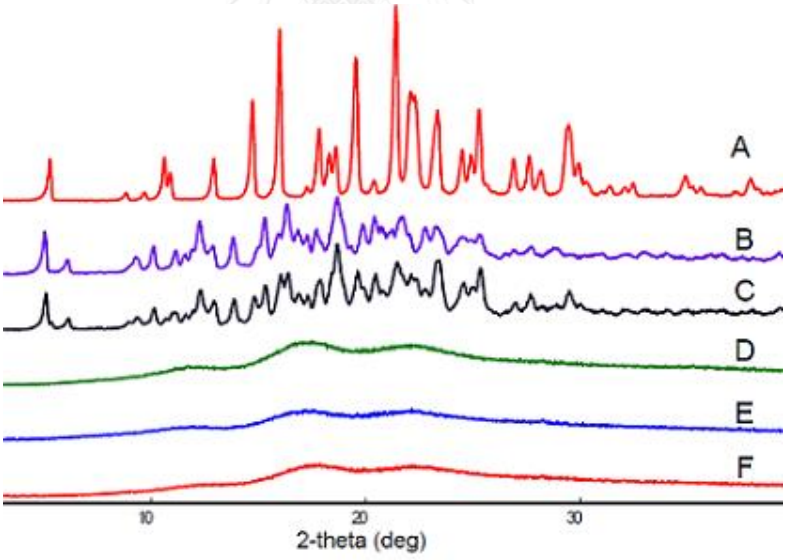

Figure 15 The PXRD spectra. (A) pure CCB, (B) pure γ-CD, (C) CCB/ physical mixture γ-CD, (D) freeze-dried CCB/γ-C, (E) freeze-dried CCB/γ-CD/HA, and (F) freeze-dried CCB/γ-CD/HPMC.

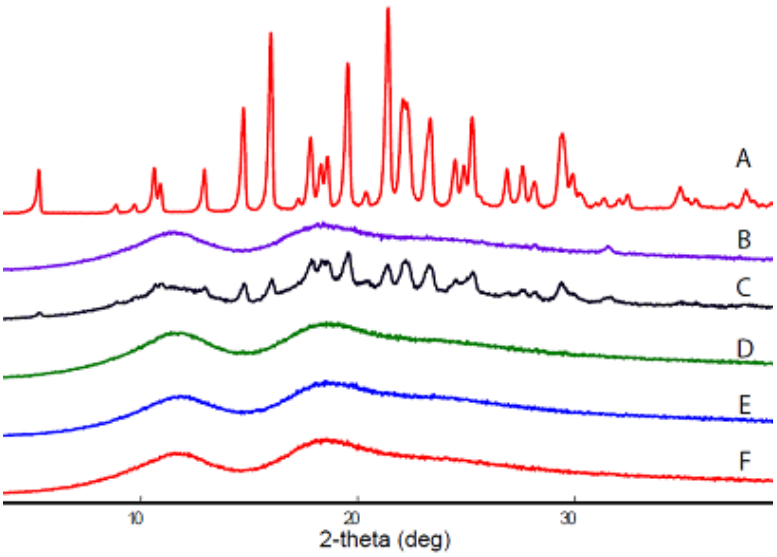

Figure 16 The PXRD spectra. (A) pure CCB, (B) pure RM-β-CD, (C) physical mixture CCB/RM-β-CD, (D) freeze-dried CCB/RM-β-CD, (E) freeze-dried CCB/RM-β-CD/HA, and (F) freeze-dried CCB/RM-β-CD/HPMC.

The diffractogram of CCB exhibited a series of intense peaks at 5.3, 10.6, 10.9, 12.9, 14.7, 16.0, 17.8, 18.3, 18.6, 19.5, 20.4, 21.4, 22.1, 23.3, 24.5, 24.9, 25.3, 26.9, 27.7 28.2 and 29.4, which were indicated of their crystallinity (Figure 15A and 16A). The γ-CD exhibited characteristic peaks at 5.0, 10.1, 11.1, 12.2, 13.8, 15.3, 15.9, 16.3, 16.8, 18.7, 20.3, 21.6 22.8 and 23.3 due to its crystalline nature (Figure 15B) while RM-β-CD did not show any peak and exhibited amorphous state (Figure 16B). Most of the principal peaks of CCB were presented in the diffraction patterns of PM of both CCB/γ-CD and CCB/RM-β-CD (Figure 15C and 16C). This indicated that there was no interaction between the pure CCB and respective CDs. In contrast to FD samples of CCB/CD binary complex (FD CCB/RM-β-CD and FD CCB/γ-CD) and ternary complex (CCB/γ-CD/HA, FD CCB/γ-CD/HPMC, FD CCB/RM-β-CD/HA, and FD CCB/RM-β-CD/HPMC), they showed a halo pattern with the disappearance of all the peaks corresponding to CCB. It was demonstrated the transformation of CCB from the crystalline to the amorphous form by possibly formation of inclusion complex with CD (Sinha et al., 2005). However, freeze drying technique preparation may affect to transformation of in solid state when the solvent was completely removed through sublimation which could not be negligible (Einfal, Planinsek, and Hrovat, 2013).

4.1.3 Fourier transform infra-red (FT-IR) spectroscopy

Figure 17 and Figure 18 show the FT-IR spectra of pure CCB, γ-CD, RM-β-CD, their PM and FD samples. The FT-IR spectra of CCB are shown in Figure 17A and 18A. Its characteristic peaks at 3,332.4 and 3,229.9 cm^{-1} attributed to N-H stretching vibration of SO_2NH_2 group, 1,346.5 and 1,158.2 cm^{-1} for the S=O asymmetric and symmetric stretching and 1,228.7 for C-F stretching. The FT-IR spectrum of γ-CD and RM-β-CD showed a broad absorption band at 3383 cm^{-1} due to -OH stretching and displayed a large band and distinct peak in the region of 1200-900 cm^{-1} (Homayouni et al., 2015). The FT-IR spectrum of CCB in PM sample showed the double peaks of N-H stretching that were slightly shifted to 3330.9 cm^{-1} and 3229.4 cm^{-1} for PM CCB/γ-CD (Figure 17C) and 3336.6 $cm^{-1}$and 3232 cm^{-1} for PM CCB/RM-β-CD (Figure 18C). The S=O stretching vibration was slightly shift to 1347.6 cm^{-1} and 1160.7 cm^{-1} for PM CCB/RM-β-CD while no shift of that in case of CCB/γ-CD. These observations indicated that there was less interaction between CCB and CD in the PM samples.

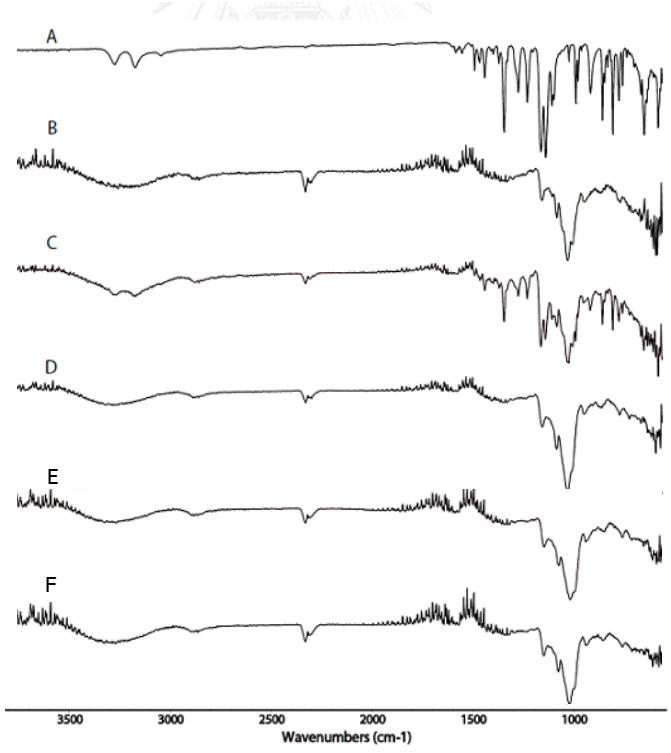

Figure 17 FT-IR spectra. (A) pure CCB, (B) pure γ-CD, (C) CCB/ physical mixture γ-CD, (D) freeze-dried CCB/γ-C, (E) freeze-dried CCB/γ-CD/HA, and (F) freeze-dried CCB/γ-CD/HPMC.

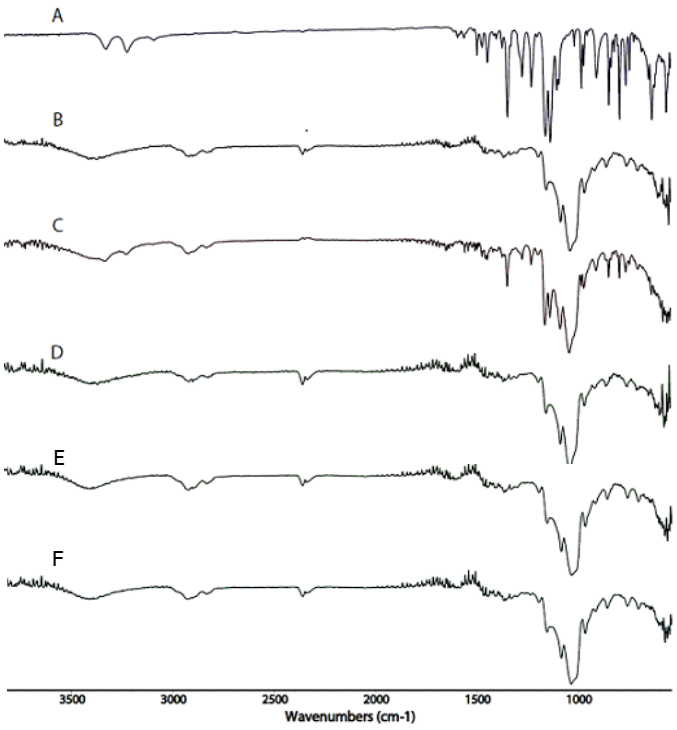

Figure 18 FT-IR spectra. (A) pure CCB, (B) pure RM-β-CD, (C) physical mixture CCB/RM-β-CD, (D) freeze-dried CCB/RM-β-CD, (E) freeze-dried CCB/RM-β-CD/HA, and (F) freeze-dried CCB/RM-β-CD/HPMC.

For FD sample of both binary complex and ternary complex, the N-H stretching bands of CCB indicated the masking of characteristic symmetric and asymmetric stretch. Likewise, the C-F stretching band and S=O stretching bands of CCB disappeared in FD samples. These results may be ascribed to the existence of some interaction between functional group (sulfonamide group or -CF_3 group) of CCB and functional group in the hydrophobic cavities of CD during inclusion complexes (Sinha et al., 2011).

4.2 Solution-state characterization

Proton nuclear magnetic resonance spectroscopy (^{1}H-NMR) studies provide information of the existence of CCB/CD inclusion complexes and suggest the conformation of guest molecules into the CD cavity. The changes in ^{1}H-chemical shifts ($\Delta\delta$) observed for the H5 proton of CCB in the presence of RM-β-CD and γ-CD were 0.045 and 0.043, respectively and displayed significant upfield (Table 10). This behavior can be associated that the H5 proton of CCB locates close to the oxygen atoms in the CD cavity which is rich in π electrons (Ganza-Gonzalez et al., 1994). And also, all aromatic protons of CCB that the presence of γ-CD showed a significant upfield shift. Whereas, all aromatic protons of CCB that solubilized in RM-β-CD displayed downfield shifts demonstrating weaker interactions i.e., Van der Waals forces between CCB and the hydrogen atoms of CD (Ventura et al., 2005).

Table 10 The ^{1}H-chemical shifts of CCB alone and in the presence of individual γ-CD and RM-β-CD.

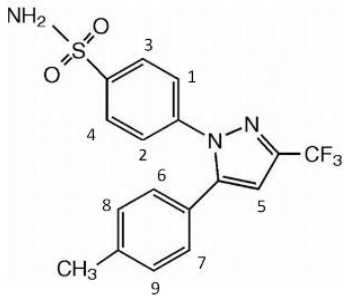

Celecoxib

Protons	Celecoxib	CCB/γ-CD	$\Delta\delta$*	CCB/RM-β-CD	$\Delta\delta^*$
-CH_3	2.206	2.183	-0.023	2.217	0.011
*H5	6.877	6.834	-0.043	6.832	-0.045
H6,H7,H8,H9	7.062	7.035	-0.027	7.076	0.014
H1,H2	7.378	7.345	-0.034	7.390	0.011
H3,H4	7.823	7.801	-0.022	7.838	0.015

$\Delta\delta^* = \delta_{complex} - \delta_{free}$

^{1}H-NMR chemical shift of RM-β-CD is summarized in Table 11. The H3 and H5 proton of glucose units are facing to the interior of the lipophilic CD cavity. The changes in ($\Delta\delta$) were generally observed for the upfield of H3 and H5 which is characteristic of the formation of an inclusion complex. As the result, the changes in $\Delta\delta$ of RM-β-CD in the presence of CCB for H3 and H5 proton were 0.092 and 0.042 indicating a significant upfield shifts. In this case, the $\Delta\delta^*$ of H3 proton was higher than that of H5 proton. It indicated that RM-β-CD formed partial inclusion of CCB (Greatbanks and Pickford, 1987). In addition, the $\Delta\delta^*$ for H1 proton of RM-β-CD was 0.097 displayed significant upfield. This result was agreed with the data obtained by Ventura et al. (2005).

Table 11 The ^{1}H-chemical shifts of RM-β-CD alone and in the presence of CCB.

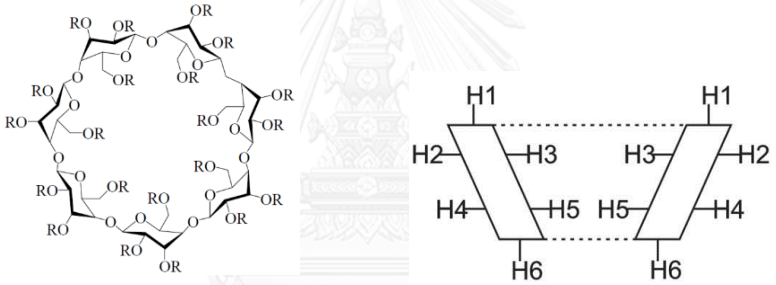

R= H or –CH_3

Protons	RM-β-CD	CCB/RM-β-CD	$\Delta\delta^*$
H1	4.941	4.844	-0.097
H2	-	-	-
*H3	3.785	3.693	-0.092
H4	3.536	3.518	-0.018
*H5	3.577	3.536	-0.042
H6	-	-	-
CH_3OC2,3	3.438	3.451	0.013
CH_3OC6	3.269	3.259	-0.010

$\Delta\delta^* = \delta_{complex} - \delta_{free}$

Table 12 The ^{1}H-chemical shifts of γ-CD alone and in the presence of CCB.

Protons	γ-CD	CCB/γ-CD	Δδ*
H1	4.991	4.994	0.003
H2	3.523	3.499	-0.024
*H3	3.815	3.840	0.025
H4	3.469	3.480	0.011
*H5	3.751	3.821	0.070
H6	3.732	3.715	-0.017

$\Delta\delta^* = \delta_{complex} - \delta_{free}$

The ($\Delta\delta^*$) of γ-CD in the presence of CCB for H3 and H5 proton were 0.025 and 0.070, respectively (Table 12). From the results, the $\Delta\delta^*$ value of H-5 proton > H3 proton and displayed significant downfield, which indicated that the totally drug molecule inserted inside the hydrophobic cavity of γ-CD.

The proposed conformation structure of CCB/RM-β-CD and CCB/γ-CD inclusion complex are shown in Figure 19. The CCB/RM-β-CD was possibly divided in 2 configuration that were 1:1 inclusion complex and 1:2 inclusion complex. Figure 19A shows the 1:1 inclusion complex; the pyrazole head group of CCB was included through the wide rim of RM-β-CD. Figure 19B shows the 1:2 inclusion complex; the CCB was included in to the cavity of the CD dimer in a configuration in which half of CCB molecule was embedded in one monomer and other half is embedded in the other monomer of CD. It was held in position due to the formation of hydrogen bonds between the hydroxyl groups or methoxy groups of the CD and the fluorine and nitrogen atoms of the CCB. Consequently, significant upfield H1 proton of RM-β-CD may be caused by interaction between hydrogen (H1) at wide rim of CD and CCB molecule during 1:2 inclusion complex formation. It corresponded to the results of phase solubility-profile study that CCB/RM-β-CD displayed A_P-type diagram (1:1 and 1:2 complex) (Higuchi et al., 1965). This proposed conformation was supported by the CCB/β-CD complex characterization of Reddy et al. (2004).

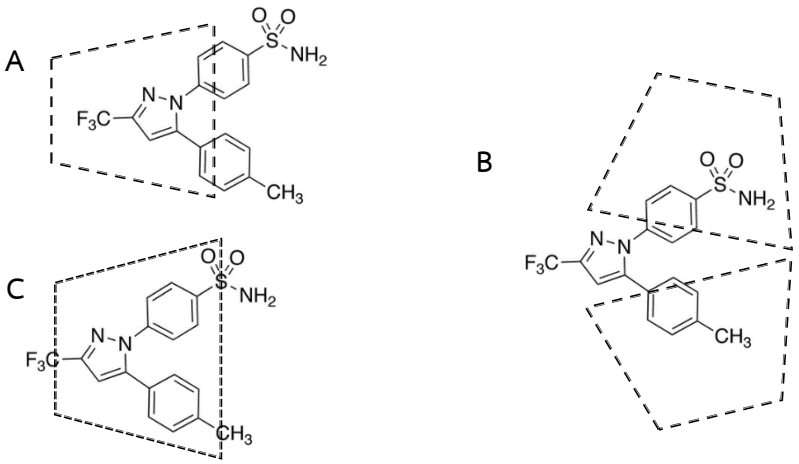

Figure 19 The proposed conformation of (A) 1:1 CCB/RM-β-CD complex, (B) 1:2 CCB/RM-β-CD complex and (C) 1:1 CCB/γ-CD complex.

And also, the proposed conformation of CCB/γ-CD is shown in Figure 19C. Due to $\Delta\delta^*$ of H5 in both CCB and γ-CD were significantly shift including all aromatic protons were upfiled shift. It was suggested that CCB was more deeply included into γ-CD cavity than of RM-β-CD cavity. For this reason, it might be due to the inner cavity diameter of γ-CD (7.5-8.3 A°) is bigger than RM-β-CD (6 A°).

5. Formulation of celecoxib ophthalmic preparation

5.1 Physicochemical and chemical characterizations of formulations

Physicochemical characterizations

The CCB eye drop formulations (F1-F6) showed a clear viscous solution while F7-F18 displayed a milky-white suspension. The pH value, osmolality, viscosity, sedimentation volume and re-dispersion time of each CCB eye drop formulation are given in Table 13 and Table 14.

Table 13 pH value, osmolality and viscosity of CCB eye drop formulations

Formulation	pH	Osmolality (mOsm/Kg)	Viscosity (mPa.s)
F1	7.37 ± 0.07	291.7 ± 9.3	2.43 ± 0.15
F2	7.34 ± 0.01	305.3 ± 18.8	4.90 ± 0.40
F3	7.32 ± 0.01	300.7 ± 4.7	9.03 ± 0.56
F4	7.38 ± 0.06	294.0 ± 8.2	2.66 ± 0.08
F5	7.40 ± 0.09	297.0 ± 12.5	8.43 ± 0.47
F6	7.36 ± 0.04	308.0 ± 14.1	14.67 ± 0.57
F7	7.34 ± 0.03	296.0 ± 11.5	2.72 ± 0.02
F8	7.37 ± 0.08	285.3 ± 4.9	8.83 ± 0.40
F9	7.39 ± 0.06	292.7 ± 7.8	15.67 ± 0.80
F10	7.31 ± 0.01	297.3 ± 7.1	2.47 ± 0.04
F11	7.35 ± 0.01	291.0 ± 4.4	7.57 ± 0.75
F12	7.43 ± 0.10	287.0 ± 1.0	15.13 ± 0.50
F13	7.38 ± 0.08	290.0 ± 7.5	2.36 ± 0.06
F14	7.35 ± 0.05	292.3 ± 11.2	8.20 ± 0.44
F15	7.43 ± 0.07	306.3 ± 13.9	16.87 ± 0.70
F16	7.41 ± 0.09	284.7 ± 3.1	2.58 ± 0.23
F17	7.36 ± 0.06	295.7 ± 2.5	6.90 ± 0.66
F18	7.37 ± 0.08	295.0 ± 3.6	15.13 ± 0.58

pH values of all formulations were in the range of 7.3-7.5. The pH value between 7 and 10 are tolerated by the eye without marked discomfort and values of pH less than 6 and above 11 always cause irritations (Kramer, Haber, and Duis, 2002). However, the pH stability of drug in formulation should be considered to avoid precipitation of the drug or its rapid degradation. Srinivasulu et al. (2012) demonstrated that CCB at the pH 7.4 had good stability and no degradation peak was observed by HPLC analysis.

Ideally, an ophthalmic eye drop should have the tonicity value closed to the lacrimal fluid that corresponding to a 0.9% sodium chloride solution (287 mOsm/kg). However, the eye can tolerate a broad range of tonicity values from 0.6 to 2% of sodium chloride solution. Hypertonic eye drop are better tolerated than hypotonic eye drops (Kramer et al., 2002). The osmolalities of all formulations ranged from 280 mOsm/kg to 324 mOsm/kg (Table 13) which were within the acceptable range (260-330 mOsm/kg).

The viscosity of CCB eye drop formulations at 25°C are displayed in Table 13. The viscosity inducing agents i.e., HPMC and HA was individual added to the aqueous ophthalmic solution and suspension to increase the viscosity for prolong contact of the drug with the eye tissues. The viscosities of formulations were between 2.36 $\pm$ 0.06 mPa.s and 16.87 $\pm$ 0.70 mPa.s. The viscosity increased with increasing the concentration of polymer. CCB eye drop suspension containing 0.5% w/v HA (F15) had the highest viscosity. However, heating method by autoclaving affected the viscosity of formulation (F1-F3). The viscosity decline from initial might be due to possible degradation of HA after exposure to temperature > 90°C for about 1 hour (Lowry and Beavers, 1994). The viscosity for ophthalmic preparation is considered optimal in the range of 15–25 mPa.s (Aldrich et al., 2013). The maximum viscosity to increase contact time should not more than 20 mPa.s. The high viscous formulations usually leave a residue on the eyelid (Kramer et al., 2002).

The good ophthalmic eye drop suspensions are uniform dispersions of solid drug particles in a vehicle. The dispersed particles in suspension should settle slowly and ease to resuspend. The easily re-dispersion of the sediment portion in a suspension is important for the uniformity of dose. A cake formation on setting is not allowed in appropriate eye drop suspension. In this study, the re-dispersion time and sedimentation volume (F) were used to evaluate the physical characteristics of ophthalmic eye drop suspensions and summarized in Table 14.

Table 14 The sedimentation volume (F) at 3, 5, 10 days and the re-dispersion time at day 5 measurement of celecoxib eye drop suspensions

Formulation	Sedimentation volume (F)			Re-dispersion time (s)
	Day 3	Day 5	Day 10	
F7	0.06 ± 0.02	0.06 ± 0.02	0.06 ± 0.02	3.8 ± 0.4
F8	0.07 ± 0.01	0.07 ± 0.01	0.07 ± 0.01	11.0 ± 0.7
F9	0.09 ± 0.01	0.08 ± 0.02	0.08 ± 0.02	22.8 ± 1.7
F10	0.36 ± 0.04	0.03 ± 0.01	0.03 ± 0.01	157.0 ± 11.5
F11	0.53 ± 0.03	0.05 ± 0.01	0.05 ± 0.01	406.3 ± 32.7
F12	0.90 ± 0.03	0.62 ± 0.02	0.62 ± 0.02	610.7 ± 40.3
F13	0.07 ± 0.01	0.07 ± 0.01	0.07 ± 0.01	4.0 ± 1.0
F14	0.08 ± 0.02	0.08 ± 0.02	0.08 ± 0.02	7.7 ± 0.6
F15	0.08 ± 0.02	0.08 ± 0.02	0.08 ± 0.02	14.3 ± 1.5
F16	0.07 ± 0.01	0.07 ± 0.01	0.07 ± 0.01	16.0 ± 1.0
F17	0.09 ± 0.01	0.09 ± 0.01	0.09 ± 0.01	14.3 ± 1.5
F18	0.10 ± 0.01	0.10 ± 0.02	0.10 ± 0.02	52.3 ± 9.0

Form the result, the height of sediment for each suspension was ultimately settled after day 5. F values of F7-F9 and F13-F15 containing HA after storage for a period of 5 days were similar. The sedimentation were rapidly formed, the supernatant were clear and the sediment were easy to re-disperse possibly indicated that they were flocculated suspensions. The flocculated suspensions showed rapid

sedimentation creating loose aggregates and formed a network-like structure (Nutan and Reddy, 2010). Whereas, the formulation of F10-F12 and F16-F18 containing HPMC were slowly formed and the supernatant were cloudy. Among the formulations have been performed, F10-F12 formulation spent more time for re-dispersing to become a uniform suspension, especially F12 (Table 14). This phenomenon was called cake formation as shown in Figure 20. Since the sediment is very closely packed and a hard cake was formed, It indicated that they were deflocculated suspension (Nutan et al., 2010). The re-dispersion time became exponentially longer when % of polymer increased in the suspension. Yasueda et al. (2004) studied the re-dispersability of 0.05% w/v fluorometholone suspensions containing HPMC at the concentration 0.001-0.01 %w/v. It was found that the formulation could re-disperse to uniform suspension. However, the increasing HPMC up to 0.5% w/v, the re-dispersion time became longer and displayed poor re-dispersability. Cake formation is the most serious of all the physical stability problems encountered in suspension. Thus, the formulation of F10, F11 and F12 containing RM-β-CD and HPMC were excluded for further study.

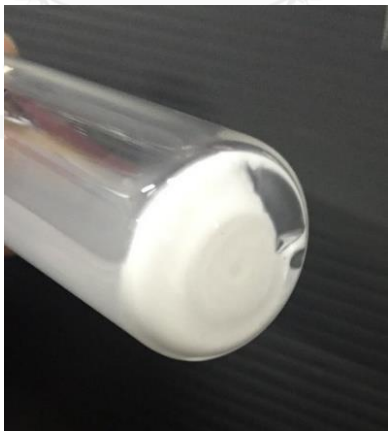

Figure 20 The appearance of cake formation of F12 after storage at room temperature for 5 days.

Chemical characterization

Table 15 exhibited total CCB content and % dissolved CCB in solution of CCB eye formulation. Regarding to the earlier result, RM-β-CD was more powerful solubilizer than γ-CD. As expected, the dissolved content of the CCB in eye drop formulation containing RM-β-CD (F7-F12) was higher than those of formulations containing γ-CD (F13-F18). On the other hand, the solid drug content (free CCB and solid CCB/CD complex) in formulations containing RM-β-CD obtained about 85-90% while more than 99% were observed in case of formulation containing γ-CD. Again, heating through autoclaving (121°C, 20 min) in CCB eye drop solution (F1-F6) lead to accelerate CCB/RM-β-CD complex to completely dissolve. Whereas, unheated formulations (F7-F12) corresponding to those formulations, 50-70% dissolved drug were existed.

Table 15 Total drug content and drug dissolved content of celecoxib eye drop formulations

Formulation	Total drug content (mg/ml)	Drug dissolved content (µg/ml)	% Total drug content	% dissolved content
F1	1.052 ± 0.014	-	105.3 ± 1.4	-
F2	1.056 ± 0.050	-	105.7 ± 5.0	-
F3	1.059 ± 0.074	-	105.9 ± 7.5	-
F4	1.061 ± 0.068	-	106.2 ± 6.7	-
F5	0.993 ± 0.044	-	99.4 ± 4.4	-
F6	1.052 ± 0.035	-	105.3 ± 3.6	-
F7	4.687 ± 0.221	558.2 ± 18.6	93.8 ± 4.4	11.16 ± 0.37
F8	4.740 ± 0.040	497.2 ± 23.3	94.8 ± 0.8	9.94 ± 0.47
F9	4.975 ± 0.113	509.0 ± 8.3	99.5 ± 2.3	10.18 ± 0.17
F10	4.856 ± 0.222	739.6 ± 45.9	97.1 ± 4.5	14.8 ± 0.92
F11	4.951 ± 0.216	707.9 ± 54.4	99.0 ± 4.3	14.16 ± 1.09
F12	4.534 + 0.024	632.8 ± 5.8	90.7 ± 0.5	12.66 ± 0.12
F13	4.808 ± 0.139	35.3 ± 5.6	96.2 ± 2.8	0.71 ± 0.12
F14	4.677 ± 0.033	28.0 ± 6.5	93.5 ± 0.7	0.56 ± 0.13
F15	4.715 ± 0.099	33.7 ± 8.0	94.3 ± 2.0	0.67 ± 0.16
F16	4.724 ± 0.189	24.7 ± 3.6	94.5 ± 3.8	0.49 ± 0.07
F17	4.848 ± 0.082	24.4 ± 2.6	97.0 ± 1.7	0.49 ± 0.05
F18	4.660 ± 0.178	23.3 ± 1.8	93.2 ± 3.6	0.47 ± 0.01

5.2 In-vitro drug permeation studies

The effect of CDs and polymer of CCB eye drop formulations on *in-vitro* permeation through a semipermeable membrane (MWCO 12–14,000 Da) were further investigated**.** Since CCB is categorized into BCS Class II which high permeability but poor solubility, the solubility of drug limited ocular bioavailability. The experiment of permeation study would be investigated by the flux pattern that received for membranes with molecular weight cut-off (MWCO 12-14,000 Da) well over the

molecular weight of CDs. Thus, both the drug and drug/CD complexes (excepting their aggregates) were able to permeate the semipermeable membranes into the receptor medium represented to permeate through an aqueous diffusion barrier at the surface of a membranes (Loftsson et al., 2002). Although the complex did not penetrate the biological membrane of eye after diffused across an aqueous diffusion barrier, the drug in the complex was in rapid dynamic equilibrium with the free drug, and increased the drug concentration gradient over the membrane which leaded to increase ocular bioavailability.

The *in-vitro* permeation profiles of CCB eye drop solutions and suspensions are shown in Figure 21 and Figure 22, respectively. Figure 23 and Figure 24 display the permeation flux (J) and apparent permeation coefficient (P_{app}) determined from the steady state region of the permeation profiles (Figure 21 and Figure 22, respectively).

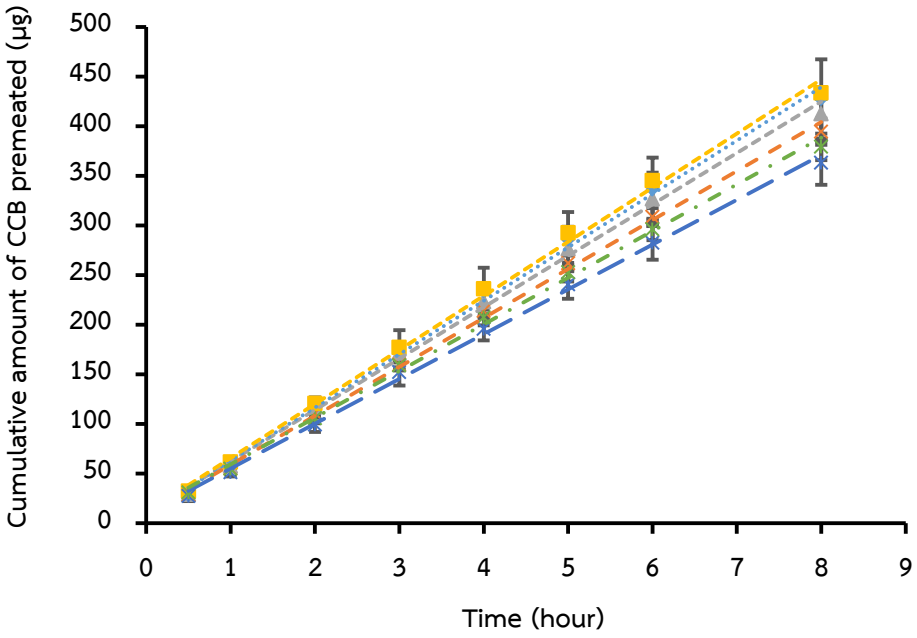

Figure 21 The permeation profiles of CCB-CD eye drop solution through semipermeable membrane (MWCO 12–14,000 Da); (▲) F1, (◆) F2, (x) F3, (■) F4, (x) F5, (x) F6

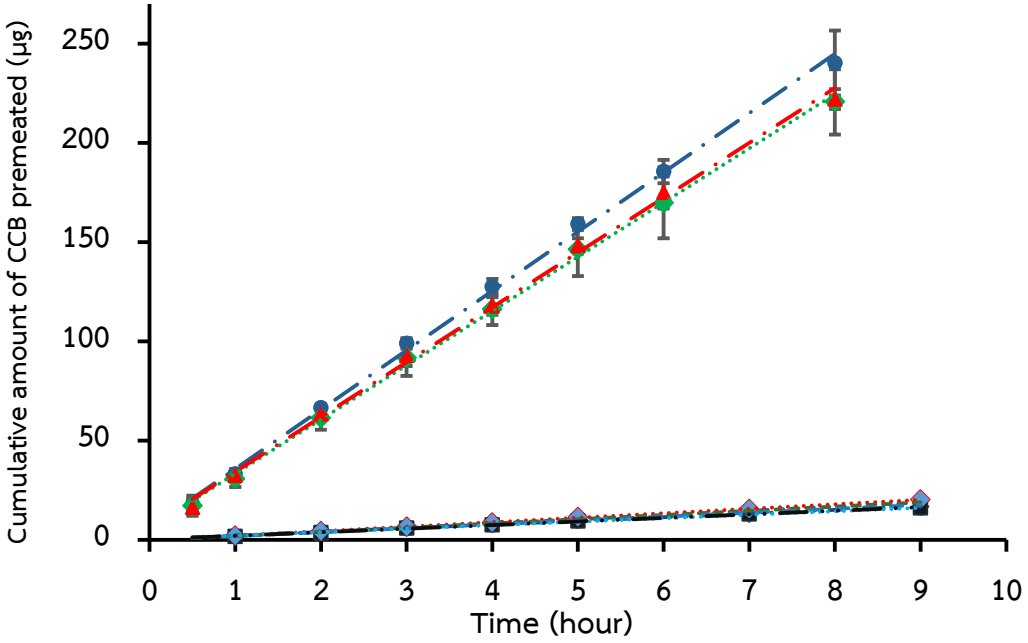

Figure 22 The permeation profiles of CCB-CD eye drop suspension through semipermeable membrane (MWCO 12–14,000 Da); (●) F7, (◆) F8, (▲) F9, (◆) F13, (◆) F14, (●) F15, (▲) F16, (●) F17, (■) F18

The flux values of 0.1% CCB ophthalmic solutions (F1-F6) were superior to those of suspensions (F7-F9) because of their completely dissolved CCB. The flux of CCB containing RM-β-CD formulations (F1-F9) was distinctly greater than γ-CD formulation (F13-F18) due to the great solubilizing efficiency of RM-β-CD. However, the P_{app} of CCB in γ-CD formulations (Figure 24) was slightly higer in all cases which probable due to smaller MW (i.e., smaller hydrodynamic radius) of CCB/γ-CD complex in case of 1:1 complex. In contrast, the inclusion complex fomation of CCB/RM-β-CD were 1:1 complex and 1:2 complex according to A_p-type profiles. This behavior presented high MW of CCB/RM-β-CD especially 1:2 complex (MW ≈ 3,005 Da) resulting in slowly premeated through semipermeable membrane. Though the concentration of polymers increases, permeation flux and, P_{app} of the formulation were not decreased. Hence, the viscosity did not influence on the permeation pattern under such circumstances. The definition of viscosity is based on the bulk properties of solutions and does not apply to individual molecules (Loftsson et al., 2002). Although P_{app} of formulations containing RM-β-CD were slighly less than the

formulation containing γ-CD (F16-F18), their flux values or the total amount of drug and their complexes were much higher which can increase drug concentration gradient over the absorption surface. Thus, the CCB formulation containing RM-β-CD in both solution and suspension forms were promising to deliver CCB to the posterior segment of the eye.

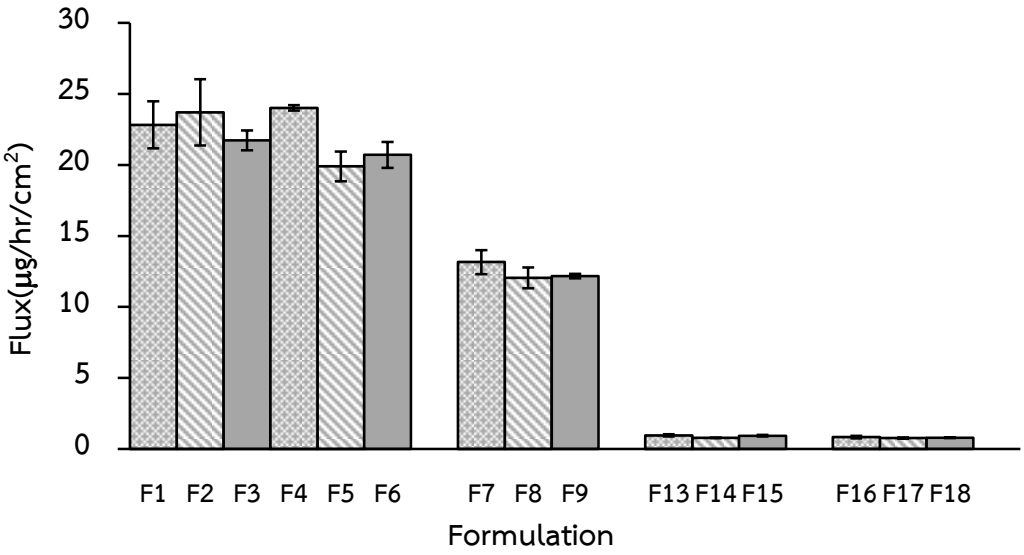

Figure 23 The permeation flux (J) of celecoxib eye drop formulation through semi-permeable membrane (MWCO 12–14,000 Da)

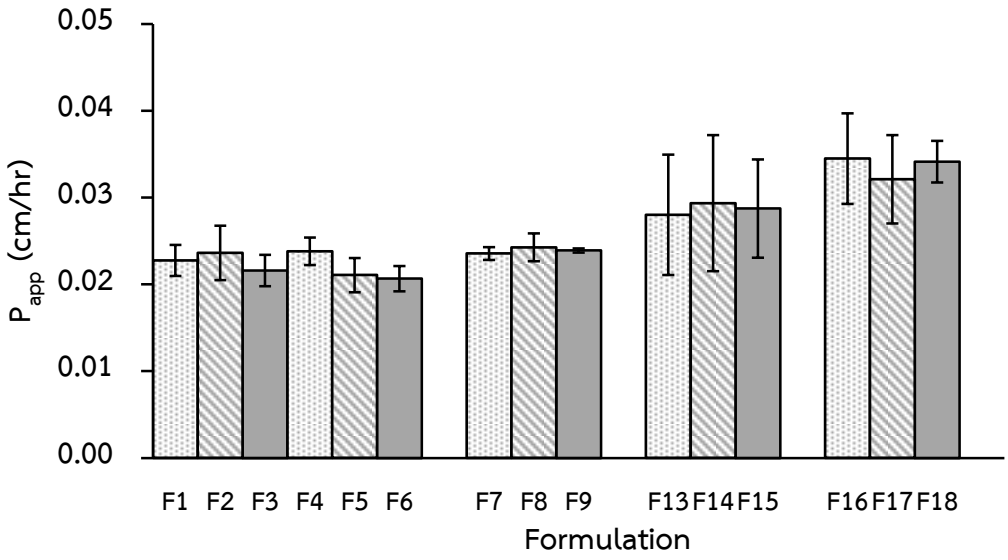

Figure 24 The apparent permeation coefficient (P_{app}) of celecoxib eye drop formulation through semi-permeable membrane (MWCO 12–14,000 Da)

5.3 In-vitro mucoadhesive studies

Table 16 and 17 demonstrate mucoadhesive properties of CCB-CD eye drop solutions and suspensions containing polymer, respectively. From the result, % drug remained for each formulation of solution (F1-F16) were not significantly different (Table 16). Thus, type of polymer and its concentrations i.e., 0.1-0.5% w/v did not affect mucoadhesive properties of CCB eye drop solution. In contrast, when increasing polymer i.e., 0.25% and 0.5% w/v to the eye drop suspension, they provided the mucoadhesive characteristics by significantly higher CCB remaining than that of solution (Figure 25). This indicated that the eye drop suspensions with polymer $\geq$ 0.25% w/v that contains solid particles i.e., free CCB and solid CCB/CD complexes would be possibly washed more slowly from the eye surface.

Table 16 Mucoadhesive properties of celecoxib eye drop solution containing HA and HPMC

Formulation	CD	Polymer	% polymer (w/v)	% Drug remained
F1	RM-β-CD	HA	0.1	0.419 ± 0.184
F2			0.25	0.338 ± 0.160
F3			0.5	0.405 ± 0.093
F4		HPMC	0.1	0.413 ± 0.183
F5			0.25	0.511 ± 0.108
F6			0.5	0.400 ± 0.135

Table 17 Mucoadhesive properties of celecoxib eye drop suspensions containing HA and HPMC

Formulation	CD	Polymer	% polymer (w/v)	% Drug remained	Mucoadhesive Ratio*
F0R	RM-β-CD	-	-	0.12 ± 0.009	1.0
F7		HA	0.1	0.656 ± 0.285	5.5
F8			0.25	1.398 ± 0.259	11.7
F9			0.5	2.243 ± 0.176	18.7
F0G	γ-CD	-	-	0.115 ± 0.012	1.0
F13		HA	0.1	0.753 ± 0.291	6.5
F14			0.25	1.422 ± 0.153	12.4
F15			0.5	3.243 ± 0.320	28.2
F16		HPMC	0.1	0.476 ± 0.238	4.1
F17			0.25	1.317 ± 0.165	11.5
F18			0.5	2.335 ± 0.338	20.3

*Mucoadhesive ratio: Compared with formulation without polymer (F0R and F0G).

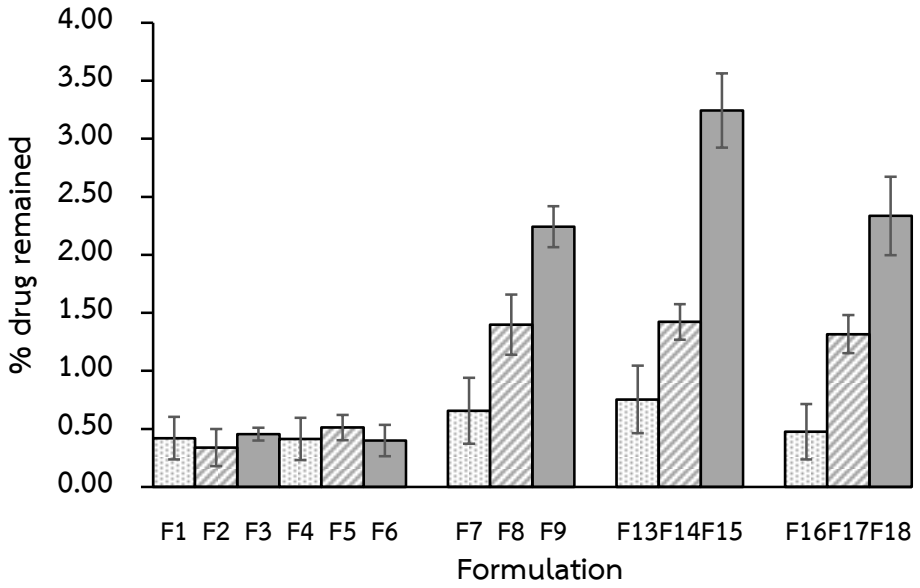

Figure 25 % drug remained of each celecoxib eye drop formulation on the mucin coated membrane

In most cases, the CCB remained in eye drop suspensions containing γ-CD was greater than the formulation containing RM-β-CD (Figure 25). This observation was due to that > 99 % CCB solid content in γ-CD formulations were adhered and slowly flushed away from the membrane surface. Regarding to the eye drop suspensions, the role of polymer (HA and HPMC) on mucoadhesive properties is concentration-dependent manner. Especially, eye drop suspension containing γ-CD and 0.5% w/v HA exhibited the greatest mucoadhesion which was 28-folds higher than that of suspension without polymer (F0G) (Table 17). According to the review of Park and Robinson (1987), generally, both anionic and cationic charged polymers showed better mucoadhesive capacity in comparison to nonionic polymer, such as cellulose derivatives or PVA. Moreover, the polyanions polymer are better than polycations polymer in terms of binding efficacy and potential toxicity. Likewise, Saettone et al. (1989) studied mucoadhesive properties of polymer with mucin-coated surfaces model. This study found that the good to excellent mucoadhesive properties were detected in formulation of tropicamide containing HA greater than formulation containing polyacrylic acid. Consequently, HA is the most promising mucoadhesive polymer for ophthalmic drug delivery.

From the above results, it was concluded that CCB-CD suspensions containing 0.5% w/v HA or HPMC (F9, F15 and F18) provided the great mucoadhesive properties which is possible to increase the residence time, consequently to enhance the ocular bioavailability. Hence, not only permeation flux but also mucoadhesive properties are the main factors to consider to develop the eye drop formulation.

6. Effect of heating method on CCB eye drop suspension (ternary complex)

The increasing complexation of CCB-CD with polymer as ternary complex can be accelerated by heating method i.e. using an autoclave (120 to 140ºC) for 20 to 40 minutes, using sonication bath at 70ºC for 1 hour and using microwaves at 40ºC for 5 minutes (Loftsson et al., 2005). Although the heating method by autoclaving is the promising method to enhance CCB-CD complexation discussed earlier in section of phase solubility profiles; in case of eye drop suspension after a cycle of autoclaving,

the change in physical appearance of formulation was observed. The solid particle in suspension were agglomerated to the larger size i.e., >2 mm (data not shown). Thus, the heating method by sonication at 70 ºC for 1 hour has been performed. In this study, the formulation of F9, F15 and F18 were selected because they showed excellent mucoadhesion and relatively good permeation parameters. The formulation F9, F15 and F18 passed through heating method were coded as F9so, F15so and F18so, respectively. This study aimed to determine the effect of heating method on physicochemical and chemical properties, particle size and permeation of CCB eye drop formulation compared with the corresponding formulations without heating process.

6.1 Physicochemical and chemical properties of heated and unheated CCB/CD suspension

pH and osmolality and viscosity of F9, F15, F18 with and without heating method are shown in Table 18. The viscosity of formulations containing HA with heating method (F9so and F15so) were slightly decreased when compared with the formulation without heating process. Again, this was due to that HA could be degraded under ultrasonic condition with heating at 70°C for 1 hour resulting in lowering viscosity value (Drimalova et al., 2005). Table 19 shows the sedimentation volume (F) and re-dispersion time of formulation with and without heating method. There were no changes in both F and re-dispersion time of formulation after heating process.

Table 18 pH value, osmolality and viscosity of celecoxib eye drop suspension with and without heating method

Formulation	pH	Osmolality (mOsm/Kg)	Viscosity (mPa.s)
F9	7.39 ± 0.06	292.7 ± 7.8	15.67 ± 0.80
F15	7.43 ± 0.07	306.3 ± 13.9	16.87 ± 0.07
F18	7.37 ± 0.08	295.0 ± 3.6	15.13 ± 0.58
F9so	7.36 ± 0.05	293.0 ± 7.5	13.97 ± 0.57
F15so	7.45 ± 0.02	296.3 ± 7.1	13.47 ± 1.06
F18so	7.38 ± 0.06	288.3 ± 3.5	16.03 ± 0.57

so: heating method by sonication at 70°C for 1 hr.

Table 19 Sedimentation volume (F) and re-dispersion time of celecoxib eye drop suspension with and without heating method

Formulation	Sedimentation volume (F)			Re-dispersion time (s)
	Day 3	Day 5	Day 10	
F9	0.09 ± 0.01	0.08 ± 0.02	0.08 ± 0.02	22.8 ± 1.7
F15	0.08 ± 0.02	0.08 ± 0.02	0.08 ± 0.02	14.3 ± 1.5
F18	0.10 ± 0.0	0.10 ± 0.02	0.10 ± 0.02	52.3 ± 9.0
F9so	0.09 ± 0.01	0.07 ± 0.01	0.07 ± 0.01	27.3 ± 2.5
F15so	0.09 ± 0.01	0.09 ± 0.01	0.09 ± 0.01	19.0 ± 3.0
F18so	0.09 ± 0.01	0.09 ± 0.01	0.09 ± 0.01	35.0 ± 5.0

so; heating method by sonication at 70°C for 1 hr.

Table 20 shows total CCB content and drug dissolved CCB content of each formulation with and without heating process. The assay content of all formulations met within the acceptance criteria with 90-110% LA. The percentage dissolved content of F9so, F15so and F18so were 46.9 ± 0.17, 1.33 ± 0.14 and 3.39 ± 0.16 % which greater than 4-folds, 2-fold 7-folds of the corresponding unheated formulations, respectively. This observation was probably due to the interaction between CCB/CD and water-soluble polymer by ion-ion, ion-dipole and dipole-dipole

electrostatic bonds, Van der Waals force (Ribeiro et al., 2003). In addition, CD, polymers and their complexes could form aggregates which enhance the solubilization of hydrophobic molecules like CCB. Regarding to accelerate ternary complex formation, it is possible to activate such interaction bonds between their components during the complexes preparation by heating method (Loftsson et al., 2005). It was shown that the heating method by sonication in water bath at 70°C for 1 hour could improve solubility of CCB probably via through ternary complex formation.

Table 20 Total drug content and drug dissolved content of celecoxib eye drop suspension with and without heating method

Formulation	Drug concentration (mg/ml)	Drug dissolved concentration (µg/ml)	% drug content	% dissolved content
F9	4.975 ± 0.113	509.0 ± 8.3	99.5 ± 2.3	10.18 ± 0.17
F15	4.715 ± 0.099	33.7 ± 8.0	94.3 ± 2.0	0.67 ± 0.16
F18	4.660 ± 0.178	23.3 ± 1.8	93.2 ± 3.6	0.47 ± 0.01
F9so	4.597 ± 0.359	2,349.2 ± 113.3	91.9 ± 7.2	46.98 ± 2.27
F15so	5.143 ± 0.278	66.3 ± 7.2	102.9 ± 5.6	1.33 ± 0.14
F18so	5.015 ± 0.156	169.5 ± 8.0	100.3 ± 3.1	3.39 ± 0.16

so; heating method by sonication at 70°C for 1 hr.

6.2 Particle size analysis

The Aggregate size distribution of CCB/CD complex in formulation.

The particle size and size distribution of the supernatant of CCB eye drop suspensions measured by DLS technique are shown in Figure 26. It demonstrated that all samples have the characteristic of aggregates size. An intensity peak at about 1–2 nm indicated the existing of non-aggregated complex as solubilized component while the second and the third peak referred to the complex aggregates of CCB/CD/polymer. Aggregates sizes of the second and the third intensity peak in

formulations ranged from 10 nm to 80 nm and 180 nm to 400 nm, respectively (Table 21). The formulations passed through heating method (F9so, F15so and F18so) displayed the complex aggregates relatively larger than those of unheated formulations. It was suggested that the increasing of aggregate sizes in formulations was influenced by heating method through inclusion and non-inclusion complexes or micelle-like assembles resulting in increasing CCB solubilization. Moreover, the aggregate sizes of formulations containing γ-CD (F15, F15so, F18 and F18so) were slightly larger than the formulations containing RM-β-CD. It is possible that the larger aggregates were self-aggregates of γ-CD in formulation (Jansook, Moya-Ortega, and Loftsson, 2010). Assuming that the most probable mechanism is the hydrogen bond related self-aggregation of γ-CD monomers (Szente, Szejtli, and Kis, 1998). However, there are various factors such as the formulation components and type of CDs which influence on the aggregate size of complex (Puskás et al., 2013; Ryzhakov et al., 2016). Numerous studies have been investigated the complex aggregates formation. The inclusion complex of CD are able to form larger aggregates in aqueous solution, which solubilized themselves or hydrophobic drugs through non-inclusion complex or micelle-like assembles (Loftsson et al., 2004). Micelle-like structures in aqueous solution consisted of trans-β-carotene β-CD and γ-CD obtained diameter of aggregates more than 200 nm (Mele, Mendichi, and Selva, 1998).

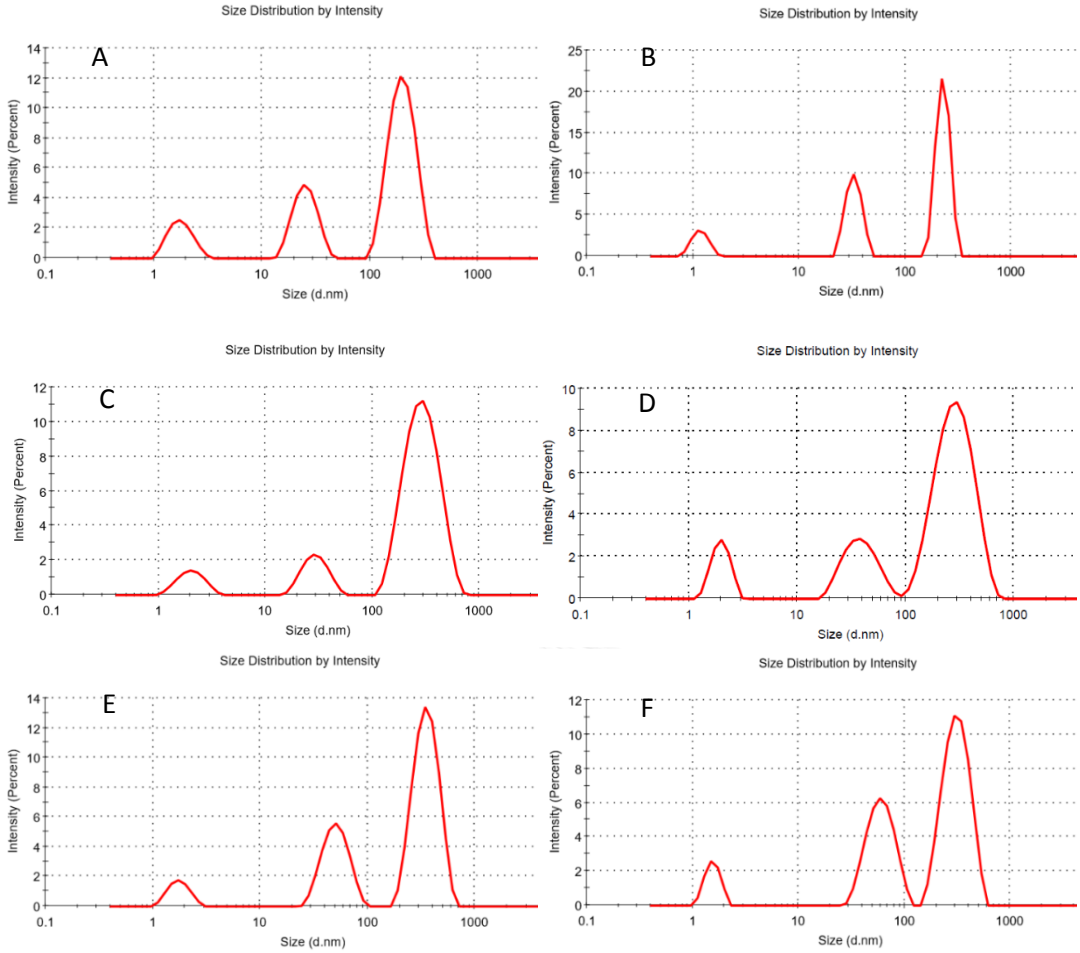

Figure 26 The aggregate size and size distribution of CCB/CD complex in formulation at 25°C in DI water determined by DLS technique; (A) F9, (B) F9so, (C) F15, (D) F15so, (E) F18, (F) F18so.

Table 21 The aggregate size and size distribution of selected CCB-CD eye drop formulations determined by DLS technique.

Formulation	Polymer	CD	Particle size (nm)
F9	0.5% HA	RM-β-CD	221.1 ± 18.1 29.2 ± 7.2 1.92 ± 0.2
F15	0.5% HA	γ-CD	307.2 ± 45.7 34.1 ± 5.4 2.0 ± 0.2
F18	0.5% HPMC	γ-CD	304.2 ± 64.4 45.2 ± 14.9 1.7 ± 0.1
F9so	0.5% HA	RM-β-CD	230.1 ± 26.7 34.0 ± 9.0 1.6 ± 0.5
F15so	0.5% HA	γ-CD	332.6 ± 32.2 48.6 ± 10.7 2.0 ± 0.3
F18so	0.5% HPMC	γ-CD	350.4 ± 35.3 58.1 ± 15.7 1.9 ± 0.4

so*, Sonication at 70°C for 1 hr

γ-CDs are carbohydrates and do self-assemble like other carbohydrates in aqueous solution. It is probable to form larger self-aggregates in aqueous solutions with opalescence and precipitation even at low concentrations. Regarding to RM-β-CD, the phase solubility of triclosan and triclocarban was determined. It displayed A_p-type diagram indicating formation of higher-order complexes and their complex aggregates were confirmed by NMR techniques (Duan et al., 2005). In addition, Puskas et al., (2013) studied the effect of glucose, urea, and inorganic salts on the complex

formation of RM-β-CD, SBE-β-CD and HP-β-CD containing cholesterol. A mixture of non-aggregated complexes with a diameter of 1-2 nm and aggregated complexes with a diameter ranging from about 100 to 1000 nm were observed by DLS technique.

The particle size of suspensions

Ophthalmic suspensions possibly used to increase the corneal retention time of a drug providing sustained and enhanced ocular bioavailability. The particles in suspensions are desired to be a micronized form (less than 10 μm in diameter) to prevent irritation or scratching of the eye (Kaur and Kanwar, 2002). Suspensions are commonly prepared by dispersing micronized drug powder in a suitable aqueous vehicle. A reduction in particle size usually improves the patient comfort and acceptable suspension (Aldrich et al., 2013). In this study, the particle in suspension was reduced by media milling technique. The particle size of suspensions was measured by optical microscope and their morphology was observed by SEM.

Table 22 the particle size of celecoxib eye drop suspension with and without heating method determined by optical microscope

Formulation	Particle size (μm) (Mean ± S.D.)
F9	3.90 ± 1.63
F15	5.13 ± 2.35
F18	4.82 ± 2.18
F9so	3.77 ± 1.85
F15so	4.43 ± 2.09
F18so	4.32 ± 2.10

so; Sonication at 70°C for 1 hr.

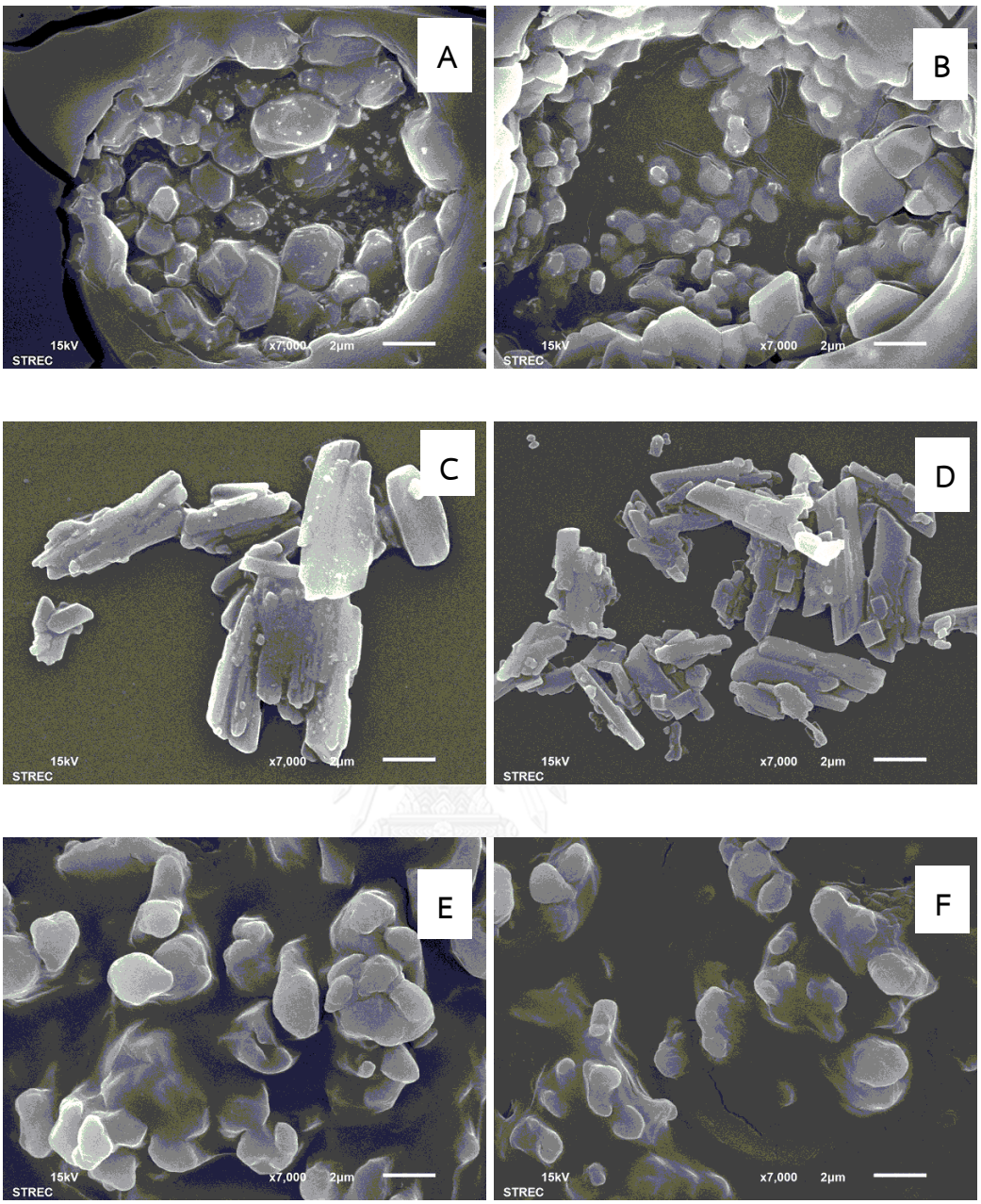

Figure 27 SEM Photographs of celecoxib eye drop formulation with and without heating method; (A) F9, (B) F9so, (C) F15, (D) F15so, (E) F18, (F) F18so

Table 22 displays the particle size of CCB eye drop suspensions and Figure 27 shows SEM Photographs of CCB eye drop suspensions. The particles size of F9so, F15so and F18so showed slightly smaller than those of unheated ones. The particle size of all CCB formulations (heated and unheated) not more than 8 µm which was acceptable for eye drop suspension's criteria. Especially, F9so eye drop suspension

(Figure 27B) showed relatively spherical shape with the smallest particle size and narrow size distribution. It ensures that our CCB-CD ophthalmic suspension did not cause to irritate to the eye. Both techniques, media mill and sonication with heating, provide synergistic effect in the particle size reduction.

6.3 In-vitro permeation of heated and unheated CCB/CD suspension

Figure 28 displays the permeation profile of heated and unheated CCB-CD eye drop suspensions through semi-permeable membrane (MWCO 12–14,000 Da). Table 23 shows the flux and P_{app} values of unheated and heated CCB eye drop suspensions (calculated from the slope of permeation profile in Figure 28). It is generalized that the increasing % dissolved CCB content, the higher amount of drug permeation through semi-permeable membrane was observed. And also, when considering to the flux permeation, the flux value of F9so and F18so were 2-folds and 4-folds higher than F9 and F18, respectively. Although % dissolved CCB content of F15so was higher than F15 about 2-folds, the permeation flux of heated formulation was not increased. Among the CCB eye drop suspension tested, CCB eye drop suspension containing RM-β-CD and HA with heating method showed the greatest flux value was observed.

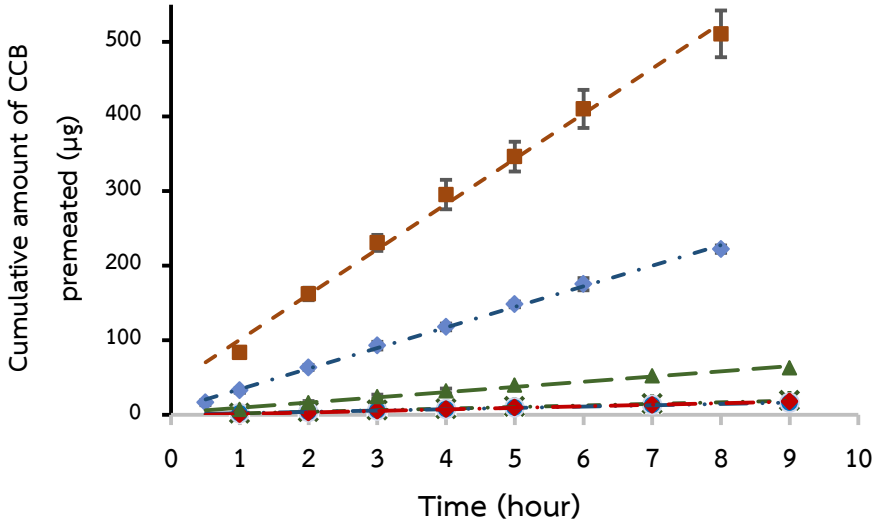

Figure 28 The permeation profile of CCB-CD eye drop suspension with and without heating method through semi-permeable membrane (MWCO 12–14,000 Da); (◆) F9, (✕) F15, (●) F18, (■) F9so, (◆) F15so, (▲) F18so

Table 23 Flux (J) and apparent permeation coefficient (P_{app}) of celecoxib eye drop suspension with and without heating method through semi-permeable membrane (MWCO 12-14,000 Da)

Formulation	Flux (µg/hr/cm^2)	P_{app} (cm/hr)
F9	12.17 ± 0.16	0.0239 ± 0.0002
F15	0.94 ± 0.06	0.0287 ± 0.0057
F18	0.79 ± 0.02	0.0341 ± 0.0024
F9so	26.72 ± 1.74	0.0114 ± 0.0010
F15so	0.93 ± 0.10	0.0141 ± 0.0017
F18so	3.06 ± 0.14	0.0181 ± 0.0008

so; heating method by sonication at 70°C for 1 hr.

However, P_{app} of all heated formulations were decreased when compared with the following unheated formulation (Table 23). It is possible that the bonds activation between the components i.e., CCB, CD and water-soluble polymers as ternary complex during the heating method were formed. The increasing interaction between CCB-CD complex and polymer leaded to the increasing the initial dissolved CCB concentration (Cd). However, due to its great interaction and retaining in polymer network resulted in decreasing P_{app} through the membrane.

6.4 In-vitro permeation through simulated artificial vitreous humor

The study of *in-vitro* permeation through artificial vitreous humor model was simulated the permeation of drug through biological membrane such as cornea and conjunctival and through vitreous humor into the posterior segment of eye. In theory, when the drug/CD complex penetrated through aqueous layer barrier, the drug in the complex was rapid dynamic equilibrium release to the “free drug”, and increased the drug concentration gradient over the membrane which was readily absorbed to the site of action. Table 24 displays the permeation flux and apparent permeation coefficient (P_{app}) of heated and unheated CCB eye drop suspensions through simulated artificial vitreous humor.

Table 24 The permeation f*lux (J) and* apparent *permeation coefficient (P_{app}) of celecoxib eye drop suspension with and without heating method through simulated artificial vitreous humor*

Formulation	Flux (μg/hr/cm^2)	P_{app} (cm/hr)
F9	1.55 ± 0.20	0.0030 ± 0.0004
F15	0.11 ± 0.05	0.0033 ± 0.0012
F18	0.17 ± 0.05	0.0075 ± 0.0027
F9so	2.98 ± 0.16	0.0013 ± 0.0001
F15so	0.14 ± 0.01	0.0022 ± 0.0003
F18so	0.34 ± 0.01	0.0020 ± 0.0002

so*; heating method by sonication at 70°C for 1 hr.

As expected, because the percentage of dissolved content of suspension containing RM-β-CD were higher, the flux values of the suspension containing RM-β-CD (F9 and F9so) showed greater than suspension containing γ-CD (F15, F15so, F18 and F18so). The flux values of F9so and F18so was 2-folds greater than F9 and F18 while its value of F15 and F15so were slightly different. The polymer enhanced CD complexation of CCB by heating method may lead to higher drug flux through the simulated artificial vitreous humor model. In this study, only free drug and mono- and dimer of CCB/CD complexes were permeated through semipermeable membrane (MWCO 3,500 Da) and artificial vitreous humor to the chamber which almost imitated the delivering of CCB to the posterior segment of eye. On account of limitation of number of CCB molecules to enter and long distance of simulated artificial vitreous humor model resulting in the decreasing of flux permeation and the P_{app} when compared to the earlier *in-vitro* permeation data. It indicated that the MWCO of semi-permeable membrane, the length and its viscosity of vitreous humor model were possibly influenced on the permeation of CCB.

However, Sigurdsson et al. (2007) demonstrated that the topical absorption following of dexamethasone containing CD eye drop application could be reached to the posterior segment of the rabbit eyes. In addition, the concentration of the drug in the retina was higher than the vitreous humor for 3-folds. It possible due to that the non-corneal absorption by diffusion of the drug through the conjunctiva, sclera,

choroid as well as systemic absorption from the conjunctival blood vessels and re-entering to the retina were occurred after the topical eye drop application (Boddu et al., 2014). Therefore, in fact, the concentration in the retina of CCB may be possibly increased via these pathway mechanisms.

From above results, F9so still exhibited the highest flux value of CCB among formulations tested which gave high drug levels in the receptor compartment. Thus, F9so eye drop suspension containing RM-β-CD and HA is the great potential formulation which can deliver CCB into the posterior segment of the eye. Due to the several factors i.e., the eye, barriers, pre-corneal clearances including the absorption pathways for topically eye drop to the posterior segment of the eye, the *in-vivo* study is required to be further study.

CHAPTER V
CONCLUSIONS

Celecoxib (CCB), a poorly water-soluble drug, its solubility can be enhanced by using cyclodextrin (CD) through inclusion complex formation. The CCB/CD complex in the aqueous solutions has thermal stability and no degradation peak was observed during the heating process.

Among selected CDs tested, RM-β-CD, β-CD derivatives, exhibited the highest complexation efficiency of CCB and presented an A_p-type phase solubility diagram. γ-CD was selected due to its safety. The addition of polymer in aqueous CD solutions provided synergistic effect of CD solubilization via ternary complex formation. HPMC showed the highest increments in solubilizing efficiency following HA and chitosan, respectively. The aggregate sizes of CCB/CD/polymer observed by DLS and TEM techniques were in the range of 250-350 nm. It was suggested that these complex aggregates could be capable of solubilizing drugs. The data obtained from the DSC, PXRD, and FT-IR studies demonstrated that CCB formed an inclusion complex with CD. The ^{1}H-NMR result indicated that CCB partially included and deeply inserted into the cavity of RM-β-CD and γ-CD, respectively.

The CCB eye drop formulation consisted of RM-β-CD and γ-CD as solubilizers, HPMC and HA as mucoadhesive polymers were developed. The physicochemical and chemical properties of all formulations were determined i.e., pH and osmolality of formulations were closely to lacrimal fluid which possibly not marked discomfort after applied. The solid particle sizes of suspensions shown below 10 μm which indicated that CCB-CD ophthalmic suspension did not irritate the eye. The percentage total drug content of all formulations met in a limit of 90-110%. In most cases, when applied the heating method, % dissolved drug content was increased. After sedimentation, they were easily re-dispersed to become uniform suspension by gently shaking; except the formulations containing RM-β-CD and HPMC.

No mucoadhesive was observed in the CCB eye drop solution while CCB eye drop suspension containing 0.25-0.5% w/v of polymers i.e., HA and HPMC had mucoadhesive properties. This was due to their solid particles parts which washed more slowly from the mucin-coated membrane. Furthermore, the CCB eye drop formulation containing HA showed the mucoadhesive properties greater than that of HPMC at 0.5% w/v while there were no significantly different in lower concentration of polymer. Thus, these formulations are possible to increase the contact time on eye surface and provide to enhance ocular bioavailability.

The *in-vitro* permeation study was investigated the drug diffuse through a semipermeable membrane. The formulations containing RM-β-CD showed distinguishable difference in greater permeation flux than formulations containing γ-CD due to higher CCB dissolved content. It indicated that the increasing of % drug dissolved content possibly lead to enhance the permeation by increasing the drug concentration gradient over the surface of membrane. Moreover, the permeation of the formulation could be improved by increasing solubility of CCB through heating method. In contrast, in the formulation containing γ-CD, the higher P_{app} was noticed because of their lower CCB/γ-CD complexes molecular weight size. However, the formulation containing RM-β-CD and HA showed the highest flux permeation through semipermeable membrane and also through simulated vitreous humor including relatively good mucoadhesion. Therefore, it can be good candidate for further study to deliver CCB to the posterior segment of the eye.

REFERENCES

Al-Muhammed, J., Ozer, A. Y., Ercan, M. T., and Hincal, A. A. (1996). In-vivo studies on dexamethasone sodium phosphate liposomes. Journal Microencapsulation, 13(3), 293-306.

Aldrich, D. S., Bach, C. M., Brown, W., Chambers, W., Fleitman, J., Hunt, D., et al. (2013). Ophthalmic Preparations 2013;39(5). 39(5). (P) \\usp-netapp2\share\SHARE\USPNF\PRINTQ\pager\xmlIn\NEP_20130828110441_S200824.xml Aug. 28, 2013 11:04:44

Amrite, A. C., Ayalasomayajula, S. P., Cheruvu, N. P., and Kompella, U. B. (2006). Single periocular injection of celecoxib-PLGA microparticles inhibits diabetes-induced elevations in retinal PGE2, VEGF, and vascular leakage. Investigative Ophthalmology & Visual Science, 47(3), 1149-1160.

Amrite, A. C., and Kompella, U. B. (2008). Celecoxib inhibits proliferation of retinal pigment epithelial and choroid-retinal endothelial cells by a cyclooxygenase-2-independent mechanism. Journal of Pharmacology and Experimental Therapeutics 324(2), 749-758.

Ayalasomayajula, S. P., and Kompella, U. B. (2003). Celecoxib, a selective cyclooxygenase-2 inhibitor, inhibits retinal vascular endothelial growth factor expression and vascular leakage in a streptozotocin-induced diabetic rat model. European Journal of Pharmacology, 458(3), 283-289.

Ayalasomayajula, S. P., and Kompella, U. B. (2004). Retinal delivery of celecoxib is several-fold higher following subconjunctival administration compared to systemic administration. Pharmaceutical Research, 21(10), 1797-1804.

Barza, M. (1978). Factors affecting the intraocular penetration of antibiotics. The influence of route, inflammation, animal species and tissue pigmentation. Scandinavian Jounal of Infectious Disease Supplement(14), 151-159.

Bin Choy, Y., Park, J. H., and Prausnitz, M. R. (2008). Mucoadhesive Microparticles Engineered for Ophthalmic Drug Delivery. Journal of Physics and Chemistry of Solids, 69(5-6), 1533-1536.

Boddu, S. H., Gupta, H., and Patel, S. (2014). Drug delivery to the back of the eye following topical administration: an update on research and patenting activity. Recent Patents on Drug Delivery & Formulation, 8(1), 27-36.

Cappello, B., Maio, C., Iervolino, M., and Miro, A. (2007). Combined effect of hydroxypropyl methylcellulose and hydroxypropyl-beta-cyclodextrin on physicochemical and dissolution properties of celecoxib. Journal of Inclusion Phenomena and Macrocyclic Chemistry, 59(3-4), 237-244.

Chaudhary, A. N., U. Gulati, N. Sharma, V. K.. Khosa R. L.. (2012). Enhancement of solubilization and bioavailability of poorly soluble drugs by physical and chemical modifications: A recent review. Journal of Advanced Pharmacy Education & Research, 2(1), 32-67.

Cheruvu, N. P., Amrite, A. C., and Kompella, U. B. (2009). Effect of diabetes on transscleral delivery of celecoxib. Pharmaceutical Research, 26(2), 404-414.

Choubey, P., Manavalan, R., Dabre, R., and Jain, G. (2013). Preformulation Studies for development of a generic capsule formulation of Celecoxib comparable to the branded (Reference) Product Innovations in Pharmaceuticals and Pharmacotherapy 1(3), 230-243.

Chowdary, K. P., and Srinivas, S. V. (2006). Influence of hydrophilic polymers on celecoxib complexation with hydroxypropyl beta-cyclodextrin. AAPS PharmSciTech, 7(3), 1-6.

Congdon, N., O'Colmain, B., Klaver, C. C., Klein, R., Munoz, B., Friedman, D. S., et al. (2004). Causes and prevalence of visual impairment among adults in the United States. Archives of Ophthalmology, 122(4), 477-485.

Davies, N. M., McLachlan, A. J., Day, R. O., and Williams, K. M. (2000). Clinical pharmacokinetics and pharmacodynamics of celecoxib: a selective cyclo-oxygenase-2 inhibitor. Clinical Pharmacokinetics, 38(3), 225-242.

Del Valle, E. M. M. (2004). Cyclodextrins and their uses: a review. Process Biochemistry, 39(9), 1033-1046.

Dhanapal, R., and Ratna, J. V. (2012). Ocular Drug Delivery System- A Review. International Journal of Innovative Drug Discovery, 2(1), 4-15.

Drimalova, E., Velebny, V., Sasinkova, V., Hromadkova, Z., and Ebringerova, A. (2005). Degradation of hyaluronan by ultrasonication in comparison to microwave and conventional heating. Carbohydrate Polymers, 61(4), 420-426.

Duan, M. S., Zhao, N., Ossurardottir, I. B., Thorsteinsson, T., and Loftsson, T. (2005). Cyclodextrin solubilization of the antibacterial agents triclosan and triclocarban: formation of aggregates and higher-order complexes. International Journal of Pharmaceutics, 297(1-2), 213-222.

Einfal, T., Planinsek, O., and Hrovat, K. (2013). Methods of amorphization and investigation of the amorphous state. Acta Pharmaceutica, 63(3), 305-334.

Felt, O., Furrer, P., Mayer, J. M., Plazonnet, B., Buri, P., and Gurny, R. (1999). Topical use of chitosan in ophthalmology: tolerance assessment and evaluation of precorneal retention. International Journal of Pharmaceutics, 180(2), 185-193.

Ganza-Gonzalez, A., Vila-Jato, J. L., Anguiano-Igea, S., Otero-Espinar, F. J., and Blanco-Méndez, J. (1994). A proton nuclear magnetic resonance study of the inclusion complex of naproxen with beta-cyclodextrin. International Journal of Pharmaceutics, 106(3), 179-185.

Gaudana, R., Ananthula, H. K., Parenky, A., and Mitra, A. K. (2010). Ocular Drug Delivery. American Association of Pharmaceutical Scientists, 12(3), 348-360.

González-Gaitano, G., Rodríguez, P., Isasi, J. R., Fuentes, M., Tardajos, G., and Sánchez, M. (2002). The Aggregation of Cyclodextrins as Studied by Photon Correlation Spectroscopy. Journal of inclusion phenomena and macrocyclic chemistry, 44(1), 101-105.

Greatbanks, D., and Pickford, R. (1987). Cyclodextrins as chiral complexing agents in water, and their application to optical purity measurements. Magnetic Resonance in Chemistry, 25(3), 208-215.

Hedges, A. R. (1998). Industrial Applications of Cyclodextrins. Chemical Reviews, 98(5), 2035-2044.

Higuchi, T., and Connors, K. A. (1965). Phase solubility techniques. Advances in Analytical Chemistry and Instrumentation, 4, 117-212.

Homayouni, A., Sadeghi, F., Nokhodchi, A., Varshosaz, J., and Afrasiabi Garekani, H. (2015). Preparation and Characterization of Celecoxib Dispersions in Soluplus®: Comparison of Spray Drying and Conventional Methods. Iranian Journal of Pharmaceutical Research, 14(1), 35-50.

Hughes, P. M., Olejnik, O., Chang-Lin, J. E., and Wilson, C. G. (2005). Topical and systemic drug delivery to the posterior segments. Advanced Drug Delivery Reviews, 57(14), 2010-2032.

Hui, H.-W., and Robinson, J. R. (1985). Ocular delivery of progesterone using a bioadhesive polymer. International Journal of Pharmaceutics, 26(3), 203-213.

Jager, R. D., Mieler, W. F., and Miller, J. W. (2008). Age-related macular degeneration. The New England Journal of Medicine, 358(24), 2606-2617.

Janoria, K. G., Gunda, S., Boddu, S. H., and Mitra, A. K. (2007). Novel approaches to retinal drug delivery. Expert Opinion on Drug Delivery, 4(4), 371-388.

Jansook, P., Moya-Ortega, M. D., and Loftsson, T. (2010). Effect of self-aggregation of gamma-cyclodextrin on drug solubilization. Journal of Inclusion Phenomena and Macrocyclic Chemistry, 68(1), 229-236.

Jansook, P., Stefansson, E., Thorsteinsdottir, M., Sigurdsson, B. B., Kristjansdottir, S. S., Bas, J. F., et al. (2010). Cyclodextrin solubilization of carbonic anhydrase inhibitor drugs: formulation of dorzolamide eye drop microparticle suspension. European Journal of Pharmaceutics and Biopharmaceutics, 76(2), 208-214.

Jenchitr, W., Ruamviboonsuk, P., Sanmee, A., and Pokawattana, N. (2011). Prevalence of age-related macular degeneration in Thailand. Ophthalmic Epidemiology, 18(1), 48-52.

Kaur, I. P., and Kanwar, M. (2002). Ocular preparations: the formulation approach. Drug Development and Industrial Pharmacy, 28(5), 473-493.

Keipert, S., Fedder, J., Böhm, A., and Hanke, B. (1996). Interactions between cyclodextrins and pilocarpine — As an example of a hydrophilic drug. International Journal of Pharmaceutics, 142(2), 153-162.

Kim, T. W., Lindsey, J. D., Aihara, M., Anthony, T. L., and Weinreb, R. N. (2002). Intraocular distribution of 70-kDa dextran after subconjunctival injection in mice. Investigative Ophthalmology & Visual Science, 43(6), 1809-1816.

Koevary, S. B. (2003). Pharmacokinetics of topical ocular drug delivery: potential uses for the treatment of diseases of the posterior segment and beyond. Current Drug Metabolism, 4(3), 213-222.

Kompella, U., Amrite, A. C., Pugazhenthi, V., and Cheruvu, N. P. S. (2010). Delivery of Celecoxib for Treating Diseases of the Eye: Influence of Pigment and Diabetes. Expert Opinion on Drug Delivery, 7(5), 631-645.

Kompella, U. B., Singh, S. R., and Sundaram, S. (2009). Methods and Compositions for Targeted Delivery of Therapeutic Agents: Google Patents, US 20090087494 A1.

Kramer, I., Haber, M., and Duis, A. (2002). Formulation Requirements for the Ophthalmic Use of Antiseptics. In A. Kramer and W. Behrens-Baumann. (Eds.), Antiseptic Prophylaxis and Therapy in Ocular Infections. Developments in Ophthalmology (Vol. 33, pp. 85-116). Basel: Karger

Kummer, M. P., Abbott, J. J., Dinser, S., and Nelson, B. J. (2007). *Artificial vitreous humor for in Vitro experiments.* Paper presented at the Annual International Conference of the IEEE Engineering in Medicine and Biology - Proceedings.

Kurz, D., and Ciulla, T. A. (2002). Novel approaches for retinal drug delivery. Ophthalmology Clinics of North America, 15(3), 405-410.

Lach, J. L., Huang, H.-S., and Schoenwald, R. D. (1983). Corneal Penetration Behavior of beta-Blocking Agents II: Assessment of Barrier Contributions. Journal of Pharmaceutical Sciences, 72(11), 1272-1279.

Lee, S.-B., Geroski, D. H., Prausnitz, M. R., and Edelhauser, H. F. (2004). Drug delivery through the sclera: effects of thickness, hydration, and sustained release systems. Experimental Eye Research, 78(3), 599-607.

Lipinski, C. A., Lombardo, F., Dominy, B. W., and Feeney, P. J. (2001). Experimental and computational approaches to estimate solubility and permeability in drug discovery and development settings. Advanced Drug Delivery Reviews, 46(1-3), 3-26.

Loftsson, T., and Brewster, M. E. (1996). Pharmaceutical applications of cyclodextrins. 1. Drug solubilization and stabilization. Journal of Pharmaceutical Sciences, 85(10), 1017-1025.

Loftsson, T., and Brewster, M. E. (2012). Cyclodextrins as functional excipients: methods to enhance complexation efficiency. Journal of Pharmaceutical Sciences, 101(9), 3019-3032.

Loftsson, T., Frikdriksdottir, H., Sigurkdardottir, A. M., and Ueda, H. (1994). The effect of water-soluble polymers on drug-cyclodextrin complexation. International Journal of Pharmaceutics, 110(2), 169-177.

Loftsson, T., Hreinsdottir, D., and Masson, M. (2005). Evaluation of cyclodextrin solubilization of drugs. International Journal of Pharmaceutics, 302(1-2), 18-28.

Loftsson, T., Hreinsdottir, D., and Stefansson, E. (2007). Cyclodextrin microparticles for drug delivery to the posterior segment of the eye: aqueous dexamethasone eye drops. Journal of Pharmacy and Pharmacology, 59(5), 629-635.

Loftsson, T., Jarho, P., Masson, M., and Jarvinen, T. (2005). Cyclodextrins in drug delivery. Expert Opinion Drug Delivery, 2(2), 335-351.

Loftsson, T., Magnúsdóttir, A., Másson, M., and Sigurjónsdóttir, J. F. (2004). Self-Association of Cyclodextrins and Cyclodextrin Complexes. Journal of Pharmaceutical Sciences, 91(11), 2307-2316.

Loftsson, T., Másson, M., and Sigurdsson, H. H. (2002). Cyclodextrins and drug permeability through semi-permeable cellophane membranes. International Journal of Pharmaceutics, 232(1–2), 35-43.

Loftsson, T., Vogensen, S. B., Brewster, M. E., and Konradsdottir, F. (2007). Effects of cyclodextrins on drug delivery through biological membranes. Journal of Pharmaceutical Sciences, 96(10), 2532-2546.

Loftssona, T., and Jarvinen, T. (1999). Cyclodextrins in ophthalmic drug delivery. Advanced Drug Delivery Reviews, 36(1), 59-79.

Lowry, K. M., and Beavers, E. M. (1994). Thermal stability of sodium hyaluronate in aqueous solution. Journal of Biomedical Material Research, 28(10), 1239-1244.

Ludwig, A. (2005). The use of mucoadhesive polymers in ocular drug delivery. Advanced Drug Delivery Reviews, 57(11), 1595-1639.

Maragos, S., Archontaki, H., Macheras, P., and Valsami, G. (2009). Effect of cyclodextrin complexation on the aqueous solubility and solubility/dose ratio of praziquantel. AAPS PharmSciTech, 10(4), 1444-1451.

Másson, M., Loftsson, T., Másson, G. s., and Stefánsson, E. (1999). Cyclodextrins as permeation enhancers: some theoretical evaluations and in vitro testing. Journal of Controlled Release, 59(1), 107-118.

Medarevic, D., Kachrimanis, K., Djuric, Z., and Ibric, S. (2015). Influence of hydrophilic polymers on the complexation of carbamazepine with hydroxypropyl-beta-cyclodextrin. European Journal of Pharmaceutical Sciences, 78, 273-285.

Mele, A., Mendichi, R., and Selva, A. (1998). Non-covalent associations of cyclomaltooligosaccharides (cyclodextrins) with trans-beta-carotene in water: evidence for the formation of large aggregates by light scattering and NMR spectroscopy. Carbohydrate Research, 310(4), 261-267.

Miranda, J. C. d., Martins, T. E. A., Veiga, F., and Ferraz, H. G. (2011). Cyclodextrins and ternary complexes: technology to improve solubility of poorly soluble drugs. Brazilian Journal of Pharmaceutical Sciences, 47, 665-681.

Mitra, A. K., Velagaleti, P. R., and Grau, U. M. (2010). Topical Drug Delivery Systems for Ophthalmic Use: Google Patents, US 20100310642 A1.

Mura, P. (2014). Analytical techniques for characterization of cyclodextrin complexes in aqueous solution: a review. Journal of Pharmaceutical and Biomedical Analysis, 101, 238-250.

Mura, P. (2015). Analytical techniques for characterization of cyclodextrin complexes in the solid state: A review. Journal of Pharmaceutical and Biomedical Analysis, 113, 226-238.

Mura, P., Faucci, M. T., and Bettinetti, G. P. (2001). The influence of polyvinylpyrrolidone on naproxen complexation with hydroxypropyl-beta-cyclodextrin. European Journal of Pharmaceutical Sciences, 13(2), 187-194.

Nagarsenker, M. S., and Joshi, M. S. (2005). Celecoxib-cyclodextrin systems: characterization and evaluation of in vitro and in vivo advantage. Drug Development and Industrial Pharmacy, 31(2), 169-178.

Nutan, M. T. H., and Reddy, I. K. (2010). General Principles of Suspensions. In A. K. Kulshreshtha, O. N. Singh and G. M. Wall (Eds.), Pharmaceutical Suspensions: From Formulation Development to Manufacturing (pp. 39-65). New York, NY: Springer New York.

Ozkiris, A. (2010). Anti-VEGF agents for age-related macular degeneration. Expert Opinion on Therapeutic Patents, 20(1), 103-118.

Pacella, E., Vestri, A. R., Muscella, R., Carbotti, M. R., Castellucci, M., Coi, L., et al. (2013). Preliminary results of an intravitreal dexamethasone implant (Ozurdex(R)) in patients with persistent diabetic macular edema. Clinical Ophthalmology, 7, 1423-1428.

Park, H., and Robinson, J. R. (1987). Mechanisms of Mucoadhesion of Poly(acrylic Acid) Hydrogels. Pharmaceutical Research, 4(6), 457-464.

Patel, J. S., and Patel, R. P. (2012). Preparation, characterization and in vitro dissolution study of Nitrazepam: Cyclodextrin inclusion complex. Journal of Pharmacy & Bioallied Sciences, 4(Suppl 1), S106-S107.

Puskás, I., Czifra, T. C., Fenyvesi, É., and Szente, L. (2013). Aggregation behavior of cyclodextrin and cholesterol in simulated human cerebrospinal fluid. Bioactive Carbohydrates and Dietary Fibre, 2(2), 157-163.

Raghava, S., Hammond, M., and Kompella, U. B. (2004). Periocular routes for retinal drug delivery. Expert Opinion Drug Delivery, 1(1), 99-114.

Rajesh, K., and Bhanudas, K. (2010). Preparation, physicochemical characterization, dissolution and formulation studies of telmisartan cyclodextrin inclusion complexes. Asian Journal of Pharmaceutics.

Rawat, S., and Jain, S. K. (2004). Solubility enhancement of celecoxib using beta-cyclodextrin inclusion complexes. Euopianr Journal of Pharmaceutics and Biopharmaceutics, 57(2), 263-267.

Reddy, M. N., Rehana, T., Ramakrishna, S., Chowdhary, K. P., and Diwan, P. V. (2004). Beta-cyclodextrin complexes of celecoxib: molecular-modeling, characterization, and dissolution studies. AAPS PharmSci, 6(1), 1-9.

Ribeiro, L. S., Ferreira, D. C., and Veiga, F. J. (2003). Physicochemical investigation of the effects of water-soluble polymers on vinpocetine complexation with beta-cyclodextrin and its sulfobutyl ether derivative in solution and solid state. European Journal of Pharmaceutical Sciences, 20(3), 253-266.

Ryzhakov, A., Do Thi, T., Stappaerts, J., Bertoletti, L., Kimpe, K., Sá Couto, A. R., et al. (2016). Self-Assembly of Cyclodextrins and Their Complexes in Aqueous Solutions. Journal of Pharmaceutical Sciences, 105(9), 2556-2569.

Saarinen-Savolainen, P., Jarvinen, T., Araki-Sasaki, K., Watanabe, H., and Urtti, A. (1998). Evaluation of cytotoxicity of various ophthalmic drugs, eye drop excipients and cyclodextrins in an immortalized human corneal epithelial cell line. Pharmaceutical Research, 15(8), 1275-1280.

Saettone, M. F., Chetoni, P., Tilde Torracca, M., Burgalassi, S., and Giannaccini, B. (1989). Evaluation of muco-adhesive properties and in vivo activity of ophthalmic vehicles based on hyaluronic acid. International Journal of Pharmaceutics, 51(3), 203-212.

Sandri, G., Bonferoni, M. C., Chetoni, P., Rossi, S., Ferrari, F., Ronchi, C., et al. (2006). Ophthalmic delivery systems based on drug-polymer-polymer ionic ternary interaction: in vitro and in vivo characterization. European Journal of Pharmaceutics and Biopharmaceutics, 62(1), 59-69.

Saokham, P., and Loftsson, T. (2017). gamma-Cyclodextrin. International Journal of Pharmaceutics, 516(1–2), 278-292.

Saraswathi, B., Balaji, A., and Umashankar, M. S. (2013). Polymers in Mucoadhesive Drug Delivery System-Lastest Updates International Journal of Pharmacy and Pharmaceutical Sciences 5(3), 423-430.

Schuette, J. M., and Warner, I. M. (1994). Structural considerations and fluorescence spectral definition of cyclodextrin/perylene complexes in the presence of 1-pentanol. Talanta, 41(5), 647-649.

Shankar Kuchekar, B., and Narkhede, M. (2007). The Effect of Water Soluble Polymers on Felodipine Aqueous Solubility and Complexing Abilities with Natural and Modified beta-Cyclodextrin. Iranian Journal of Pharmaceutical Sciences, 3(4), 197-202.

Shen, C., Yang, X., Wang, Y., Zhou, J., and Chen, C. (2012). Complexation of capsaicin with beta-cyclodextrins to improve pesticide formulations: effect on aqueous solubility, dissolution rate, stability and soil adsorption. Journal of Inclusion Phenomena and Macrocyclic Chemistry, 72(3), 263-274.

Sigurdardottir, A. M., and Loftsson, T. (1995). The effect of polyvinylpyrrolidone on cyclodextrin complexation of hydrocortisone and its diffusion through hairless mouse skin. International Journal of Pharmaceutics, 126(1), 73-78.

Sigurdsson, H. H., Konraethsdottir, F., Loftsson, T., and Stefansson, E. (2007). Topical and systemic absorption in delivery of dexamethasone to the anterior and posterior segments of the eye. Acta Ophthalmologica Scandinavica 85(6), 598-602.

Sinha, V. R., Anitha, R., Ghosh, S., Nanda, A., and Kumria, R. (2005). Complexation of celecoxib with beta-cyclodextrin: characterization of the interaction in solution and in solid state. Journal of Pharmaceutical Sciences, 94(3), 676-687.

Sinha, V. R., Nanda, A., Chadha, R., and Goel, H. (2011). Molecular simulation of hydroxypropyl-beta-cyclodextrin with hydrophobic selective Cox-II chemopreventive agent using host-guest phenomena. Acta Poloniae Pharmaceutica, 68(4), 585-592.

Srinivasulu, D., Sastry, B. S., Rajendra, P. Y., and OM, P. G. (2012). Separation and determination of process-rerated impurities of celecoxib in bulk drugs using reversed phase liquid chromatography. Famacia, 60(3), 436-447.

Szente, L., Szejtli, J., and Kis, G. L. (1998). Spontaneous opalescence of aqueous gamma-cyclodextrin solutions: complex formation or self-aggregation. Journal of Pharmaceutical Sciences, 87(6), 778-781.

Thomas, P. J., Clapton, S. D., Hemant, A., and Ashim, K. M. (2003). Mucoadhesive Polymers in Ophthalmic Drug Delivery Ophthalmic Drug Delivery Systems, Second Edition (pp. 409-435): CRC Press.

Tirucherai, G. S., and Mitra, A. K. (2003). Effect of hydroxypropyl beta cyclodextrin complexation on aqueous solubility, stability, and corneal permeation of acyl ester prodrugs of ganciclovir. AAPS PharmSciTech, 4(3), 1-12.

Uekama, K., Hirayama, F., and Irie, T. (1998). Cyclodextrin Drug Carrier Systems. Chemical Reviews, 98(5), 2045-2076.

Urtti, A., and Salminen, L. (1993). Minimizing systemic absorption of topically administered ophthalmic drugs. Survey of Ophthalmology, 37(6), 435-456.

Velagaleti, P., Anglade, E., Khan, J., Gilger, B. C., and Mitra, A. K. (2010). Topical delivery of hydrophobic drugs using a novel mixed nanomicellar technology to treat diseases of the anterior & posterior segments of the eye. Drug Delivery Technology 10(4), 42-47.

Ventura, C. A., Giannone, I., Paolino, D., Pistara, V., Corsaro, A., and Puglisi, G. (2005). Preparation of celecoxib-dimethyl-beta-cyclodextrin inclusion complex: characterization and in vitro permeation study. European Journal of Medicinal Chemistry, 40(7), 624-631.

Vyas, S. P., Mysore, N., Jaitely, V., and Venkatesan, N. (1998). Discoidal niosome based controlled ocular delivery of timolol maleate. Pharmazie, 53(7), 466-469.

Xu, J., Heys, J. J., Barocas, V. H., and Randolph, T. W. (2000). Permeability and diffusion in vitreous humor: implications for drug delivery. Pharmaceutical Research, 17(6), 664-669.

Yasueda, S.-i., Inada, K., Matsuhisa, K., Terayama, H., and Ohtori, A. (2004). Evaluation of ophthalmic suspensions using surface tension. European Journal of Pharmaceutics and Biopharmaceutics, 57(2), 377-382.

Yousef, F. O., Zughul, M. B., and Badwan, A. A. (2007). The modes of complexation of benzimidazole with aqueous beta-cyclodextrin explored by phase solubility, potentiometric titration, 1H-NMR and molecular modeling studies. Journal of Inclusion Phenomena and Macrocyclic Chemistry, 57(1), 519-523.

Yuzawa, M., Tamakoshi, A., Kawamura, T., Ohno, Y., Uyama, M., and Honda, T. (1997). Report on the nationwide epidemiological survey of exudative age-related macular degeneration in Japan. International Ophthalmology, 21(1), 1-3.

Zimmer, A., and Kreuter, J. (1995). Microspheres and nanoparticles used in ocular delivery systems. Advanced Drug Delivery Reviews, 16(1), 61-73.

APPENDICES

APPENDIX A

HPLC VALIDATION

1. Specificity

Figure A-1 and A-2 demonstrate the chromatograms of PBS, α-CD, β-CD, γ-CD, RM-β-CD, HP-β-CD, chitosan, hyaluronic acid, HPMC, BAC, EDTA, mobile phase and various concentrations of standard solution of CCB. CCB was eluted as a distinct peak with the retention time of 11.2-11.9 minutes and peak solvent which has a retention time of 1.5-2.0 minutes. All of excipients in formulation had no peak which interfere CCB peak when were injected in the same condition. This resulted indicated that it was specific to detect CCB content without interferences.

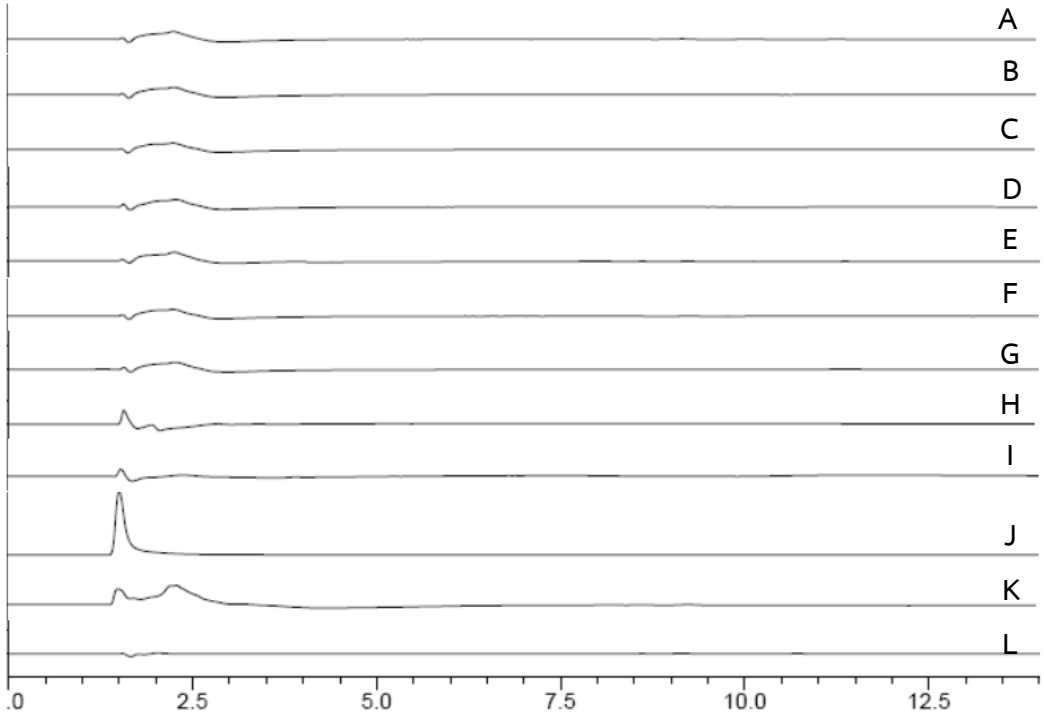

Figure A- 1 The HPLC chromatograms of (A) PBS pH 7.4, (B) α-CD, (C) β-CD, (D) γ-CD, (E) RM-β-CD, (F) HP-β-CD, (G) chitosan, (H) hyaluronic acid, (I) HPMC, (J) BAC, (K) EDTA, and (L) mobile phase

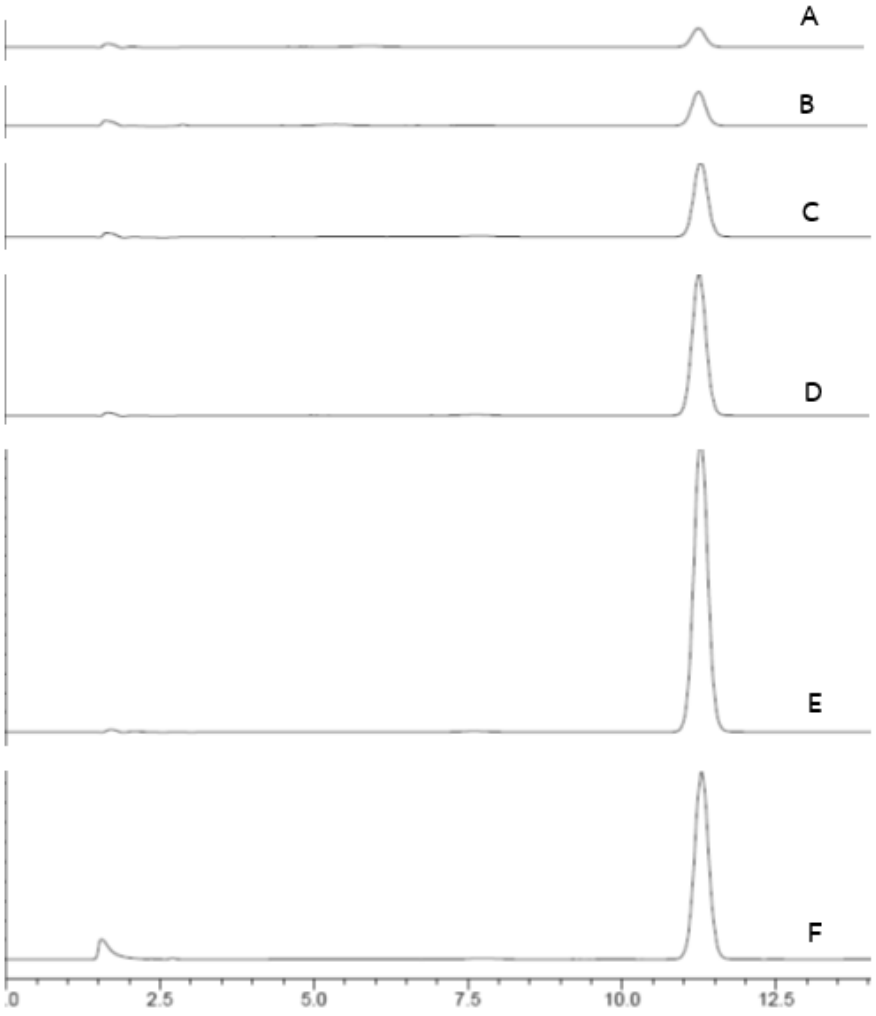

Figure A- 2 The HPLC chromatograms of the standard solution of CCB (A) 0.5 µg/ml, (B) 1.0 µg/ml, (C) 2.0 µg/ml, (D) 4.0 µg/ml, (E) 8.0 µg/ml and (F) 5% w/v CCB suspension in mobile phase

2. Linearity

The chromatograms of CCB dissolved in mobile phase (acetonitrile: water; 55:45) are demonstrated in figure A-2. The retention time of CCB was about 11.22-11.86 minutes. The calibration curve was plotted between the peak area and concentration of CCB in µg/ml. The results are shown in table A-1, A-2, A-3 and figure A-3, A-4, A-5. The linear regression analysis was performs with the coefficient of determination (R^2) of 0.9998-1.0000. These results concluded that the HPLC condition was acceptable to determine the amount of CCB in the formulation

Table A- 1 Data of calibration curve of standard CCB solutions (N0.1)

CCB concentration (µg/ml)	Peak areas of CCB				SD	% CV
	area(r1)	area(r2)	area(r3)	Mean		
0.0499	3050	3058	3025	3044	17.2	0.6
0.4985	30401	30726	30368	30498	197.9	0.6
0.9970	57801	57725	58023	57850	154.8	0.3
1.9940	126574	126759	126343	126559	208.4	0.2
3.9880	236050	235307	237969	236442	1373.6	0.6
7.9760	487569	493384	493479	491477	3385.0	0.7
15.9520	999161	998997	999980	999379	526.6	0.1

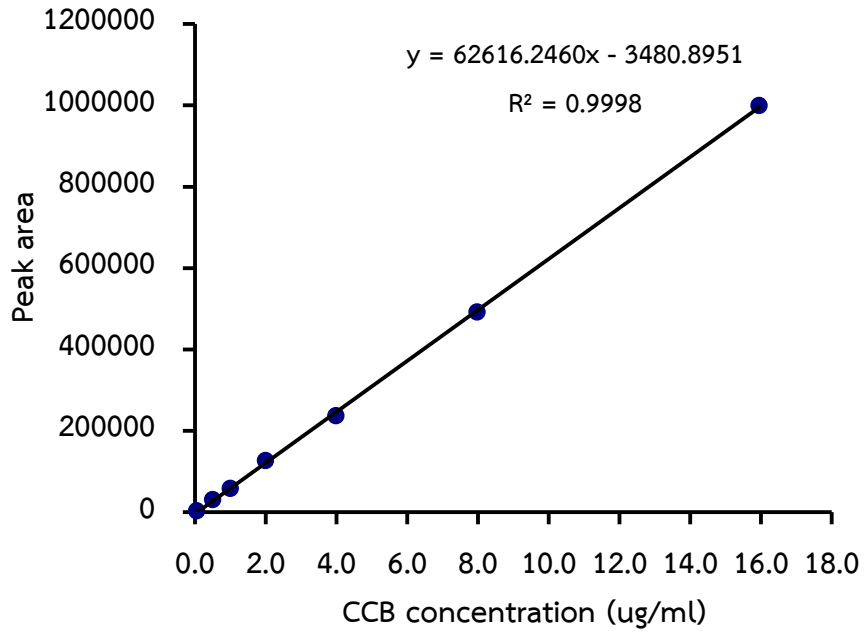

Figure A- 3 Calibration curve of standard CCB solutions by HPLC method (N0.1)

Table A- 2 Data of calibration curve of standard CCB solutions (N0.2)

CCB concentration (µg/ml)	Peak areas of CCB				SD	% CV
	area(r1)	area(r2)	area(r3)	Mean		
0.0500	3172	3187	3202	3187	15.0	0.47
0.4995	30414	30063	30364	30280	189.9	0.63
0.9990	57546	57795	58594	57978	547.5	0.94
1.9980	126995	127655	128075	127575	544.4	0.43
3.9960	248599	250490	251486	250192	1466.4	0.59
7.9920	488857	495720	496273	493617	4131.3	0.84
15.9840	1001129	1000613	1001507	1002113	448.8	0.04

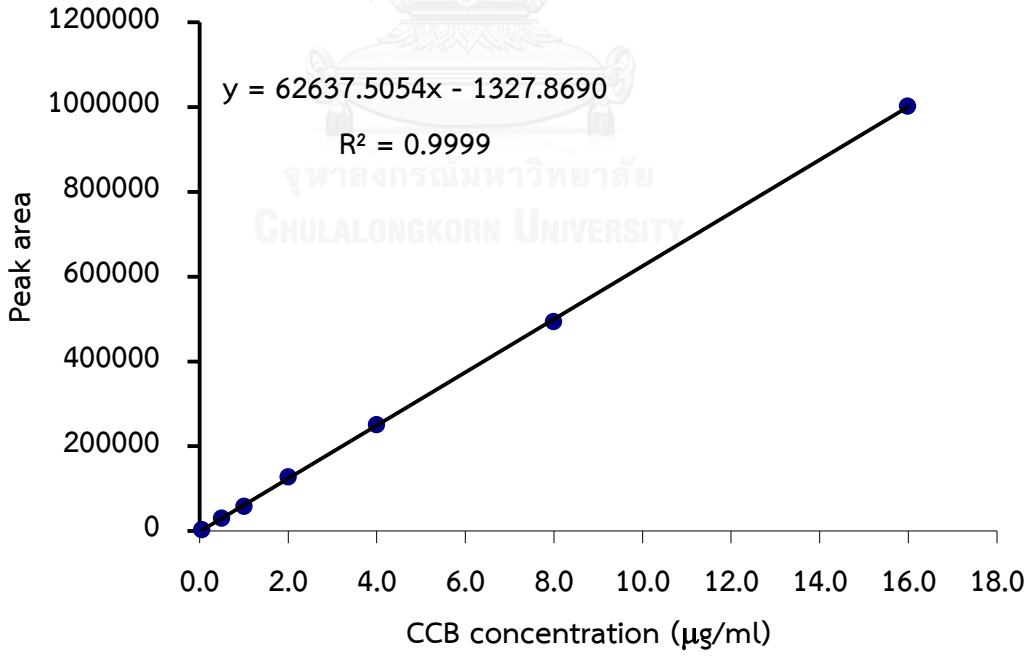

Figure A- 4 Calibration curve of standard CCB solutions by HPLC method (N0.2

Table A- 3 Data of calibration curve of standard CCB solutions (N0.3)

CCB concentration (µg/ml)	Peak areas of CCB				SD	% CV
	area(r1)	area(r2)	area(r3)	Mean		
0.0499	3124	3097	3148	3123	25.5	0.82
0.4985	30944	30313	31042	30766	395.6	1.29
0.9970	58805	58800	59040	58882	137.1	0.23
1.9940	125959	125906	125045	125637	513.1	0.41
3.9880	250474	252212	252161	251616	989.0	0.39
7.9760	496709	497952	499222	497961	1256.5	0.25
15.9520	997053	997185	992696	995645	2554.5	0.26

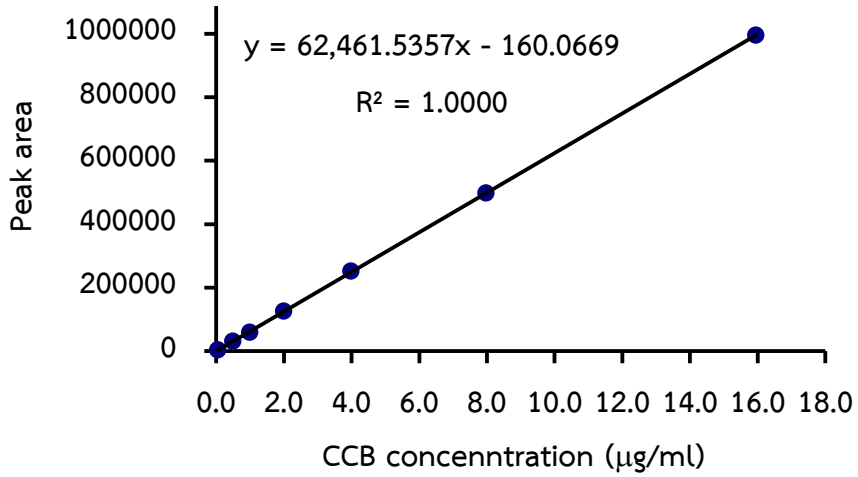

Figure A- 5 Calibration curve of standard CCB solutions by HPLC method (N0.3)

3. Precision

Table A-4 and A-5 shows data of within run precision and between run precision of CCB assayed by the HPLC method, respectively. The percentage of coefficient of variation (%CV) values of peak area in both within run and between run precisions

were low (0.24-0.80% and 0.14-1.43%, respectively). Consequently, the HPLC condition could be used to determine the amount of CCB over a period of time studies

Table A- 4 Data of within run precision of CCB analyzed by HPLC method.

CCB Conc.	Peak areas of CCB							
(µg/ml)	(n1)	(n2)	(n3)	(n4)	(n5)	mean	SD	% CV
0.0499	3050	3029	3073	3040	3089	3056.20	24.49	0.80
1.9940	126574	126942	126072	127526	126007	126624.20	730.18	0.58
15.9520	999161	1000331	997332	1002228	1003463	1000503.00	2430.18	0.24

Table A- 5 Data of between run precision of CCB analyzed by HPLC method.

CCB Conc.	Peak areas of CCB						
(µg/ml)	N	Day 1	Day 2	Day 3	Mean	SD	% CV
0.0499	n1	3050	3069	3039	3052.67	15.18	0.50
	n2	3029	3049	3065	3047.67	18.04	0.59
	n3	3073	3134	3070	3092.33	36.12	1.17
	n4	3040	3023	3087	3050.00	33.15	1.09
	n5	3089	3111	3056	3085.33	27.68	0.90
	Average	3056.2	3077.2	3063.4	3065.60	10.67	0.35
1.9940	n1	126574	126341	126224	126379.67	178.18	0.14
	n2	126942	126671	126124	126579.00	416.69	0.33
	n3	126072	126873	126318	126421.00	410.31	0.32
	n4	127526	128750	125177	127151.00	1815.78	1.43
	n5	126007	127678	124241	125975.33	1718.72	1.36
	Average	126624.2	127262.6	125616.8	126501.20	829.77	0.66
15.9520	n1	999161	1001765	994778	998568.00	3531.05	0.35
	n2	1000331	1001454	997375	999720.00	2107.02	0.21
	n3	997332	1000380	996954	998222.00	1878.42	0.19
	n4	1002228	1001622	992395	998748.33	5510.48	0.55
	n5	1003463	1001507	995932	1000300.67	3907.74	0.39
	Average	1000503	1001345.6	995486.8	999111.80	3167.49	0.32

4. Accuracy

Table A-6, A-7 and A-8 demonstrate the percentage of analytical recovery in each concentration of CCB for three determinations. The mean percentage recoveries were 100.6%, 100.5% and 100.9% with the %CV of percentage recovery were low 0.4%, 0.9% and 1.0%, respectively. Form the result indicated that the HPLC method could be used to accurately determine CCB within the concentration range of 0.05-16.0 µg/ml.

Table A- 6 Data of accuracy of CCB analyzed by HPLC method (No.1)

Actual conc.	Peak areas				Mean analytical	%
(µg/ml)	area(r1)	area(r2)	area(r3)	Mean	concentration	discovery
4.09	256765	258267	257370	257467.3	4.1	100.8
5.03	313625	315024	314467	314372.0	5.0	100.1
6.09	383543	381029	385351	383307.7	6.1	100.8
					Mean	100.6
					SD	0.4
					%CV	0.4

Table A- 7 Data of accuracy of CCB analyzed by HPLC method (No.2)

Actual conc.	Peak areas				Mean analytical	%
(µg/ml)	area(r1)	area(r2)	area(r3)	Mean	concentration	discovery
4.09	259062	257830	258775	258555.7	4.1	101.3
4.98	307434	310449	309932	309271.7	5.0	99.5
6.08	377914	384307	383575	381932.0	6.1	100.6
					Mean	100.5
					SD	0.9
					%CV	0.9

Table A- 8 Data of accuracy of CCB analyzed by HPLC method (No.3)

Actual conc. (µg/ml)	Peak areas				Mean analytical concentration	% discovery
	area(r1)	area(r2)	area(r3)	Mean		
4.09	261331	260322	259187	260280.0	4.2	101.9
5.01	312739	313047	313324	313036.7	5.0	100.1
6.01	378545	378296	375762	377534.3	6.0	100.6
					Mean	100.9
					SD	1.0
					%CV	1.0

APPENDIX B

PHYSICOCHEMICAL PROPERTIES

Table B- 1 The pH data of each formulation

Formulation	CD	Polymer	% polymer (w/v)	pH				
				n1	n2	n3	Average	S.D.
F1	RM-β-CD	HA	0.10	7.3	7.38	7.44	7.37	0.07
F2			0.25	7.35	7.33	7.35	7.34	0.01
F3			0.50	7.32	7.32	7.33	7.32	0.01
F4	RM-β-CD	HPMC	0.10	7.43	7.32	7.41	7.39	0.06
F5			0.25	7.49	7.41	7.31	7.40	0.09
F6			0.50	7.34	7.34	7.41	7.36	0.04
F7	RM-β-CD	HA	0.10	7.31	7.37	7.35	7.34	0.03
F8			0.25	7.46	7.30	7.37	7.38	0.08
F9			0.50	7.37	7.46	7.35	7.39	0.06
F10	RM-β-CD	HPMC	0.10	7.32	7.30	7.32	7.31	0.01
F11			0.25	7.36	7.35	7.36	7.36	0.01
F12			0.50	7.38	7.54	7.37	7.43	0.10
F13	γ-CD	HA	0.10	7.32	7.47	7.35	7.38	0.08
F14			0.25	7.37	7.30	7.39	7.35	0.05
F15			0.50	7.36	7.49	7.44	7.43	0.07
F16	γ-CD	HPMC	0.10	7.32	7.42	7.49	7.41	0.09
F17			0.25	7.32	7.33	7.43	7.36	0.07
F18			0.50	7.38	7.44	7.29	7.37	0.08
F9so	RM-β-CD	HA	0.50	7.35	7.41	7.32	7.36	0.05
F15so	γ-CD	HA	0.50	7.43	7.45	7.47	7.45	0.02
F18so		HPMC	0.50	7.33	7.45	7.38	7.39	0.06

Table B- 2 The osmolality data of each formulation

Formulation	CD	Polymer	% polymer (w/v)	Osmolality (mOsm/Kg)				
				n1	n2	n3	Average	S.D.
F1	RM-β-CD	HA	0.10	298	296	281	291.7	9.3
F2			0.25	294	295	327	305.3	18.8
F3			0.50	306	299	297	300.7	4.7
F4	RM-β-CD	HPMC	0.10	285	296	301	294.0	8.2
F5			0.25	296	310	285	297.0	12.5
F6			0.50	293	321	310	308.0	14.1
F7	RM-β-CD	HA	0.10	285	295	308	296.0	11.5
F8			0.25	291	282	283	285.3	4.9
F9			0.50	295	284	299	292.7	7.8
F10	RM-β-CD	HPMC	0.10	291	296	305	297.3	7.1
F11			0.25	293	294	286	291.0	4.4
F12			0.50	286	287	288	287.0	1.0
F13	γ-CD	HA	0.10	282	297	291	290.0	7.5
F14			0.25	288	305	284	292.3	11.2
F15			0.50	291	310	318	306.3	13.9
F16	γ-CD	HPMC	0.10	282	284	288	284.7	3.1
F17			0.25	293	296	298	295.7	2.5
F18			0.50	291	296	298	295.0	3.6
F9so	RM-β-CD	HA	0.50	285	300	294	293.0	7.5
F15so	γ-CD	HA	0.50	290	304	295	296.3	7.1
F18so		HPMC	0.50	288	292	285	288.3	3.5

Table B- 3 The viscosity data of each formulation

Formulation	CD	Polymer	% polymer (w/v)	Viscosity (mPa.s)				
				n1	n2	n3	Average	S.D.
F1	RM-β-CD	HA	0.10	2.4	2.3	2.6	2.43	0.15
F2			0.25	4.5	4.9	5.3	4.90	0.40
F3			0.50	8.4	9.2	9.5	9.03	0.57
F4	RM-β-CD	HPMC	0.10	2.6	2.8	2.6	2.66	0.08
F5			0.25	8.6	7.9	8.8	8.43	0.47
F6			0.50	15.3	14.2	14.5	14.67	0.57
F7	RM-β-CD	HA	0.10	2.7	2.7	2.7	2.72	0.02
F8			0.25	9.1	8.8	8.6	8.83	0.25
F9			0.50	16.5	15.6	14.9	15.67	0.80
F10	RM-β-CD	HPMC	0.10	2.4	2.5	2.5	2.47	0.05
F11			0.25	7.6	7.3	7.8	7.57	0.25
F12			0.50	14.7	15.5	15.2	15.13	0.40
F13	γ-CD	HA	0.10	2.3	2.4	2.4	2.36	0.06
F14			0.25	7.5	8.7	8.4	8.20	0.62
F15			0.50	16.3	16.9	17.4	16.87	0.55
F16	γ-CD	HPMC	0.10	2.4	2.5	2.8	2.58	0.23
F17			0.25	6.3	7.6	6.8	6.90	0.66
F18			0.50	14.5	15.3	15.6	15.13	0.57
F9so	RM-β-CD	HA	0.50	13.5	14.6	13.8	13.97	0.57
F15so	γ-CD	HA	0.50	13.3	14.6	12.5	13.47	1.06
F18so		HPMC	0.50	15.4	16.5	16.2	16.03	0.57

Table B- 4 The re-dispersion time data of each suspension

Formulation	CD	Polymer	% polymer (w/v)	Re-dispersion time (s)				
				n1	n2	n3	Mean	S.D.
F7	RM-β-CD	HA	0.10	4	4	4	3.8	0.4
F8			0.25	10	11	12	11.0	0.7
F9			0.50	23	25	21	22.8	1.7
F10	RM-β-CD	HPMC	0.10	156	146	169	157.0	11.5
F11			0.25	443	380	396	406.3	32.7
F12			0.50	641	626	565	610.7	40.3
F13	γ-CD	HA	0.10	5	4	3	4.0	1.0
F14			0.25	8	7	8	7.7	0.6
F15			0.50	13	16	14	14.3	1.5
F16	γ-CD	HPMC	0.10	15	17	16	16.0	1.0
F17			0.25	13	16	14	14.3	1.5
F18			0.50	58	42	57	52.3	9.0
F9so	RM-β-CD	HA	0.50	25	27	30	27.3	2.5
F15so	γ-CD	HA	0.50	19	16	22	19.0	3.0
F18so		HPMC	0.50	30	35	40	35.0	5.0

Table B- 5 The sedimentation volume of suspension

Formulation	CD	Polymer	% polymer (w/v)	Sedimentation Volume at 5 day				
				n1	n2	n3	Mean	S.D.
F7	RM-β-CD	HA	0.10	0.06	0.08	0.04	0.06	0.02
F8			0.25	0.08	0.06	0.06	0.07	0.01
F9			0.50	0.06	0.10	0.08	0.08	0.02
F10	RM-β-CD	HPMC	0.10	0.04	0.02	0.04	0.03	0.01
F11			0.25	0.04	0.06	0.04	0.05	0.01
F12			0.50	0.60	0.64	0.62	0.62	0.02
F13	γ-CD	HA	0.10	0.08	0.06	0.08	0.07	0.01
F14			0.25	0.08	0.06	0.10	0.08	0.02
F15			0.50	0.10	0.06	0.08	0.08	0.02
F16	γ-CD	HPMC	0.10	0.08	0.06	0.06	0.07	0.01
F17			0.25	0.08	0.08	0.10	0.09	0.01
F18			0.50	0.10	0.12	0.08	0.10	0.02
F9so	RM-β-CD	HA	0.50	0.06	0.08	0.08	0.07	0.01
F15so	γ-CD	HA	0.50	0.08	0.08	0.10	0.09	0.01
F18so		HPMC	0.50	0.10	0.08	0.08	0.09	0.01

Table B- 6 The particle size data of ternary complexes

complex	Particle size (nm)				
	n1	n2	n3	Mean	S.D.
CCB/RM-β-CD/HA	250.8	276.6	323.6	283.7	36.9
	2.3	1.9	1.9	2.0	0.2
CCB/RM-β-CD/HPMC	277.8	329.2	328.3	311.8	29.4
	2.1	1.6	2.5	2.1	0.5
CCB/γ-CD/HA	255.3	248.7	314.2	272.7	36.1
	1.9	1.9	1.8	1.9	0.02
CCB/ γ-CD/HPMC	301.2	305.7	317.5	308.1	8.4
	2.3	2.0	2.0	2.1	0.1

Table B- 7 The particle size data in supernatant of formulation

Formulation	CD	Polymer	Particle size (nm)				
			n1	n2	n3	Mean	S.D.
F3	RM-β-CD	0.5% HA	183.6	268.9	245.5	232.7	44.1
			12.1	11.9	18.1	14.1	3.5
			1.4	1.6	2.2	1.7	0.4
F9	RM-β-CD	0.5% HA	237.5	224.1	201.6	221.1	18.1
			24.6	37.5	25.6	29.2	7.2
			1.8	2.1	1.8	1.9	0.2
F15	γ-CD	0.5% HA	264.7	301.5	355.5	307.2	45.7
			40.3	29.9	32.2	34.1	5.4
			2.2	2.1	1.8	2.0	0.2
F18	γ-CD	0.5% HPMC	232.5	357.3	322.7	304.2	64.4
			28.2	51.5	55.9	45.2	14.9
			1.7	1.8	1.7	1.7	0.0
F9so	RM-β-CD	0.5% HA	204.9	258.1	227.3	230.1	26.7
			25.6	43.5	32.9	34.0	9.0
			2.0	2.1	1.2	1.8	0.5
F15so	γ-CD	0.5% HA	295.7	355.3	346.8	332.6	32.2
			40.0	60.6	45.3	48.6	10.7
			2.0	1.7	2.4	2.0	0.3
F18so	γ-CD	0.5% HPMC	315.9	348.9	386.4	350.4	35.3
			61.2	41.2	72.1	58.2	15.7
			1.6	2.4	1.9	1.9	0.4

Table B- 8 Data of % dissolved drug content of suspension F7-F13 and F9so

Formulation		CD	Polymer	Conc. (µg/ml)	% dissolved			
					Mean	SD	Mean	S.D.
F7	n1	RM-β-CD	0.1% HA	579.6	558.2	18.6	11.2	0.4
	n2			547.0				
	n3			547.9				
F8	n1	RM-β-CD	0.25% HA	475.3	497.2	23.3	9.9	0.5
	n2			521.7				
	n3			494.6				
F9	n1	RM-β-CD	0.5% HA	506.0	509.0	8.3	10.2	0.2
	n2			518.3				
	n3			502.7				
F9so	n1	RM-β-CD	0.5% HA	2250.5	2349.2	113.3	47.0	2.3
	n2			2473.0				
	n3			2324.2				
F10	n1	RM-β-CD	0.1% HPMC	689.7	739.6	45.9	14.8	0.9
	n2			780.2				
	n3			748.9				
F11	n1	RM-β-CD	0.25% HPMC	760.0	707.9	54.4	14.2	1.1
	n2			712.3				
	n3			651.4				
F12	n1	RM-β-CD	0.5% HPMC	632.3	632.8	5.8	12.7	0.1
	n2			627.2				
	n3			638.8				
F13	n1	γ-CD	0.1% HA	28.9	35.3	5.8	0.7	0.1
	n2			36.9				
	n3			40.0				

Table B- 9 Data of % dissolved drug content of suspension F14-F18, F15so and F18so

Formulation		CD	Polymer	Conc. (µg/ml)	% dissolved			
					Mean	SD	Mean	S.D.
F14	n1	γ-CD	0.25% HA	20.6	28.0	6.5	0.6	0.1
	n2			30.2				
	n3			33.0				
F15	n1	γ-CD	0.5% HA	42.6	33.7	8.0	0.7	0.2
	n2			31.6				
	n3			26.9				
F15so	n1	γ-CD	0.5% HA	65.3	66.3	7.2	1.3	0.1
	n2			73.9				
	n3			59.6				
F16	n1	γ-CD	0.1% HPMC	27.2	24.7	3.6	0.5	0.1
	n2			20.6				
	n3			26.4				
F17	n1	γ-CD	0.25% HPMC	24.8	24.4	2.6	0.5	0.1
	n2			26.7				
	n3			21.6				
F18	n1	γ-CD	0.5% HPMC	21.9	23.3	1.8	0.5	0.0
	n2			25.4				
	n3			22.7				
F18so	n1	γ-CD	0.5% HPMC	174.4	169.5	8.0	3.4	0.2
	n2			173.8				
	n3			160.3				

Table B- 10 Data of % total drug content of suspension F1-F16

Formulation		CD	Polymer	Conc. (µg/ml)	% Content			
					Mean	SD	Mean	S.D.
F1	n1	RM-β-CD	0.1% H	1059.9	1052.8	14.2	105.3	1.4
	n2			1036.5				
	n3			1062.0				
F2	n1	RM-β-CD	0.25% HA	1018.8	1056.5	50.5	105.7	5.0
	n2			1036.9				
	n3			1113.8				
F3	n1	RM-β-CD	0.5% HA	1003.5	1059.5	74.9	106.0	7.5
	n2			1144.6				
	n3			1030.6				
F4	n1	RM-β-CD	0.1% HPMC	996.4	1061.7	68.6	106.2	6.9
	n2			1055.6				
	n3			1133.2				
F5	n1	RM-β-CD	0.25% HPMC	972.7	993.9	44.5	99.4	4.4
	n2			1045.1				
	n3			964.0				
F6	n1	RM-β-CD	0.5% HPMC	1011.5	1052.9	35.9	105.3	3.6
	n2			1073.5				
	n3			1073.7				

Table B- 11 Data of % total drug content of suspension F7-F12 and F9so

Formulation		CD	Polymer	Conc. (µg/ml)	% Content			
					Mean	SD	Mean	S.D.
F7	n1	RM-β-CD	0.1% HA	4440.5	4687.8	221.3	93.8	4.4
	n2			4867.0				
	n3			4756.0				
F8	n1	RM-β-CD	0.25% HA	4731.2	4740.0	40.8	94.8	0.8
	n2			4784.5				
	n3			4704.4				
F9	n1	RM-β-CD	0.5% HA	4940.1	4975.9	113.5	99.5	2.3
	n2			5102.9				
	n3			4884.6				
F9so	n1	RM-β-CD	0.5% HA	4242.4	4597.4	359.4	91.9	7.2
	n2			4961.1				
	n3			4588.8				
F10	n1	RM-β-CD	0.1% HPMC	4742.6	4856.6	222.8	97.1	4.5
	n2			4713.9				
	n3			5113.4				
F11	n1	RM-β-CD	0.25% HPMC	4809.6	4951.2	216.5	99.0	4.3
	n2			5200.4				
	n3			4843.7				
F12	n1	RM-β-CD	0.5% HPMC	4508.3	4534.5	24.3	90.7	0.5
	n2			4539.2				
	n3			4556.1				

Table B- 12 Data of % total drug content of suspension F13-F18, F15so and F18so

Formulation		% CD	Polymer	Conc. (µg/ml)	% Content			
					Mean	SD	Mean	S.D.
F13	n1	γ-CD	0.1% HA	4648.7	4808.4	139.1	96.2	2.8
	n2			4872.9				
	n3			4903.6				
F14	n1	γ-CD	0.25% HA	4639.1	4677.3	33.9	93.5	0.7
	n2			4703.9				
	n3			4688.8				
F15	n1	γ-C	0.5% HA	4822.5	4715.3	99.0	94.3	2.0
	n2			4696.2				
	n3			4627.2				
F15so	n1	γ-CD	0.5% HA	4915.3	5143.2	278.8	102.9	5.6
	n2			5454.1				
	n3			5060.2				
F16	n1	γ-CD	0.1% HPMC	4887.4	4724.8	189.0	94.5	3.8
	n2			4517.5				
	n3			4769.5				
F17	n1	γ-CD	0.25% HPMC	4790.7	4848.7	82.8	97.0	1.7
	n2			4943.5				
	n3			4811.9				
F18	n1	γ-CD	0.5% HPMC	4557.7	4660.7	178.8	93.2	3.6
	n2			4557.3				
	n3			4867.1				
F18so	n1	γ-CD	0.5% HPMC	4867.0	5015.3	156.8	100.3	3.1
	n2			5179.3				
	n3			4999.6				

APPENDIX C

MUCOADHESIVE PROPERTIES

Table C- 1 The % drug remained for each F1-F7 formulation on mucin coated membrane

formulation		drug remained (µg)	drug remained Mean (µg)	drug remained S.D.	% drug remained	% drug remained Mean	% drug remained S.D.
F1	n1	0.23	0.222	0.099	0.44	0.419	0.18
	n2	0.12			0.22		
	n3	0.31			0.59		
F2	n1	0.14	0.177	0.080	0.28	0.34	0.16
	n2	0.27			0.52		
	n3	0.12			0.21		
F3	n1	0.21	0.216	0.062	0.41	0.41	0.09
	n2	0.28			0.49		
	n3	0.16			0.31		
F4	n1	0.29	0.218	0.091	0.58	0.41	0.18
	n2	0.12			0.22		
	n3	0.25			0.44		
F5	n1	0.20	0.254	0.052	0.40	0.51	0.11
	n2	0.27			0.51		
	n3	0.30			0.62		
F6	n1	0.13	0.212	0.077	0.25	0.40	0.13
	n2	0.28			0.52		
	n3	0.23			0.43		
F7	n1	2.18	1.517	0.579	0.98	0.66	0.28
	n2	1.16			0.48		
	n3	1.21			0.51		

Table C- 2 The % drug remained for each F8-F16 formulation on mucin coated membrane

formulation		drug remained (µg)	drug remained		% drug remained	% drug remained	
			Mean (µg)	S.D.		Mean	S.D.
F8	n1	2.92	3.311	0.591	1.23	1.40	0.26
	n2	3.03			1.27		
	n3	3.99			1.70		
F9	n1	5.64	5.573	0.314	2.28	2.24	0.18
	n2	5.23			2.05		
	n3	5.85			2.39		
F13	n1	2.53	1.796	0.636	1.09	0.75	0.29
	n2	1.43			0.59		
	n3	1.42			0.58		
F14	n1	2.90	3.328	0.377	1.25	1.42	0.15
	n2	3.47			1.47		
	n3	3.62			1.54		
F15	n1	7.24	7.643	0.716	3.00	3.24	0.32
	n2	8.47			3.61		
	n3	7.22			3.12		
F16	n1	0.51	1.110	0.528	0.21	0.48	0.24
	n2	1.51			0.67		
	n3	1.31			0.55		

Table C- 3 The % drug remained for each F17, F18 and F0G of formulation on mucin coated membrane

formulation		drug remained (µg)	drug remained		% drug remained	% drug remained	
			Mean (µg)	S.D.		Mean	S.D.
F17	n1	3.06	3.196	0.454	1.28	1.32	0.17
	n2	3.70			1.50		
	n3	2.83			1.17		
F18	n1	5.28	5.688	0.746	2.02	2.34	0.34
	n2	5.23			2.30		
	n3	6.55			2.69		
F0R	n1	0.33	0.306	0.0187	0.13	0.120	0.0092
	n2	0.30			0.12		
	n3	0.29			0.11		
F0G	n1	0.27	0.302	0.0329	0.11	0.115	0.0119
	n2	0.34			0.13		
	n3	0.29			0.11		

APPENDIX D

PERMEATION

Table D- 1 The permeation profiles of F1 through semipermeable membrane

Time (Hr.)	Cumulative release of F1 (µg)			Mean (µg)	SD
	n1	n2	n3		
0.5	27.74	29.73	29.15	28.87	1.02
1	58.09	56.44	57.48	57.34	0.84
2	115.43	119.63	116.33	117.13	2.21
3	175.76	174.41	163.02	171.06	7.00
4	229.87	229.55	209.65	223.03	11.58
5	285.46	285.96	257.91	276.44	16.05
6	343.25	333.65	303.47	326.79	20.76
8	431.26	422.03	384.53	412.60	24.75
Slope	54.658	53.163	47.522	51.78	3.76
R^2	0.9974	0.9964	0.9966		

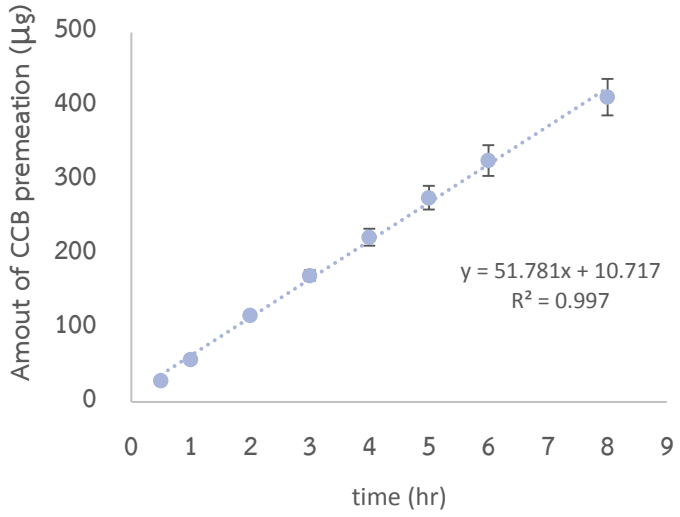

Figure D- 1 The permeation profiles of F1 through semipermeable membrane

Table D- 2 The permeation profiles of F2 through semipermeable membrane

Time (Hr.)	Cumulative release of F2 (µg)			Mean (µg)	SD
	n1	n2	n3		
0.5	25.70	30.76	26.64	27.70	2.69
1	58.70	64.47	53.16	58.78	5.65
2	119.24	125.97	107.43	117.55	9.39
3	168.05	196.92	159.08	174.68	19.78
4	229.74	259.01	210.43	233.06	24.46
5	281.61	315.12	258.59	285.11	28.43
6	333.81	369.49	303.54	335.61	33.02
8	423.11	469.19	388.13	426.81	40.66
slope	53.403	59.247	48.688	53.78	5.29
R^2	0.9970	0.9960	0.9975		

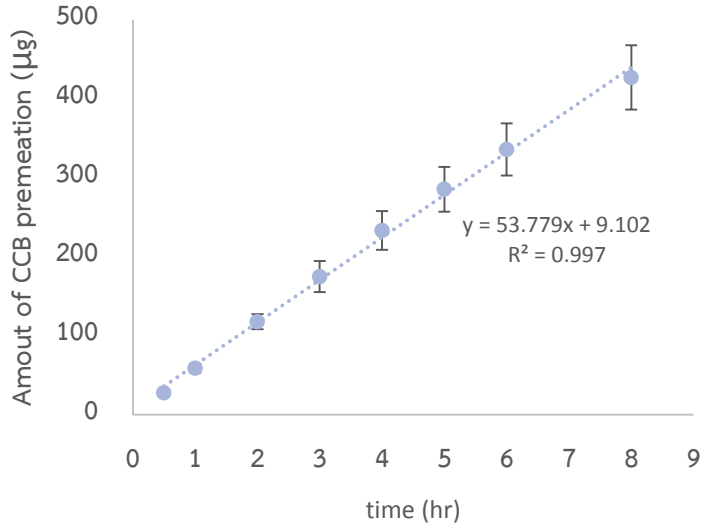

Figure D- 2 The permeation profiles of F2 through semipermeable membrane

Table D- 3 The permeation profiles of F3 through semipermeable membrane

Time (Hr.)	Cumulative release of F3 (µg)			Mean (µg)	SD
	n1	n2	n3		
0.5	29.41	28.43	26.77	28.20	1.33
1	56.38	55.40	53.11	54.96	1.68
2	115.93	109.91	107.07	110.97	4.53
3	160.29	161.50	156.83	159.54	2.42
4	220.55	213.21	207.68	213.82	6.46
5	269.56	261.87	253.80	261.75	7.88
6	318.32	307.01	300.76	308.70	8.90
8	408.05	394.41	381.38	394.61	13.34
Slope	50.948	49.176	47.810	49.31	1.57
R^2	0.9980	0.9979	0.9973		

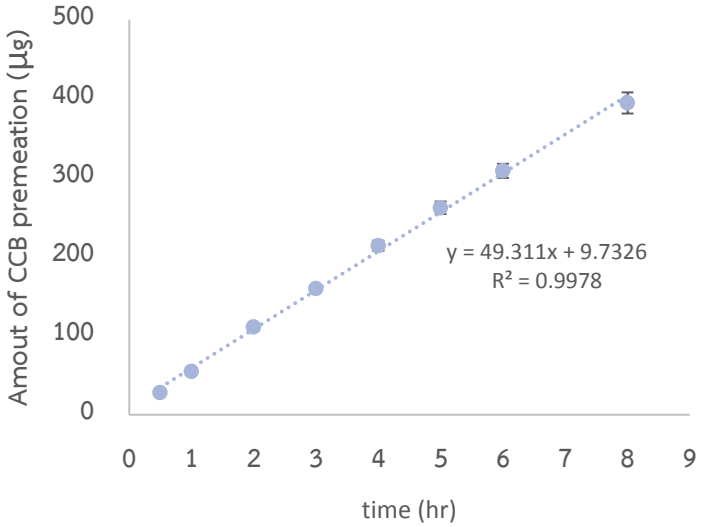

Figure D- 3 The permeation profiles of F3 through semipermeable membrane

Table D- 4 The permeation profiles of F4 through semipermeable membrane

Time (Hr.)	Cumulative release of F4 (µg)			Mean (µg)	SD
	n1	n2	n3		
0.5	33.55	33.03	29.69	32.09	2.09
1	62.27	62.35	59.81	61.47	1.45
2	120.36	124.81	116.36	120.51	4.22
3	174.10	181.66	175.03	176.93	4.12
4	234.84	239.41	234.32	236.19	2.80
5	294.26	297.69	285.48	292.47	6.30
6	352.85	345.77	336.41	345.01	8.25
8	428.42	440.08	431.84	433.44	6.00
Slope	54.360	54.975	54.146	54.49	0.43
R^2	0.9946	0.9971	0.9979		

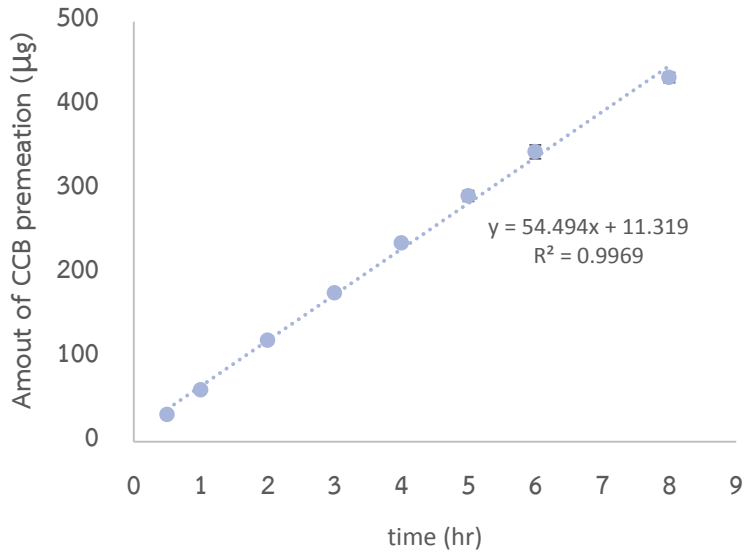

Figure D- 4 The permeation profiles of F4 through semipermeable membrane

Table D- 5 The permeation profiles of F5 through semipermeable membrane

Time (Hr.)	Cumulative release of F5 (µg)			Mean (µg)	SD
	n1	n2	n3		
0.5	33.27	23.16	25.78	27.40	5.25
1	55.35	47.23	50.65	51.08	4.08
2	107.02	92.37	98.72	99.37	7.35
3	166.25	139.15	151.25	152.22	13.58
4	205.93	183.43	197.42	195.60	11.36
5	253.42	225.49	242.35	240.42	14.06
6	296.43	263.49	287.71	282.54	17.06
8	383.03	339.47	366.72	363.07	22.01
Slope	47.011	42.486	46.003	45.17	2.38
R^2	0.9975	0.9978	0.9978		

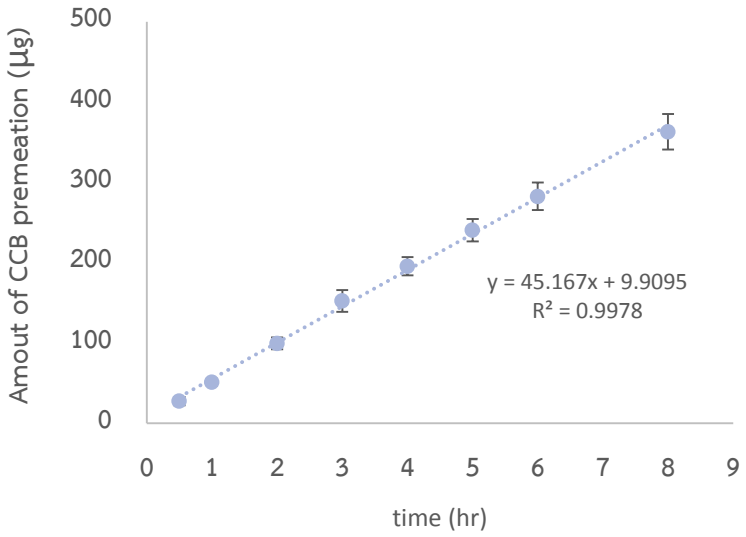

Figure D- 5 The permeation profiles of F5 through semipermeable membrane

Table D- 6 The permeation profiles of F6 through semipermeable membrane

Time (Hr)	Cumulative release of F6 (µg)			Mean (µg)	SD
	n1	n2	n3		
0.5	29.78	36.02	26.54	30.78	4.82
1	56.74	53.00	54.21	54.65	1.91
2	111.70	102.71	103.10	105.84	5.08
3	164.38	153.92	158.89	159.06	5.23
4	215.54	199.67	207.25	207.49	7.94
5	261.95	243.19	253.82	252.99	9.41
6	304.73	284.05	299.41	296.06	10.74
8	390.14	364.20	383.35	379.23	13.45
Slope	48.407	44.604	47.989	47.00	2.09
R^2	0.9968	0.9978	0.9977		

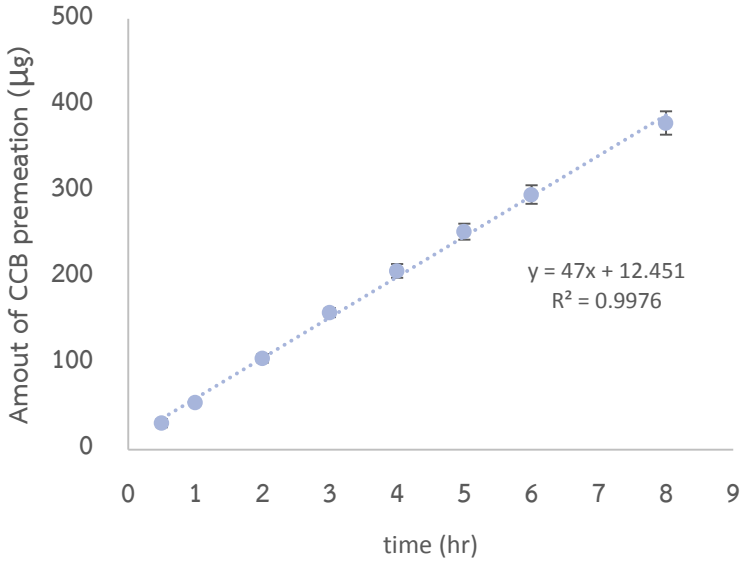

Figure D- 6 The permeation profiles of F6 through semipermeable membrane

Table D- 7 The permeation profiles of F7 through semipermeable membrane

Time (Hr.)	Cumulative release of F7 (µg)			Mean (µg)	SD
	n1	n2	n3		
0.5	16.09	21.28	15.74	17.70	3.10
1	33.60	35.07	30.37	33.01	2.40
2	67.72	67.31	64.27	66.44	1.88
3	101.30	99.22	95.99	98.84	2.68
4	132.02	125.07	125.08	127.39	4.01
5	161.85	159.32	155.97	159.05	2.95
6	192.12	183.93	180.62	185.56	5.92
8	259.01	230.14	231.20	240.12	16.37
Slope	32.053	28.452	29.101	29.87	1.92
R^2	0.9995	0.996	0.9967		

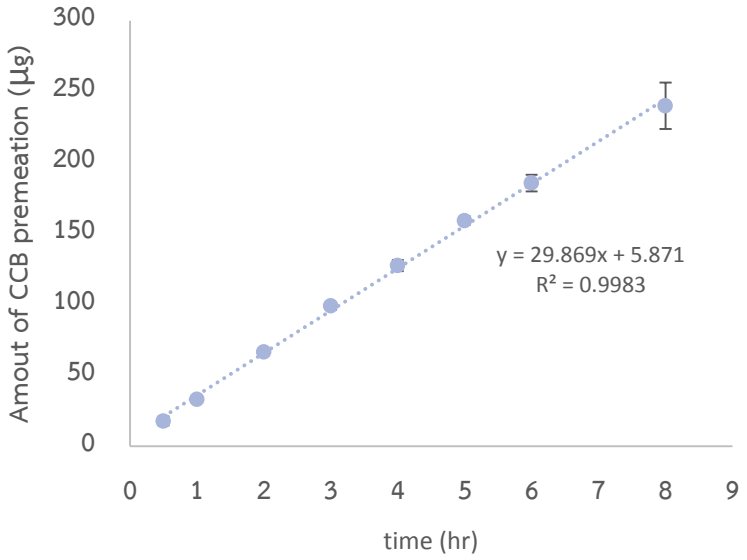

Figure D- 7 The permeation profiles of F7 through semipermeable membrane

Table D- 8 The permeation profiles of F8 through semipermeable membrane

Time (Hr.)	Cumulative release of F8 (µg)			Mean (µg)	SD
	n1	n2	n3		
0.5	15.65	22.84	12.86	17.11	5.15
1	30.31	34.87	26.71	30.63	4.09
2	61.96	66.78	55.18	61.31	5.83
3	91.88	100.59	82.32	91.60	9.14
4	116.17	124.15	108.07	116.13	8.04
5	143.98	160.81	134.15	146.31	13.48
6	-	182.43	157.12	169.77	17.90
8	225.86	233.88	202.20	220.65	16.47
Slope	27.921	28.664	25.452	27.31	1.68
R^2	0.9990	0.9968	0.9978		

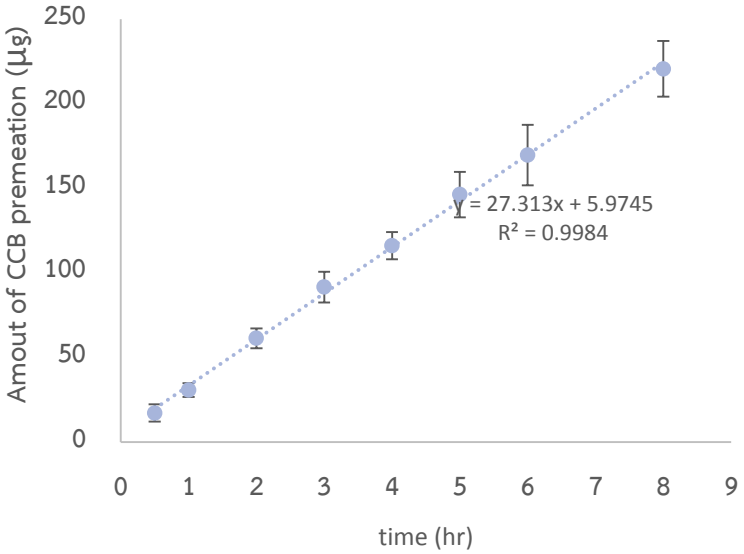

Figure D- 8 The permeation profiles of F8 through semipermeable membrane

Table D- 9 The permeation profiles of F9 through semipermeable membrane

Time (Hr.)	Cumulative release of F9 (µg)			Mean (µg)	SD
	n1	n2	n3		
0.5	13.91	20.27	14.82	16.33	3.44
1	30.74	36.14	30.66	32.51	3.14
2	61.44	67.50	61.08	63.34	3.61
3	88.01	98.29	91.90	92.73	5.19
4	113.40	122.38	117.49	117.76	4.50
5	144.73	152.16	147.27	148.05	3.77
6	169.32	184.25	171.48	175.02	8.07
8	223.39	226.23	216.46	222.03	5.02
Slope	27.743	27.899	27.205	27.62	0.36
R^2	0.9991	0.9961	0.996		

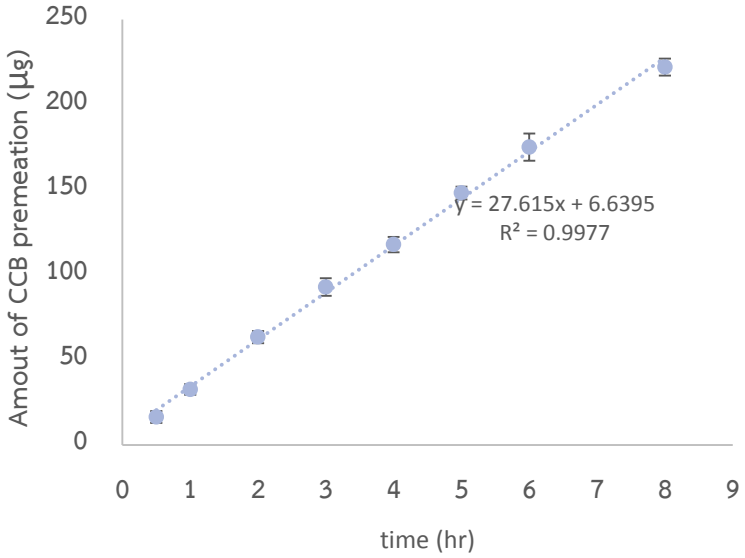

Figure D- 9 The permeation profiles of F9 through semipermeable membrane

Table D- 10 The permeation profiles of F13 through semipermeable membrane

Time (Hr.)	Cumulative release of F13 (µg			Mean (µg)	SD
	n1	n2	n3		
1	2.23	1.65	1.85	1.91	0.30
2	4.56	4.19	4.13	4.29	0.23
3	7.24	5.90	6.43	6.52	0.67
4	9.40	7.85	8.62	8.62	0.78
5	12.95	9.48	11.40	11.28	1.74
7	17.16	13.79	15.17	15.38	1.70
9	20.58	-	19.69	20.13	0.63
Slope	2.358	1.967	2.227	2.26	0.20
R^2	0.9921	0.9971	0.9986		

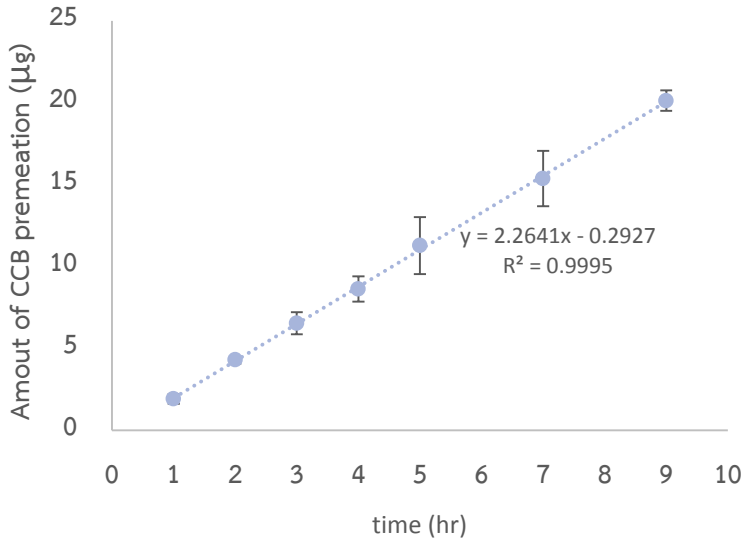

Figure D- 10 The permeation profiles of F13 through semipermeable membrane

Table D- 11 The permeation profiles of F14 through semipermeable membrane

Time (Hr.)	Cumulative release of F14 (µg)			Mean (µg)	SD
	n1	n2	n3		
1	-	1.28	1.66	1.47	0.27
2	5.65	3.35	3.90	4.30	1.20
3	7.40	4.78	6.64	6.27	1.34
4	9.25	6.33	7.53	7.70	1.46
5	11.99	8.01	9.57	9.86	2.01
7	14.94	11.59	12.48	13.00	1.73
9	18.05	15.83	16.21	16.70	1.19
Slope	1.796	1.774	1.789	1.84	0.01
R^2	0.9922	0.9966	0.9955		

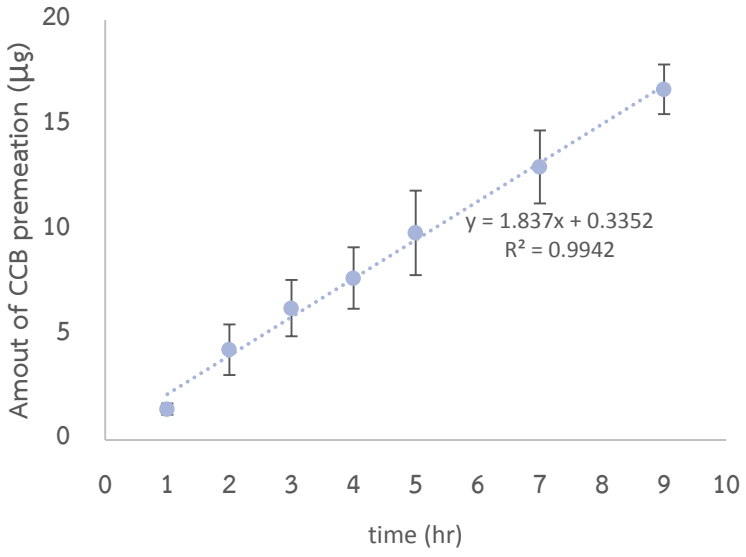

Figure D- 11 The permeation profiles of F14 through semipermeable membrane

Table D- 12 The permeation profiles of F15 through semipermeable membrane

Time (Hr.)	Cumulative release of F15 (µg)			Mean (µg)	SD
	n1	n2	n3		
1	1.97	1.95	1.47	1.80	0.28
2	4.35	4.25	3.63	4.08	0.39
3	6.50	6.49	5.34	6.11	0.66
4	8.43	8.19	7.27	7.96	0.61
5	10.67	11.19	9.84	10.57	0.68
7	15.13	15.49	13.26	14.62	1.20
9	19.18	19.99	17.40	18.85	1.33
Slope	2.148	2.260	1.983	2.13	0.14
R^2	0.9991	0.9987	0.9986		

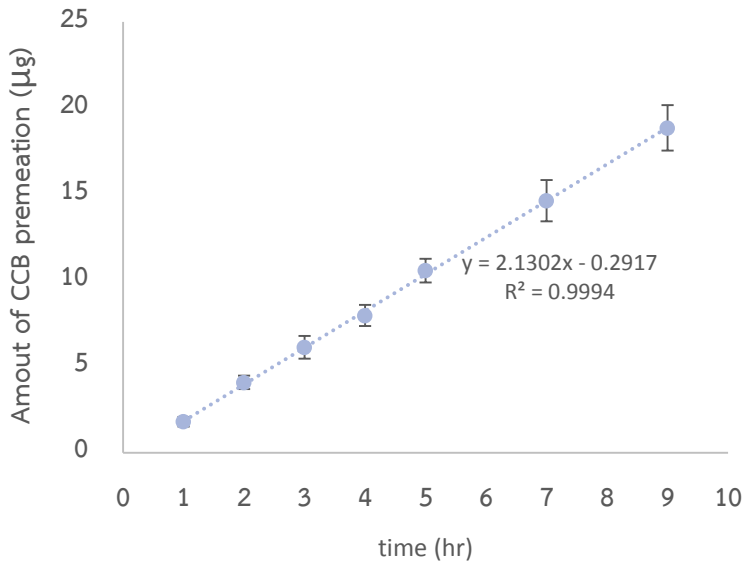

Figure D- 12 The permeation profiles of F15 through semipermeable membrane

Table D- 13 The permeation profiles of F16 through semipermeable membrane

Time (Hr.)	Cumulative release of F16 (µg)			Mean (µg)	SD
	n1	n2	n3		
1	1.59	1.94	1.26	1.60	0.34
2	3.81	3.20	3.69	3.57	0.32
3	6.53	6.08	6.08	6.23	0.26
4	7.87	7.24	7.94	7.68	0.38
5	11.41	8.78	9.96	10.05	1.32
7	14.52	12.60	13.96	13.70	0.99
9	18.53	15.91	17.26	17.23	1.31
Slope	2.120	1.857	1.759	1.96	0.19
R^2	0.9925	0.9937	0.9952		

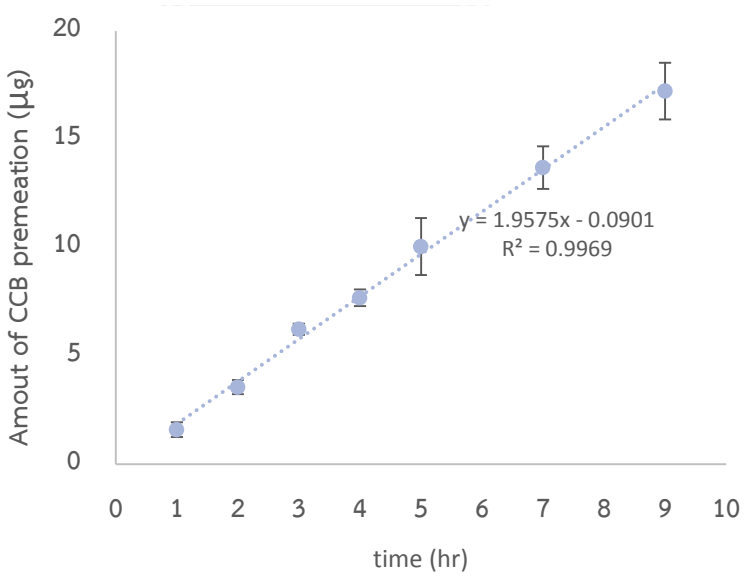

Figure D- 13 The permeation profiles of F16 through semipermeable membrane

Table D- 14 The permeation profiles of F17 through semipermeable membrane

Time (Hr.)	Cumulative release of F17 (µg)			Mean (µg)	SD
	n1	n2	n3		
1	2.45	2.13	1.28	1.95	0.60
2	4.45	3.32	3.20	3.66	0.69
3	5.95	5.16	5.33	5.48	0.42
4	8.07	6.98	7.41	7.48	0.55
5	9.97	8.67	9.49	9.38	0.65
7	13.11	11.79	13.16	12.69	0.78
9	16.57	15.33	15.67	15.86	0.64
Slope	1.761	1.668	1.844	1.76	0.09
R^2	0.9986	0.9988	0.9926		

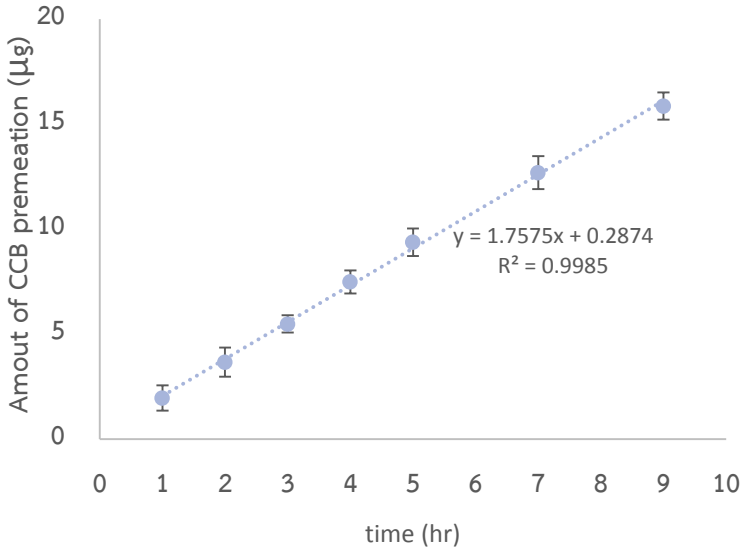

Figure D- 14 The permeation profiles of F17 through semipermeable membrane

Table D- 15 The permeation profiles of F18 through semipermeable membrane

Time (Hr.)	Cumulative release of F18 (µg)			Mean (µg)	SD
	n1	n2	n3		
1	2.30	1.20	1.23	1.57	0.62
2	4.57	3.36	2.95	3.63	0.84
3	6.82	5.29	5.19	5.77	0.91
4	8.05	7.37	6.79	7.40	0.63
5	10.23	9.21	8.90	9.45	0.70
7	13.39	13.19	12.36	12.98	0.55
9	16.62	15.33	15.82	15.92	0.65
Slope	1.763	1.808	1.834	1.80	0.04
R^2	0.9966	0.9905	0.9989		

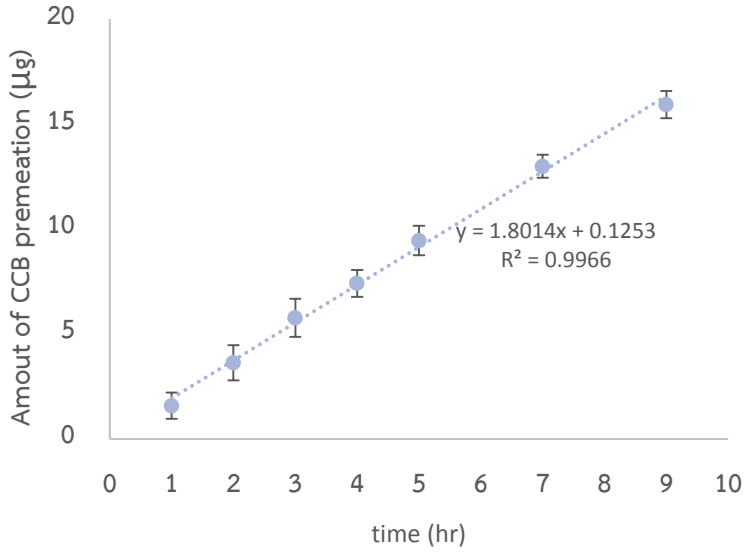

Figure D- 15 The permeation profiles of F18 through semipermeable membrane

Table D- 16 The permeation profiles of F9so through semipermeable membrane

Time (Hr.)	Cumulative release of F9so (µg)			Mean (µg)	SD
	n1	n2	n3		
1	85.06	86.77	77.70	83.18	4.82
2	164.34	169.04	152.56	161.98	8.49
3	237.34	235.99	218.08	230.47	10.75
4	305.48	307.43	272.31	295.07	19.74
5	356.97	358.25	323.00	346.07	19.99
6	423.24	426.47	380.72	410.14	25.53
8	535.27	521.37	475.58	510.74	31.23
Slope	63.752	62.012	56.202	60.66	3.95
R^2	0.9953	0.9917	0.9938		

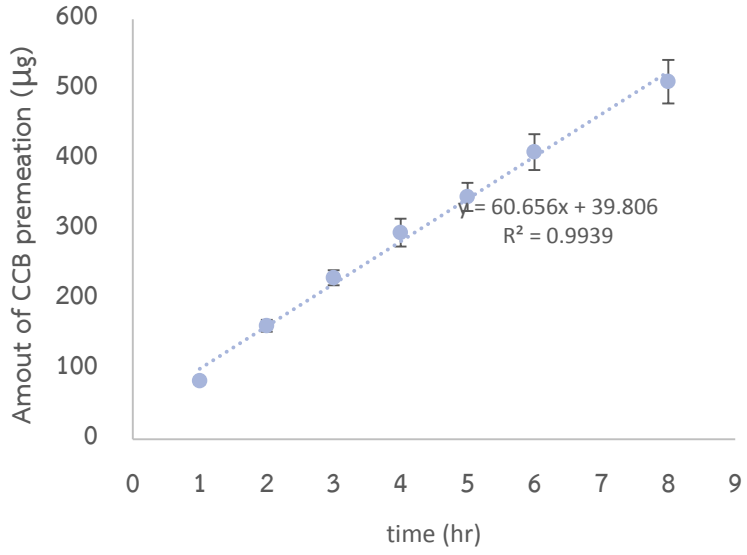

Figure D- 16 The permeation profiles of F9so through semipermeable membrane

Table D- 17 The permeation profiles of F15so through semipermeable membrane

Time (Hr.)	Cumulative release of F15so (µg)			Mean (µg)	SD
	n1	n2	n3		
1	0.73	0.24	0.39	0.45	0.25
2	3.29	2.40	2.79	2.82	0.45
3	5.18	5.04	4.95	5.06	0.11
4	7.88	6.28	7.24	7.13	0.80
5	11.24	8.31	9.21	9.59	1.50
7	14.21	13.02	12.09	13.11	1.06
9	19.61	16.94	15.87	17.47	1.93
Slope	2.3339	2.0769	1.8997	2.10	0.22
R^2	0.9936	0.9973	0.9926		

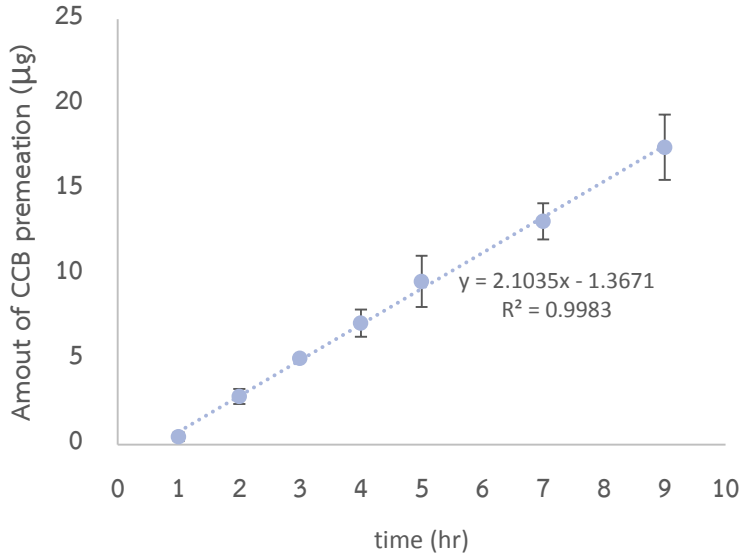

Figure D- 17 The permeation profiles of F15so through semipermeable membrane

Table D- 18 The permeation profiles of F18so through semipermeable membrane

Time (Hr.)	Cumulative release of F18so (µg)			Mean (µg)	SD
	n1	n2	n3		
1	7.76	7.14	6.10	7.00	0.84
2	17.96	15.25	14.46	15.89	1.84
3	26.84	22.46	23.29	24.20	2.33
4	35.29	30.65	30.03	31.99	2.87
5	43.16	38.76	36.86	39.59	3.23
7	55.25	49.99	50.12	51.79	3.00
9	67.05	61.11	60.19	62.79	3.72
Slope	7.3261	6.7763	6.7678	6.96	0.32
R^2	0.9876	0.9923	0.9918		

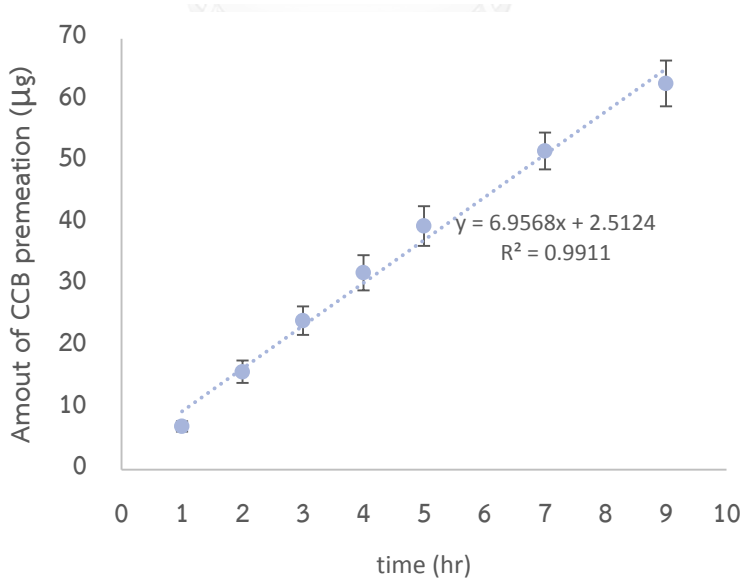

Figure D- 18 The permeation profiles of F18so through semipermeable membrane

Table D- 19 The permeation profiles of F3 through simulated vitreous humor

Time (Hr.)	Cumulative release of F3 (µg)			Mean (µg)	SD
	n1	n2	n3		
4	2.35	1.94	1.72	2.00	0.32
5	4.78	4.26	3.73	4.26	0.52
6	8.51	7.49	6.97	7.66	0.78
7	13.25	11.57	11.14	11.99	1.11
8	19.34	17.15	16.44	17.64	1.51
9	26.81	23.30	23.21	24.44	2.05
10	34.49	29.52	29.93	31.31	2.76
15	81.44	70.98	72.44	74.95	5.66
Slope	8.6814	7.5487	7.8127	8.01	0.59
R^2	0.995	0.9937	0.9943		

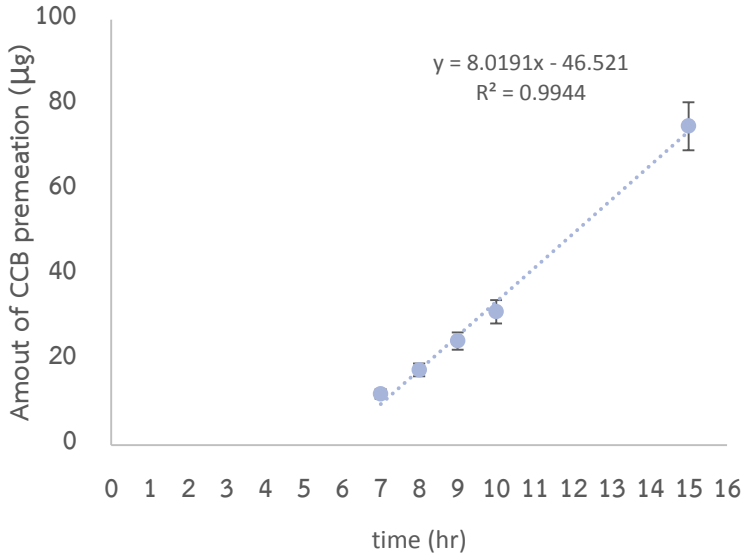

Figure D- 19 The permeation profiles of F3 through simulated vitreous humor

Table D- 20 The permeation profiles of F9 through simulated vitreous humor

Time (Hr.)	Cumulative release of F9 (µg)			Mean (µg)	SD
	n1	n2	n3		
4	0.95	0.97	1.31	1.08	0.20
5	1.78	2.18	2.68	2.21	0.45
6	3.21	3.71	4.34	3.76	0.57
7	4.97	5.70	6.75	5.81	0.90
8	7.32	8.34	9.56	8.41	1.12
9	9.77	11.49	13.09	11.45	1.66
10	12.56	14.44	16.36	14.45	1.90
15	28.67	34.54	37.31	33.51	4.41
Slope	3.0080	3.6678	3.8839	3.52	0.46
R^2	0.996	0.9940	0.9957		

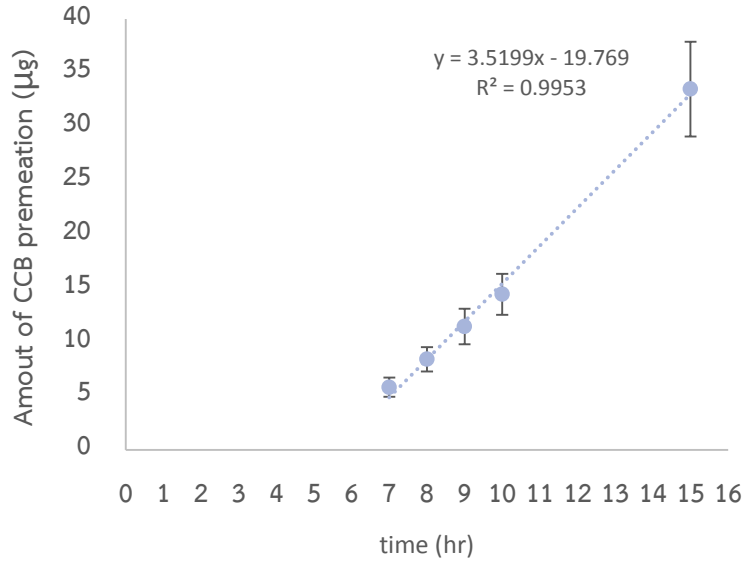

Figure D- 20 The permeation profiles of F9 through simulated vitreous humor

Table D- 21 The permeation profiles of F15 through simulated vitreous humor

Time (Hr)	Cumulative release of F15 (µg)			Mean (µg)	SD
	n1	n2	n3		
16	4.63	1.47	2.92	3.01	1.58
20	5.99	2.07	3.89	3.98	1.96
22	6.93	2.33	4.37	4.55	2.30
24	7.67	2.64	5.21	5.18	2.52
26	8.89	2.97	5.60	5.82	2.97
28	9.12	3.10	5.85	6.02	3.01
Slope	0.3787	0.1399	0.2541	0.26	0.12
R^2	0.9981	0.9935	0.9934		

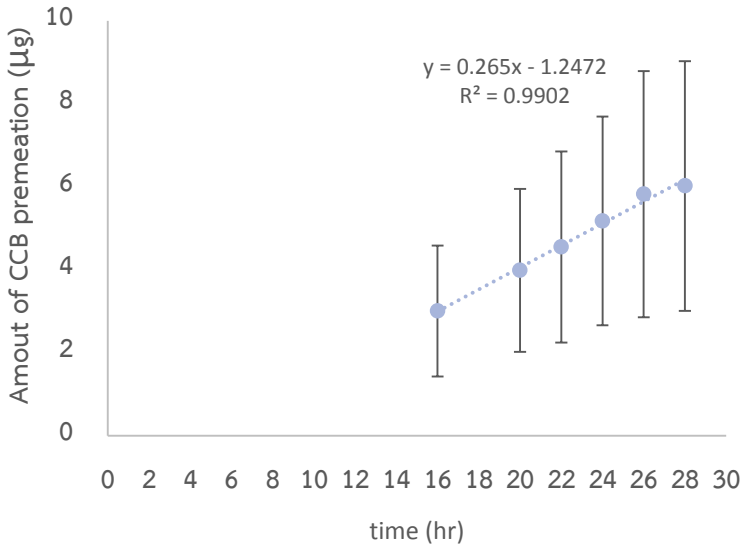

Figure D- 21 The permeation profiles of F15 through simulated vitreous humor

Table D- 22 The permeation profiles of F18 through simulated vitreous humor

Time (Hr.)	Cumulative release of F18 (µg)			Mean (µg)	SD
	n1	n2	n3		
16	4.69	3.27	2.87	3.61	0.96
20	7.30	4.28	4.11	5.23	1.79
22	7.66	4.94	4.81	5.80	1.61
24	9.04	5.62	5.49	6.72	2.02
26	9.95	6.36	6.21	7.51	2.11
28	10.89	7.89	7.86	8.88	1.74
Slope	0.5085	0.3094	0.3341	0.42	0.11
R^2	0.9973	0.9924	0.9989		

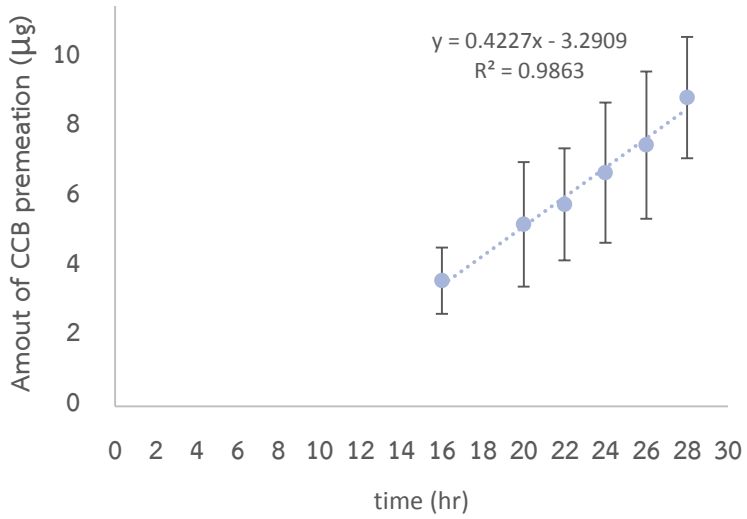

Figure D- 22 The permeation profiles of F18 through simulated vitreous humor

Table D- 23 The permeation profiles of F9so through simulated vitreous humor

Time (Hr.)	Cumulative release of F9so (µg)			Mean (µg)	SD
	n1	n2	n3		
7	13.14	14.35	12.26	13.25	1.05
8	18.49	19.35	17.14	18.33	1.12
10	30.36	31.44	28.21	30.00	1.64
12	44.61	44.23	40.30	43.05	2.38
14	61.03	59.44	55.45	58.64	2.88
16	77.40	74.20	70.41	74.00	3.50
Slope	7.1589	6.6764	6.4559	6.76	0.36
R^2	0.9943	0.9964	0.994		

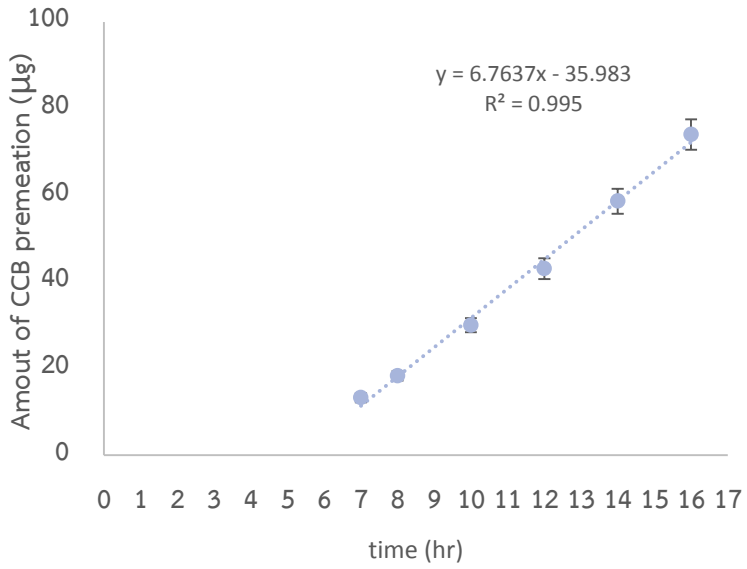

Figure D- 23 The permeation profiles of F9so through simulated vitreous humor

Table D- 24 The permeation profiles of F15so through simulated vitreous humor

Time (Hr)	Cumulative release of F15so (µg)			Mean (µg)	SD
	n1	n2	n3		
17	6.97	6.07	6.37	6.47	0.46
18	7.34	6.43	6.64	6.80	0.48
20	8.32	7.10	7.33	7.58	0.65
22	9.18	7.45	8.19	8.27	0.87
24	9.50	8.18	8.84	8.84	0.66
26	9.88	8.86	9.24	9.32	0.52
Slope	0.3344	0.3006	0.3357	0.32	0.02
R^2	0.9818	0.9931	0.9904		

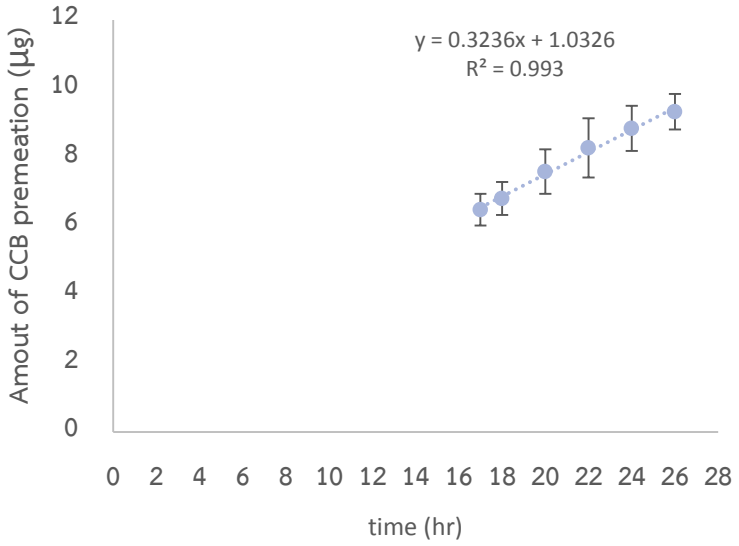

Figure D- 24 The permeation profiles of F15so through simulated vitreous humor

Table D- 25 The permeation profiles of F18so through simulated vitreous humor

Time (Hr.)	Cumulative release of F18so (µg)			Mean (µg)	SD
	n1	n2	n3		
17	12.51	11.55	11.31	11.79	0.64
18	13.80	12.54	12.55	12.96	0.73
20	15.23	13.98	14.25	14.49	0.66
22	16.37	15.81	15.21	15.80	0.58
24	18.66	17.01	17.12	17.60	0.92
26	19.52	18.53	18.98	19.01	0.49
Slope	0.7771	0.7696	0.8122	0.79	0.02
R^2	0.9927	0.997	0.9915		

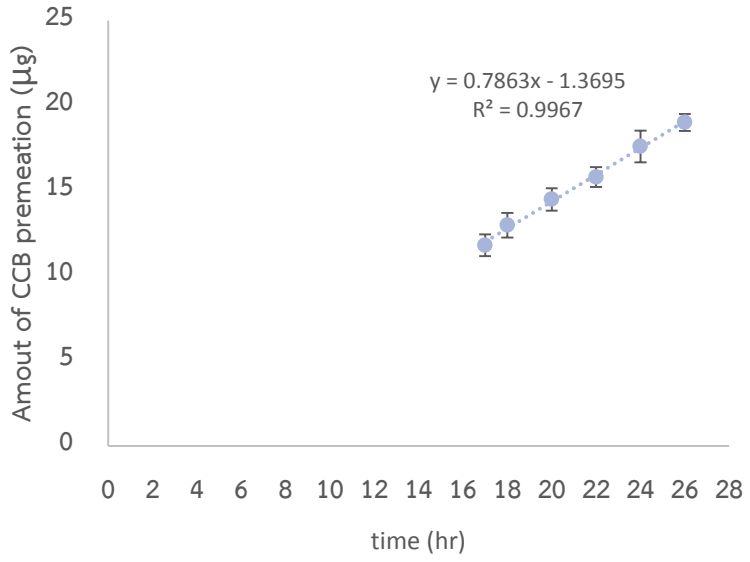

Figure D- 25 The permeation profiles of F18so through simulated vitreous humor

VITA

Pol.Cap. Pakin Kulsirachote was born on February 22, 1982 in Bangkok, Thailand. He graduated the bachelor degree of Pharmaceutical Science with a second class honors from Faculty of Pharmaceutical Science, Prince of Songkla University, Hat Yai, Thailand in 2005. He had worked at OLIC (Thailand) Ltd., Ayuthaya, Thailand for 5 years and had worked at IDS manufacturing Co.,Ltd., Pathumthani, Thailand for 1 year. After that, he worked at Police General Hospital, Bangkok, Thailand for 4 years before entering the Master's Degree in Pharmaceutics program, Faculty of Pharmaceutical science in 2014 at Chulalongkorn University, Bangkok, Thailand.